DEVELOPMENT AND APPLICATIONS
OF
H-INFINITY CONTROL

A THESIS

Submitted in the fulfilment of the requirement for the award of the degree of

DOCTOR OF PHILOSOPHY

by

Sikander Hans

(Registration No. 901604013)

Under the Supervision of

Dr. Smarajit Ghosh

Professor

Department of Electrical and Instrumentation Engineering

THAPAR INSTITUTE
OF ENGINEERING & TECHNOLOGY
(Deemed to be University)

Department of Electrical and Instrumentation Engineering

THAPAR INSTITUTE OF ENGINEERING & TECHNOLOGY

(Deemed to be University u/s 3 of UGC Act., 1956)

Patiala-147004, Punjab (INDIA)

March-2022

CERTIFICATE

I hereby certify that the work which is being presented in thesis entitled "***Development and Applications of H-Infinity Control***" submitted to the Department of Electrical and Instrumentation Engineering, Thapar Institute of Engineering and Technology (Deemed to be University), Patiala in the fulfilment of the requirements for the award of degree of "**Doctor of Philosophy**" is an authentic record of my own research work carried out under the guidance of **Dr. Smarajit Ghosh** and refers other research work, which are duly listed in the reference section.

The matter presented in this thesis has not been submitted in part or full for the award of any degree in any other University or Institute.

11/03/2022

(SIKANDER HANS)
Registration No. 901604013

This is to certify that the above statement made by the candidate is correct and true to the best of my knowledge.

S. Ghosh 11-03-2022

(Dr. SMARAJIT GHOSH)
Professor
Department of Electrical and Instrumentation Engineering
Thapar Institute of Engineering & Technology (Deemed to be University)
Patiala, Punjab, India

Dedicated

to my

Father Shri Ram Singh Hans

&

Mother Smt. Maya Devi

ABSTRACT

The working of BLDC motor is along with the controller to reduce the torque ripple and improve the speed. The controller variables are tuned through the sensing algorithm and the disturbances are avoided. H∞ controller is used to synthesize the guaranteed performance of certain applications as well as it provides maximum gain at any situation. Due to high order, the H-Infinity controllers can prompt to demand for immense control efforts along with certain analysis are essential for designing a particular system. In agreement with modelling conditions like design concern, inconvenient depletion at maximum frequency and bandwidth requirements, the H-Infinity controllers has afforded with a closed loop feedback. In literature, various methods are assembled about loop shaping of H-infinity and modelling of H-infinity controller among that loop shaping of H-infinity is more prominent as the performance weights are placed at the designing phase. The brushless direct current motor needs the electronic speed controllers to run the motor, which is superior to the brushed direct current motor because of its efficiency and better operating speed. The brushless direct current motor is designed with the novelty of fixed order H-infinity controller. The appropriate weight and transfer functions has been used for designing the controller. The improved particle swarm optimization algorithm to obtain the optimal position of rotor. The new controller can reduce the torque as much as possible so that speed is high and analysed the performance of torque, speed and back electro-motive force compared with existing controllers such as fuzzy proportional plus integral plus derivative, sensing algorithm and fuzzy proportional plus derivative controller and results show that the proposed technique gives better results than the other existing controllers. Continuous Stirred Tank Reactor (CSTR) are designed with H∞ controllers. H-infinity (H∞) controller based disturbance rejection along with utilization of the Water Wave Optimization (WWO) algorithm . In general, the algorithmic framework of WWO algorithm is simple, and easy to implement with a small-size population and only a few control parameters. This deals with the focuses on the conflicts of CSTR such as variation in temperature and product concentration. The elimination of these issues is performed with the help of WWO algorithm along with the controller operation. The planned work gives the enhanced performance by means of disturbance rejection The obtained results are then compared with the existing methods like PID controller, ANN algorithm and ADRC controller.

The overall process is implemented in the MATLAB working platform and the results are compared with the preceding methods to show the expected performance and the proposed technique gives better results than the other existing controllers.

ACKNOWLEDGEMENTS

I want to express my heartiest gratitude, indebtedness, and sincere appreciation to my esteemed supervisor, **Dr. Smarajit Ghosh** (Professor, Electrical and Instrumentation Engineering Department, TIET), for his continuous inspiration, support, guidance, encouragement, advice, patience and feedback throughout my Ph.D. I felt very grateful and blessed to have worked under his supervision. He always motivated me to achieve my research goals. Most of the novel ideas found in this thesis are the result of our numerous discussions. His editorial comments were very meaningful and significant for writing this thesis.

I am thankful to Dean of Research and Sponsored Projects **Dr. Rafat Siddique** for his support during the thesis work. I would like to express my heartfelt gratitude towards **Dr. Prakash Gopalan** (Director, TIET, Patiala), and **Dr. R.S. Kaler** (Head, Electrical and Instrumentation Engineering Department), for providing me with the facilities and support to complete this research work. I am also thankful to **Dr. Gurbinder Singh** (Registrar, TIET, Patiala) for his support in the smooth proceeding of the administrative needs associated with the work.

I would like to thank the esteemed members of my Doctoral Committee, **Dr. Neeraj Kumar, Dr. Sunil K. Singla and Dr. Vishal Srivastava** for their constructive comments and regularly ensuring the progress of my research work. I would like to thank the faculty and staff members of the Electrical and Instrumentation Engineering Department. I would like to thank my relatives and buddies for their moral support during my work.

Most importantly, I acknowledge the people who mean a lot to me, my parents, **Shri. Ram Singh Hans** and **Smt. Maya Devi**, for showing faith in me and giving me liberty to choose what I desired. I salute you all for the selfless love, care, pain and sacrifice you did to shape my life. Although you hardly understood what I researched on, you were willing to support any decision I made. I would never be able to pay back the love and affection showered upon by my parents.

Thanks to my sister **Dr. Neetu** and **Yograj Goondli (Jijaji)** for her selfless love, care and dedicated efforts which contributed a lot for completion of my thesis.

I am extremely grateful to my brother **Ravinder Sohan Hans** and **Parveen hans (Priya)** for his continuous encouragement, support, and positive feedback. He always motivates me during my difficult time.

I am especially thankful to my wife **Bhawana** for making this entire journey easy and comfortable through providing unconditional support and moral encouragement.

Special thanks to my brother cute son **Maanu (Maanav Ram Hans)** and Sister three lovely kids **Peehu, Ladoo and Kushi** whose smiling faces always made me enthusiastic in achieving my goal.

Last but not least this thesis is dedicated to a very special gift to me from almighty God my son **Shanu (Vihaan Ram Hans)** whose existence boosted my confidence for the completion of the thesis. I will always feel sorry to them for the time I spent during my work when they want it most.

I am indebted to my family for showering their blessings all the time and always stood beside me in difficult times. I am thankful to my **Grand Mother Ram Kauri** and **Mother-in-Law Kanta Rani.**

It's my fortune to gratefully acknowledge the support of my friends, **Pankaj jood, Shubham Chaudhary, Abhay Krishan (Bhoot Bhai), Aman Kataria**, **Tamoghana Bhattacharya** for their support and generous care throughout the research tenure. They were always beside me during the happy and hard moments to push me and motivate me.

(Sikander Hans)

TABLE OF CONTENTS

LIST OF TABLES

LIST OF FIGURES

LIST OF ABBREVIATION

S.NO	Abbreviation	
1	WWO	Water Wave Optimization
2	IPSO	Improved Particle Swarm Optimization
3	BLDC	Brushless Direct Current
4	CSTR	Continuous Stirred Tank Reactor
5	PD	Proportional Derivative
6	PID	Proportional Integral Derivative
7	PMSM	Permanent Magnet Synchronous Motor
8	ECM	Electronically Commutated Motors
9	PI	Proportional Integral
10	TSMC	Terminal Sliding Mode Controller
11	CNC	Computer Numerical Control
12	CD	Compact Disk
13	DVD	Digital Versatile Disk
14	SISO	Single Input Single Output
15	BEMF	Back Electro Motive Force
16	PDF	Probability Density Function
17	EEG	Electroencephalogram
18	DOF	Degree Of Freedom

19	ELM	External Linear Model
20	PH	Potential of Hydrogen
21	COD	Chemical Oxygen Demand
22	LMI	Linear Matrix Inequality
23	ARDC	Active Disturbance Rejection Controller
24	ANN	Artificial Neural Network
25	SPWM	Sinusoidal Pulse Width Modulation
26	COA	Centre Of Area
27	FCM	Fuzzy Clustering Method
28	EOB	Elite Opposition Based strategy
29	TD	Tracking Differentiator
30	ESO	Extended State Observer
31	MIMO	Multi Input Multi Output
32	SG	Steam Generator
33	CS	Compressed Sensing
34	DC	Direct Current
35	SMC	Sliding Mode Control
36	DMD	Dynamic Mode Decomposition
37	MPC	Model Predictive Controller
38	NTSTD	Neutral Type System With Time Delay

39	ANFIS	Adaptive Neuro-Fuzzy Inference System
40	ISMC	Integral Sliding Mode Control
41	LCAMC	Lines Cluster Approaching Mode Control
42	NLSEF	Non Linear State Error Feedback Control Law
43	DC	Direct Current
44	RPM	Revolutions per minute

CHAPTER 1

INTRODUCTION

1.1 Electric motors

In our day-to-day life, electric motors became an essential part. The device which converts electrical energy into mechanical energy is named an electric motor. The process of conversion is normally achieved over the formation of a magnetic field according to current flowing into many coils. In alternating current (AC), the electric charges flow changes its direction periodically. AC is the most commonly used and most preferred electric power for household equipment, office, and buildings, etc. It was first tested, based on the principles of Michael Faraday in 1832 using a Dynamo Electric Generator. Alternating current can be identified in waveform called a sine wave and Direct current (DC) the flow of direct current does not change periodically. The current electricity flows in a single direction in a steady voltage. The major use of DC is to supply power to electrical devices and also to charge batteries. The domain of the drive systems has consistently prevailed by DC machines. Most of the basic utilizations have been on fans and pumps where discharge control accomplished by speed restraint has afforded a reduction in the entire system energy loss over the need of conventional flow control valves, dampers, or inlet guide vanes. In most of the situations, the efficiency and attainment of the overall mechanism were enlarged as well [1]. Currently, DC machines are used by various industrial drives. Even though the machine is overpriced, the converter apparatus and control fundamentals needed are somewhat quiet in DC drives. The motor classifications are detailed in Figure 1.1, the electric motor deals with an arrangement of steel laminations and copper coils [2]. As disputed to DC machines, AC machines will reveal multi variable structures, nonlinear and highly coupled with many elementary decoupled control frameworks. Proportionate restrain performance of AC drives commonly needs more convoluted control algorithms achieved by quick real-time signal processing. Also, in some of the modern advancements in microcomputers, microelectronics and power electronics have makes it feasible for embedding experienced control functions at a sustainable price.

1.2 Classification of motors

Electronically commutated motors (ECM) are also be named as Brushless direct current motors (BLDC) or else as synchronous motors [3]. The synchronous motors are energized by direct current electricity through a switching power supply or an inverter, this generates an AC electric current to run the motor in a single phase through a closed-loop controller [4].

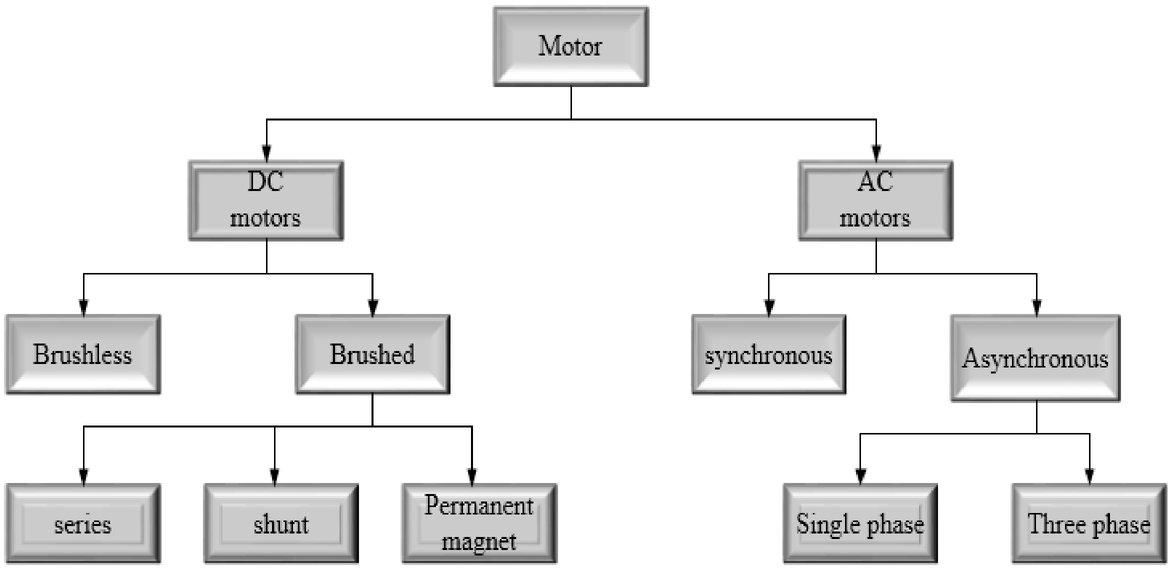

Figure 1.1: Types of motors

The speed and torque of the motor are governed by the controller which affords pulse current to the motor windings. The structure of a brushless motor system is generally similar to the permanent magnet synchronous motor (PMSM).

1.3 Differentiation of AC and DC motor

Normally both the AC and DC motors perform the same function of converting electrical energy into mechanical energy, they are mechanized, designed, and controlled differently. The power source is considered the most basic variation. AC motors will get power with alternating current (AC) whereas DC motors will get power with direct current (DC), likewise an AC-to-DC power converter or DC power supplies, batteries. The field motors wounded by DC are designed along with commutator and brushes that encapsulate the conservation, speed limitations and the life assurance of the brushed DC motors are frequently diminished. AC induction motors will not consider brushes as these motors are extremely craggy and experience durability. The concluding fundamental dissimilarity is controlling speed as the speed control of a DC motor is restrained by differing the armature winding's current whereas the speed control of an AC motor is restrained by changing the frequency, which is frequently performed by adjustable frequency drive control.

1.4 Brushless DC motor

Normally, a brushless DC motor is extensively drawn for an audible appliance like a tape recorder, the brushless DC motor gently rotates in converse with a DC motor which having brushes. Anyhow, mostly brushless DC motors are almost huge in the direction along the rotary shaft [5]. The direction of the magnetic field is perpendicular to the rotary shaft in the brushless DC motor. It is challenging to construct a flat brushless DC motor of such type, after all the height of the empowered conductor to produce rotational force is diminished [6].

When compared to other motors BLDC motors have more benefits than brushed DC motors and induction motors, like a superior speed vs torque characteristic, lengthy operating life, low noise operation, higher speed levels, great dynamic response [7]. In a classic motion sequence, the motor will move in move out various times at saturation region. Some of the other concerns such as mechanical inertia, payload deviations, gravity force, erosion, and Coriolis force defects (in the state of multilink operators) which may also be disclosed in the electromechanical dynamics, and therefore, it is essential that a dynamic compensator need to be constructed to handle this unpredictability. Because of evolution in materials and design, the price of the Brushless DC Motor has abstained since its appearance. Some of the applications used by the BLDC Motor are industrial engineering, transportation heating, and ventilation, end-user electronics, model engineering [8].

1.5 H∞ controller

To harmonize controllers in the control theory technique, stabilization can be accomplished with assured functioning using the H∞ (H-infinity) technique. A control designer explicit the controlling issues by considering them as a mathematical optimization issue after that identifies the controller which clears up its optimization. The H∞ controller method has the convenience through the traditional control methods as they can be eagerly relevant for the defects that concerning diversified systems with cross-coupling among the channels. Also, like that H∞ method demerits will comprise the range of mathematical compassionate required for affixing them profitably along with the use to logically exact system framework can be restrained. Then the essential factor came to know is the emerging controller, which is excellent in terms of arbitrary cost function and it cannot naturally define the excellent controller based on the familiar achievement measures drawn to assess controllers including energy dispensed, setting time, etc. [9]. Consequently, H-Infinity controllers can induce demand for large control efforts because of a high order. Further, the model can also be based on a particular system with the need for certain analysis. In coherent to the design conditions like design concern, maximum frequency depletion, the bandwidth requirement of the closed-loop plant, the H-Infinity controllers afford closed-loop feedback. Different methods are presented in the literature to model H-infinity controller and H-infinity loop shaping. The H-infinity loop shaping is considered as broadly approved amid them because the performance specifications will be submerged at the modeling phase by resembling performance weights [10]. The number of theoretical advantages makes of H-infinity method in control theory an attractive one. Some of the benefits are the elimination of disturbances to a high level, increased stability, and so on. As related to the given inputs to the blended weight H-infinity controllers such as bandwidth requirement, higher frequency disturbance lessening provides a closed-loop reaction of the system. Practically, H-infinity controllers may prompt vast control effort necessity. Moreover, the outline may also rely on the particular system and can require its specific analysis. At the point when H-infinity optimal control approach is connected to a plant, additional recurrence ward weights are consolidated in the plant and are chosen to show specific stability and performance determinations applicable to the outlined objective characterized in starting.

The control theory is profoundly related to the H-infinity monitoring system in each application. The control process is utilized for receiving the adjustment of controllers with upgraded working. The clarification behind the expanded consideration in this methodology is a result of the availability of the procedure in multi-variate systems. The vulnerability in demonstrating a plant is an overweighing issue in the field of robust control theory [11]. While presenting the H-infinity control, it is important to discuss Kalman channels. In the prior days, the Kalman channels were utilized for tackling flying machine-related issues from which it is formed to take care of technical related matters. In any case, specialists discovered trouble in the use of Kalman channels as a result of the mathematical way of the noise display in industrial applications. Therefore, there is a need to build up an alternative control strategy, which answers for displaying mistakes and statistical noise [12]. The variety from the Kalman channel to the H-infinity channel doesn't expect terms for noise and diminishes the estimation mistake. Therefore, it is called the minimax channel.

The number of theoretical advantages makes of H-infinity method in control theory an attractive one. Some of the benefits are the elimination of disturbances to a high level, increased stability, and so on. As related to the given inputs to the blended weight H-infinity controllers such as bandwidth requirement, higher frequency disturbance lessening provides a closed-loop reaction of the system. Practically, H-infinity controllers may prompt vast control effort necessity. Moreover, the outline may also rely on the particular system and can require its specific analysis. At the point when H-infinity optimal control approach is connected to a plant, additional recurrence ward weights are consolidated in the plant and are chosen to show specific stability and performance determinations applicable to the outlined objective characterized in starting.

H-infinity control technique had a huge effect on the advancement of control systems. These days the method had turned out to be completely developed. Also, it connects with mechanical issues. The H-infinity strategies are utilized as apart of the control hypothesis to synthesize controllers accomplishing strong execution or adjustment. The H-infinity ideal control hypothesis is an elective technique to plan a controller to ensure the implementation with the most pessimistic scenario worst disturbance. The controller incorporates the voltage control as the outer circle and the present control as the inner circle.

Models are showing a flow of systems that typically contains some inaccuracies when compared with the real system. For the most part, brought about by improvements in the model,dismissing of a few elements is affecting the flow or general displaying mistake. However, this may be an issue when outlining a control of the system – the exact model required for the appropriate plan of a controller. The whole objective is to describe a monitor equipped for balancing out even 'the direct outcome imaginable' speaking to the most corrupted model. Such a controller is then capable of controlling the practical system. Therefore, the works in the control-based mechanism go for the H-infinity controller.

1.6 Limitation of H ∞ controller design

The H∞ controller techniques combine a huge level of mathematical considerate. The mathematical formulations of H∞ controller required to apply them correctly. The sensibly excellent model of the system needs to be restrained. The problem constitution is essential since any harmonized controller will be excellent in the developed sense.

1.7 Types of controllers

The controller is regarded as a comparative device that collects an input signal from a measured task variable, then the measured value is matched with the setpoint or pre-determined control point value and the suitable quantity of output signal needed by the terminal control factor is examined for establishing corrective action in the control loop [13]. The digital algorithms and electrical signals are utilized an electronic controller to carry out corrective, comparative, and receptive functions.

There are different types of controllers like PID, ANFIS, I&C, ARDC, SMC, etc. Every controller has its special specifications and feasible applications. Among them, fuzzy logic PI and PID controllers are already drawn for Brushless DC motors [14]. In a Magnetic Levitation (Maglev) system, SMC and FOSMC are used to regulate the position of a ferromagnetic ball against gravity [15]. DED control approach is developed using a PI frequency controller and a neural network frequency controller. [16]. Like that ARDC controllers are also already drawn for CSTR operation. Due to the simplicity of functions and robustness, Proportional Integral Derivative (PID) controllers, which is an industrial control process applied primarily in various operating conditions [17]. The derivative time constant, integral time constant, and proportional gain are the significant parameters that are used for designing the controllers.

Many reasons are considered for designing new techniques of PI controllers. Among that one of the important purposes is that the controller is broadly spread. Then, due to the enhanced designing approaches the controllers can be applied in tuning and auto-tuning devices as it is very useful [18]. As a standby, the Active disturbance rejection control (ADRC) has come to proceed and that integrates quiet applications confessed from the traditional PID-type controller approach together with modern model-based methods. The designing unpredictability and effective disturbances of the ADRC can be noted from that a coarse process method is significant for modeling a controlled loop therefore, the ADRC can be more captivating [19].

1.8 Applications of controllers

The controllers are the active parts of the device. It can be used in most electrical and electronic appliances. Like that controllers can be drawn for small-scale and large-scale purposes. The type of controller will be varying according to the purposes [20]. The controllers have various utilizations in control of aircraft, air traffic control, automotive industry, mechanical system, switching power converters, and also in several fields [21]. There is a sudden change in the formation and parameter of the dynamic system, which can be induced by equipment failures or faults, deviations in the environmental disorder, or subsystems interconnections.

CHAPTER 2

LITERATURE SURVEY

The H-infinity controller is discussed from the basic application to the electrical and instrumentation application. The usage of this controller is discussed below in every application from the fundamental. Initially, it is used for the control in aerospace systems and mechanical systems as the controller technique. The part before the need for an H-infinity controller presented with the systems having delay control based on H-infinity systems in operation, which could be eliminated by the H-infinity controller.

2.1 Background

The principal issue in the engineering control system outline perpetually incorporates the online criticism control of an indeterminate, typically nonlinear, physical process. The creator forthe most part likes to work with and benefits by a methodical way to deal with the planned issue; such precise methodologies are frequently the consequence of past outline understanding. Unmistakably, an all-inclusive engineering design approach must consider:

- Sensor and Actuator constraints
- The required parameters
- Errors in measurement
- Errors in Actuator
- Sensitivity in design
- Unpredictable disturbance effects
- The computational requirement in online versus off-line
- Simpler design

Athans [22] represented how the accessible fundamental of ideal control and estimation for the charged straight quadratic-Gaussian issue gives such a bound together arrangement system. Itis extraordinary that the arrangement method gives favored control over the direct quadratic Gaussian. The H-infinity control plan can deal with the two issues:

1. For all interrupted inputs the maximum error intensity is reduced with limited intensity.
2. The stability of shunt loop in addition to systems uncertainty with limited H-infinity regulations.

2.2 Position analysis of brushless DC motor

The commutation control technique planned at decreasing commutation torque ripple in the sensor less brushless direct current motor was discussed by J.Kim ***et al*** [23]. As a result of low construction cost and relatively high capability, these types of motors are drawn for low price applications. On another way, they display great torque ripple characteristics created by non-ideal commutation current. This factor will restraint their utilization area, usually for low voltage purposes. To reduce torque ripple for the whole speed space, confer to three commutation control techniques an extensive study of commutation torque ripple was done. Then an excellent vector orbit for low torque ripple was designed and finally, the performance of the planned method was checked through simulation and experimental results.

In the digital innovation of speed controlling section, the brushless DC motor along with the approach for calculating the rotating speed of the motor was dependent on the signals rotor position sensor was discussed by M. Baszynski and S. Pirog [24]. The proposed technique concedes an increment in the frequency measurement (twelve measurements per four-pole motor and six measurements per rotation for a two-pole motor), and then the analyzed outputs were not concerned by the disarrangement ascend of the sensor also given details about the theoretical formation of a series PI controller.

The construction and digital employment of a fuzzy controller for attaining enhanced achievement of brushless direct current servomotor drive were discussed by N.Yadaiah ***et al***. By various operating schemes like parameter deviations, load disruptions, and difference in reference speed. The performance of fuzzy and PID controller occupying BLDC servomotor drive was inspected [25]. These BLDC motors are widely used in space vehicles, electric vehicles, robotics, aerospace, machinery system, and industrial control appliance. Some of the types of applications on conventional controllers such as PI, P, and PID are drawn with the BLDC servomotor drive restraint system to attain suitable transient and steady-state feedback, and finally, design and employment of fuzzy controller are conferred and its attainment was correlated with PID controller to display its efficiency to trace fault and versatility of fuzzy controller in control applications.

J.M.Patel et al. [26] proposed an approach for controlling the Pulse Width Modulation. The simulation of Brushless DC Motor was performed by Sinusoidal Pulse Width Modulation (SPWM). The rotor position was sensed by the Hall Sensors, and then six sensed signals were obtained based on the hall signal. An error signal could be determined by comparing the actual and reference speed. Further, the Triangle Wave Generator was utilized to compare the attained error signal. Ultimately, the absolute error signal was achieved. The result would be six pulses if the preceding six signals were added with the error signal and the obtained six gate pulse was specified into the Inverter Circuit.

2.3 Need of H∞ controller

The direct employment of the H∞ technique for the power control of a sensor less brushless DC motor was discussed by K.Vinida and M.Chacko [27]. This affords an excellent dynamic performance when correlated to the conventional PI controller and the comparison of the determined outputs was also described. Particle Swarm Optimization (PSO) method was selected to establish good weight choice of H∞ controller and the PSO algorithm deals in slight awareness function in minimum frequency level and quiet integral sensitivity system in maximum frequency level. The agreement needed for disturbance elimination, excellent reference tracing, and being unresponsive to create noise and error. The shortened torque ripple together with an upgraded steady-state error by 25% and rise time by 0.6% commonly provides excellent robust attainment, minimum vibration, and less noise.

The process was concerned with the fixed horizon H∞ defect estimation issue for a set of nonlinear imaginary time-varying functions with both inconstantly appearing faults and fading channels were discussed by H.Gao ***et al*** [28]. The system function was dependent on nonlinearities such as Lipschitz and the error appear in an irregular path directed by a group of dispersed white sequences like Bernoulli. The altered speculative rice fading model describes the system measurements that transfer by the fading channels. The reason for the consigned issue was to compose a time-varying defect estimator like that, in the existence of channel fading and irregular fault appearing, at the given range assessed by an H∞ norm in mean square sensibility. By using the speculative analysis approach, tolerable conditions are created to assure the dynamic system under examination, which fulfills the specified attainment compulsion on the error detection, and next to a repeated linear matrix difference access was engaged to design the desired error evaluation gains and finally, simulation results determine the efficiency of the occurred fault evaluation design scheme.

The defect of the observer positioned integral sliding mode controller was discussed by Z.Liu ***et al*** for functioning undetermined Neutral Type System with Time Delay (NTSTD). Depending on the sliding mode observer, an ISMC approach is kept ahead [29]. An acceptable technique of powerful asymptotic strength was proposed for sliding mode dynamics and a fault system with interruption depletion level was expressed by LMI. After that, an SMC law has created and hence the achievements of the sliding surface described in the state approximate field have been assured. At last, a simulation pattern is conferred to establish the utility of the attained result.

The H∞ controller was commonly preferable for inverters, which provides continuous power supply and yields better output that satisfies with the IEC 62040-3 Standard were discussed by S.P. Ribas ***et al*** [30]. In a system, an expanded state apace scheme was provided, and then considering it a better avoidance of load disturbances and asymptotic tracking of the reference were guaranteed by resonant controllers and digitally executing the control signal. It was displayed in a state in which better results were not obtained by the H∞ optimal state feedback controller due to maximum control gains. Further, to clear up this issue, an H∞ suboptimal controller was introduced. A control gain was obtained by suboptimal controlled which tends to proper output, satisfying with the restrictions from the IEC 62040-3 Standard. The performance was compared with the state feedback controller, and it establishing improved performance even in the simple model. As a result, output impedance over a particular frequency was obtained by the H∞ norm of the closed-loop system. Moreover, a better admittance value is also determined for a linear load by applying a small gain theorem along with stability while establishing a constant power supply.

2.4 Appliance of continuous stirred tank reactor

The classic illustration of a chemical industrialized appliance was a continuous stirred tank reactor (CSTR). Whose dynamics perform a considerable section of the second-order nonlinear system were investigated by Q.Zhu ***et al*** [31]. It also verified that modeling an excellent control scheme for the CSTR was very complex. External disruption attenuation and state estimation are the two troublesome problems in CSTR control. Primarily industrial progress restraint quick and robust feedback was necessary. Directed by this desired attainment and challenging defects the gained performance terminal sliding mode control (TSMC) structure which was introduced for CSTR, and would evaluate the system state and maintain the system gained tracing fault to zero. The correlative durability analysis was conferred in terms of the Lyapunov technique. Comparative examples are determined by using MATLAB simulations to approve the capability of the proposed approach.

In the wastewater treatment process, to decrease the organic element and microbe present in sludge by anaerobic digestion, a continuous stirred tank reactor (CSTR) is generally used. B.Zamora ***et al.*** describe an analytical of the fluid dynamic attitude of a CSTR to enhance the vigorously [32]. The effect of construction arrangement and power of the incorporate system on the adequate amount of the CSTR is evaluated. The analytical model is clarified under an unsteady state by considering the progression of the stream during the start and stop conditions of the mixing system. The periodic rule of the mixing system keeps the adequate volume among 94% and 99% was attained. The results obtained would direct to the possible energy optimization of the mixing system of CSTR.

The category of dynamic nature feasible for an individual first-order reaction which transmits in a stirred tank reactor are restricted according to the values of the parameter and marks in parameter area drawn to determine the different capabilities were discussed by A.Uppal [33]. The analytical principle is introduced to conclude the presence and performance aspect of restraint cycles as an objective of the system parameters. The classification of dynamic nature concluded is illustrated by analytical estimation of the temperature and concern direction. Various kinds of modern phenomena for this issue are noticed and explained in terms of the parameter plot area. The theory and inquiry techniques would calmly discover further types of the reaction system.

In the age of growing industrialization, the need for modern policy to improve outcome and the implementation of Adaptive Model Predictive Controller has been modeled to manage temperature flow of CSTR (continuous stirred tank reactor) and the results were compared with Model Predictive Controller (MPC) were discussed by U.V. Ratnakumari and M.B. Triven. For chemical industries and processing, the Continuous Stirred Tank Reactor (CSTR) plays a major role. CSTR was an energetic strong nonlinear plant that considers several variables namely concentrations and temperature, that are forced as a controlled at the industrial process [34]. The model predictive control was considered as a reference by the adaptive MPC model and the predictive control was designed by adaptation mechanism. For a nonlinear dynamic system, the adaptive MPC has attained constraint handling, performance, secured scheduling of gain, and optimization than existing approaches like model predictive, fuzzy, and PID.

2.5 Applications of IPSO and WWO algorithm

One of the significant research fields is known as fuzzy clustering, and that can be applied to solve many real-world issues. Several fuzzy clustering methods are there, from that fuzzy c-means (FCM) are more popular due to their efficiency and simplicity. However, FCM has some weaknesses, specifically its ability to slip into local minima. Taking this weakness into consideration, various optimization-based fuzzy clustering techniques were introduced by R.M. Souza ***et al***. Among these techniques, and few approaches are based on a metaheuristic optimization, including (PSO), a hybrid model that integrates a metaheuristic clustering approach like FCM [35]. The hybrid PSO and FCM methods have enhanced accuracy than traditional partitional clustering methods. However, the PSO-based clustering approach has poor execution time than the partitional clustering method and the present PSO algorithms need tuning the range of the parameter before determining the proper solution. These shortcomings are solved by hybrid approaches for fuzzy. The technique which is called FCM–IDPSO and FCM2–IDPSO, integrates FCM with a recent technique of PSO and IDPSO, which dynamically varies the parameters of PSO parameters during execution. The main goal is to establish a proper balance between exploration and exploitation, eliminates slipping into local minima speedy and so better solution could be attained. Finally, in comparison with other approaches, the hybrid approach has achieved better. Directional Overcurrent Relay (DOCR) coordination computation allowing for desired and high-level accuracy in interrelated power systems is very challenging and is a highly constraint-oriented optimization problem [36]. Analysis of the effectiveness of a newly described optimization technique, Teaching Learning Based Optimization (TLBO), in protective relay coordination compared with an extensively used optimization technique, Particle Swarm Optimization (PSO). The Battery energy storage system is optimally sized using particle swarm optimization according to the level of smoothing power requirement [37].

Modern Multiple-Input Multiple-Output (MIMO) communication techniques place massive demands on embedded processing resources in terms of throughput, latency, and resource utilization. State-of-the-art MIMO detector algorithms, such as Fixed-Complexity Sphere

Decoding (FSD), rely on efficient channel preprocessing involving numerous calculations of the pseudo-inverse of the channel matrix by QR Decomposition (QRD) and ordering [38].

Water wave optimization (WWO) is a novel metaheuristic approach that imitates shallow water wave theory was discussed by Y. Zhou ***et al***. which has a simple structure, easy realization, and good performance even with a small population. To enhance the convergence speed and calculation precision even further, the process of elite opposition-based strategy water wave optimization (EOBWWO) was developed, and it has been applied for function optimization and structural engineering design problems [39]. There are three major optimization strategies in the improvement: elite opposition-based (EOB) learning strategy improves population diversity, local neighborhood search strategy is introduced to enhance local search in breaking operation, and improved propagation operator established the improved algorithm with a better steadiness between exploitation and exploration. EOBWWO algorithm was verified by using 20 benchmark functions and two structure engineering design problems and the performance of EOBWWO was compared against those of the state-of-the-art methods. The estimated results showed that the WWO approach has faster convergence speed, higher calculation precision, with the exact solution being even obtained on some benchmark functions and a higher degree of stability than other comparative algorithms.

2.6 Research gap

- Design novel-fixed order H-infinity controller
- The position of the rotor can be analyzed.
- Torque ripple minimization is applied, when the rotor speed is at 3000 the torque will be 0.65
- Reduction of error in CSTR, such as variation in Temperature and product concentration.

2.7 Aim of the research

- BLDC motor is designed by using the fixed order H∞ controller.
- Weight function and Transfer function are used to design the controller.
- Proposed Controller reduced the torque of BLDC motor and also enhance the speed.
- By using the IPSO algorithm, the optimal position of the rotor can be obtained and improved the performance of BLDC motor.
- Designing a CSTR w.r.t temperature and product concentration.

- Eliminate the disturbances in CSTR by using the H∞ controller-based WWO algorithm.
- Planned work compared with exiting controllers.
- The entire work based on MATLAB programming.

2.8 Objectives

The following objective have been fulfilled in the research

- **Objective 1:** To develop the continuous fixed order H-infinity control.
- **Objective 2:** To apply the developed H-infinity control for performance improvement of DC motor.
- **Objective 3:** To consider disturbance as constraint for formulating optimization in developing H-infinity control.
- **Objective 4:** To apply the H-infinity control for robust performance of a dynamic system.

2.9 Organization of the research

- The introduction part of BLDC motor, CSTR, H∞ controller, and the algorithms like IPSO and WWO are explained in **chapter 1**.
- The recent works related to our proposed methodology are discussed in **chapter 2**. Objectives, research gap, aim of the research and organization of the research have also been highlighted in the chapter.
- **Chapter 3** deals with the position analysis of BLDC motor using fixed order H∞ controller based on improved particle swarm optimization algorithm (IPSO) and the existing methods like fuzzy PID controller, fuzzy PD controller, and sensing algorithm are explained in detail.
- **Chapter 4** deals with the H∞ controller-based disturbance rejection in CSTR using water wave optimization (WWO) and the existing methods like the ANN algorithm and ADRC are explained in detail.
- The results of weight function and transfer function of the H∞ controller, speed of the rotor, and position of the rotor and back EMF of the BLDC motor are explained in **chapter 5**.

- The results of CSTR with and without disturbance, error reduction by using the WWO algorithm, and comparison results with existing and proposed methods are given in **chapter 6.**
- The overall conclusion and future scope part is detailed in **chapter 7**.

CHAPTER 3

POSITION ANALYSIS OF BRUSHLESS DIRECT CURRENT MOTOR USING FIXED ORDER H- INFINITY CONTROLLER BASED ON IMPROVED PARTICLE SWARM OPTIMIZATION ALGORITHM

3.1 Introduction

The Brushless DC motor requires the electronic speed controllers to operate the motor, which is preferable to the Brushed DC motor because of its efficiency and excellent operating speed. In the past, the PI controllers were drawn due to their simple structure. But it has load disturbance, control complexity, and some parametric deviations. The above facts can be avoided by the proposed controller. The Brushless DC motor is designed with the novelty of fixed order H-infinity controller. The convenient weight functions and transfer functions are used for designing the controller. The controller is applied to the Brushless DC motor to attain the position. This paper uses an improved particle swarm optimization algorithm to obtain the excellent position of the rotor. The new controller can reduce the torque as much as possible so that the speed is high. The brushless direct current motor is designed in a MATLAB environment. The performance of the torque, speed, and back EMF voltage is verified and compared with the existing controllers such as fuzzy proportional integral derivative, sensing algorithm, and fuzzy proportional derivative controller.

3.2 Brushless DC motor

The brushless DC motor (BLDC) is a permanent magnet synchronous electric motor that consumes direct current (DC) electric and it also achieves an electronic restraint commutation system. The technique of generating rotational torque in the motor by altering phase current over at a convenient time is named a commutation system. On the contrary, to a mechanical commutation system, trapezoidal permanent magnet motors are also obtained as brushless DC motors. BLDC motor are designed specifically to be operated in a mode where they are frequently stopped with the rotor in a defined angular position. Depends motor power and RPM.

The standard brushed kind DC motor is not like in which the brushes connect with the commutator on the rotor to create an electric way among the DC electric origin and rotor armature windings. The specifications of the BLDC motor are initiated in Table 3.1. The BLDC motor utilizes electrical commutation with the permanent stator and magnet rotor with a series of coils. The permanent magnet spins and the current passing conductors are set in this motor.

Table 3.1: Specifications of BLDC motor

Parameters	Specifications
Maximum power	952KW
Rotor inertia	0.1340Kgm^2
Torque constant	0.088Nm/A
Phase inductance	2.3mH
Phase resistance	1.95Ω
Voltage constant	0.088V.s/rad
Speed range	3000 rpm
Rated current (Max.)	100 amp
Motor feedback	Hall effect sensor

The transistors or silicon restrained rectifiers convert the armature coils at the exact rotor location as it were the armature field is in space quadrature with the rotor field poles. Therefore, the power operating on the rotor makes it revolve. Usually, the hall sensors or the rotary encoders are highly utilized to identify the spot of the rotor and are located on all sides of the stator. The diagram of the BLDC motor is shown in Figure 3.1. The response of the spot of the rotor from the sensor supports to decide at what time to button the armature current. Selection a suitable motor rating for the application depend upon peak torque required for the application, RMS torque required and operating speed.

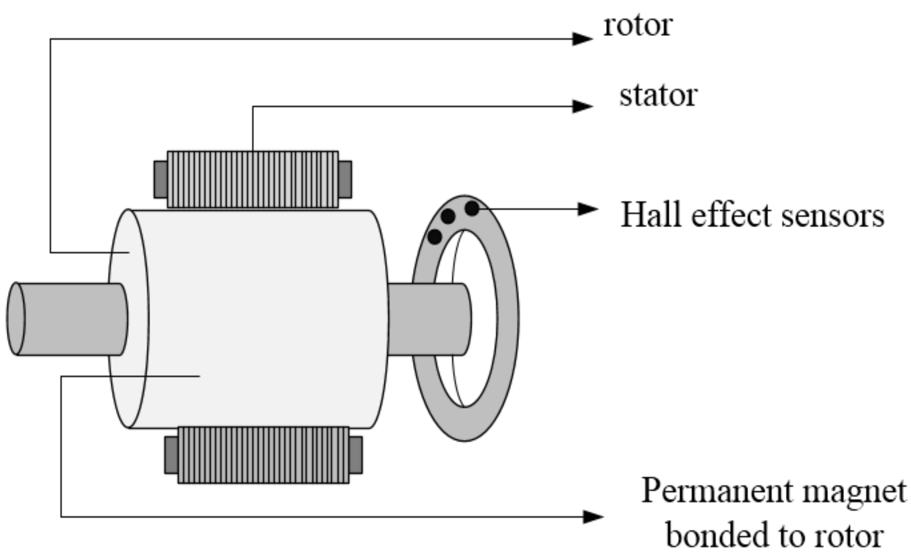

Figure 3.1: Diagram of the BLDC motor

This electrical commutation organization removes the commutator planning and brushes in a DC motor and therefore the more dependable and the fewer loud process is attained. The BLDC motors can ride at high speeds because of the lack of brushes. The proficiency of the BLDC motors is usually 85 to 90 ratios, while the brushed type DC motors are 75 to 80 ratios effectual. Extensive types of BLDC motors are accessible varying from slight power level to constituent intensity, and great power levels.

Usually, the brushless DC motor will not use the brushes. In the brushed motor, the brushes transport current by the commutator through the coils on the rotor and now the question here is how the brushless motor transfer the current into the rotor coils. This process will not happen because the coils are not placed on the rotor. Rather, the coils will not rotate because the rotor is a permanent magnet, but they are nailed exactly in the particular area on the stator. There is no essential for brushes and commutator. Because the coils do not move.

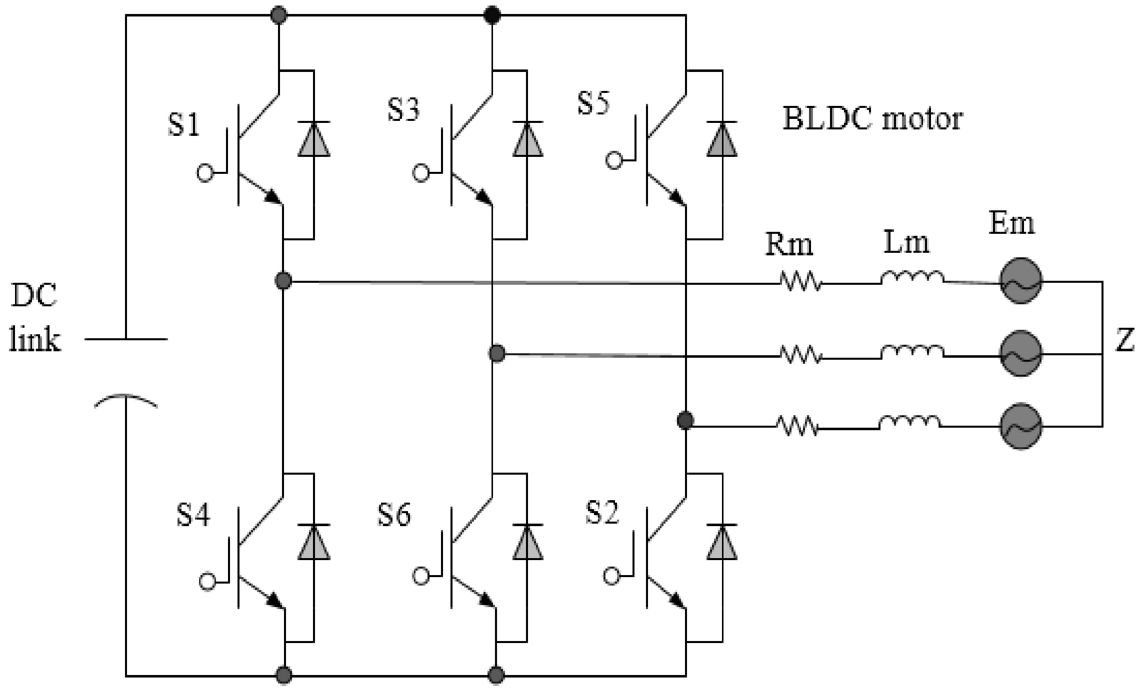

Figure 3.2: Equivalent circuit of BLDC motor

The brushes of a traditional motor transfer power to the rotor windings and once it is strengthened it becomes a stable magnetic field. The equivalent circuit for the BLDC motor is depicted in Figure 3.2, the friction between the fixed brushes and a revolving metal connect with the rotating rotor makes wear. Moreover, because of the weak brush to metal contact and arcing, power can be wasted. For the reason that the BLDC motor distributes with the brushes rather than utilizing an "electronic commutator," the dependability and the effectiveness of the motor are developed by removing this source of wear and power damage.

One of the most concentrated areas on various motor manufactures, brushless DC motor has become progressively the favored choice in most of the appliances, peculiarly in the area of motor control mechanism [40]. When compared to brushed DC motor, brushless DC motor is more preferable in many approaches, like that in capability to operate in high speed, high efficiency, and excellent heat distraction.

3.3 Construction of BLDC motor

Brushless DC motors can be manufactured in various physical compositions. Based on the stator windings, the motors can be designed as single-phase, two-phase, or three-phase motors. Most commonly three-phase brushless DC motors along permanent magnet rotors are drawn. When related to three-phase induction motor together with conventional DC motor have many similarities in the process of motor designing. Similar to all other motors this motor also had stator and rotor sections.

3.3.1 Stator

Normally, to bear the windings stator part of the brushless DC motor is built by stacked steel laminations. These windings are located in slots that are significantly cleft on the interior boundary of the stator. The diagrammatic representation of the stator is shown in Figure 3.3, these windings can be positioned either in star or delta connection. However, three-phase star-connected stators are available in most brushless DC motors. Every single winding is composed of various interconnected coils, although one or more coils are located in every single slot. To design an equal number of poles, all of these windings are dispersed over the stator boundary.

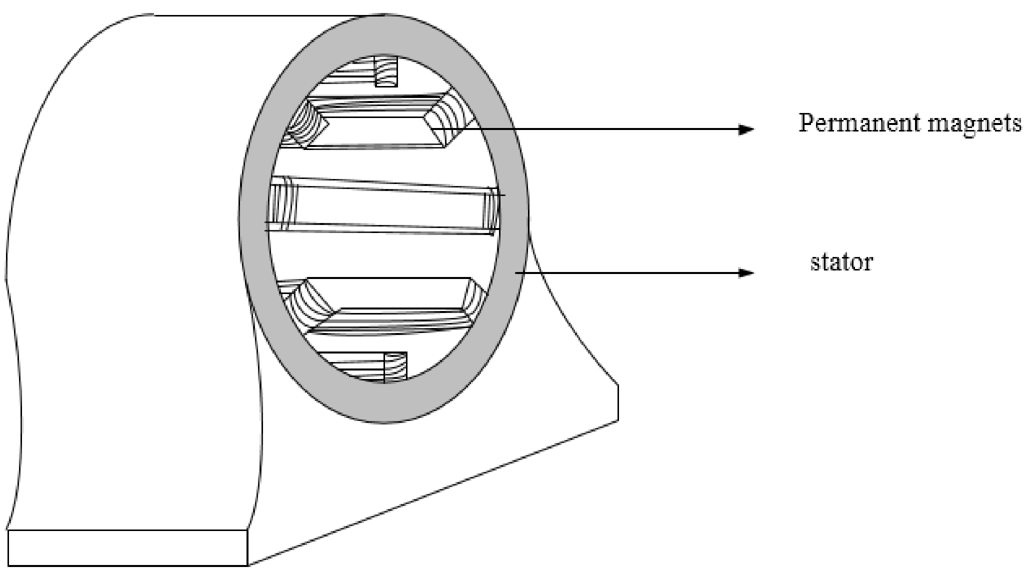

Figure 3.3: Stator diagram of BLDC motor

The stator in the BLDC motor may be an electromagnet or else a permanent magnet. If the stator is an electromagnet, the coil which empowers is called field winding or field coil. To decrease the loading debt in the motor, developers constantly use copper as operating materials in windings. Aluminum material is not used because of its low-level electrical conductivity, may be replacement of other material in fractional horsepower motors, especially, when the motors are drawn for a very small-time duration.

An AC alternator can generate power beyond numerous great current powers producing coils linked in parallel, rejecting the use of the commutator. Locating the field coils on the rotor permits for an economical slip ring mechanism to alternate high voltage, low-level current power to the revolving field coil. Before choosing the stator exact rating of the voltage has been check depending on the power supply ability. For robotics, automation, and small mobilizing applications, 48V or low voltage brushless DC motors are approved. For automation systems and industrialized appliances, 100V or high rating motors are drawn.

3.3.2 Rotor

Brushless DC motors consolidate a permanent magnet in the rotor. The total number of poles in the rotor can differ from 2 to 8 pole combinations with another north and south poles based on the application concern. To attain supreme torque in the motor, the flux density of the objective becomes high. The desired magnetic material for the rotor is required to yield the needed magnetic field density.

Some of the different types of the rotor are given below,

a) *Squirrel cage rotor:*

The squirrel cage rotor will rotate at a speed lower than the stator revolving magnetic field or else synchronous speed. The fundamental inauguration of the rotor current for the motor torque is afforded by the rotor slip. Which is the distribution to the slip. The structure of the squirrel cage rotor is shown in Figure 3.4, when the slip speed reduces the rotor speed will get increase. While raising the slip will lead to increasing the induced motor current, in other term this will raises the rotor current, appearing in a large torque for raising the load requirements.

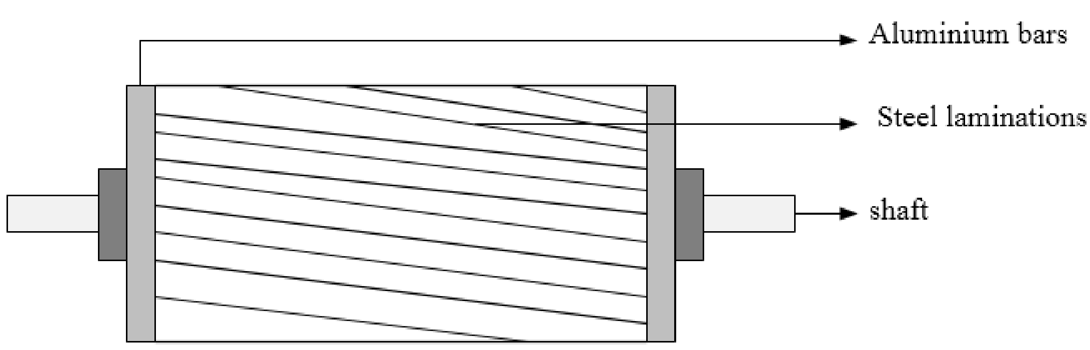

Figure 3.4: Squirrel cage rotor

b) Salient pole rotor:

The salient pole rotor will operate at a speed less than 1500 rpm. This rotor functions at a speed below 1500 rpm (revolutions per minute) and 40% of the classed torque beyond agitation. It has a huge diameter and very small axial length. The diagrammatic representation of the salient pole rotor is shown in Figure 3.5, for the salient pole rotor air gap is the Air gap is unreliable and has very low Rotor has low mechanical stability.

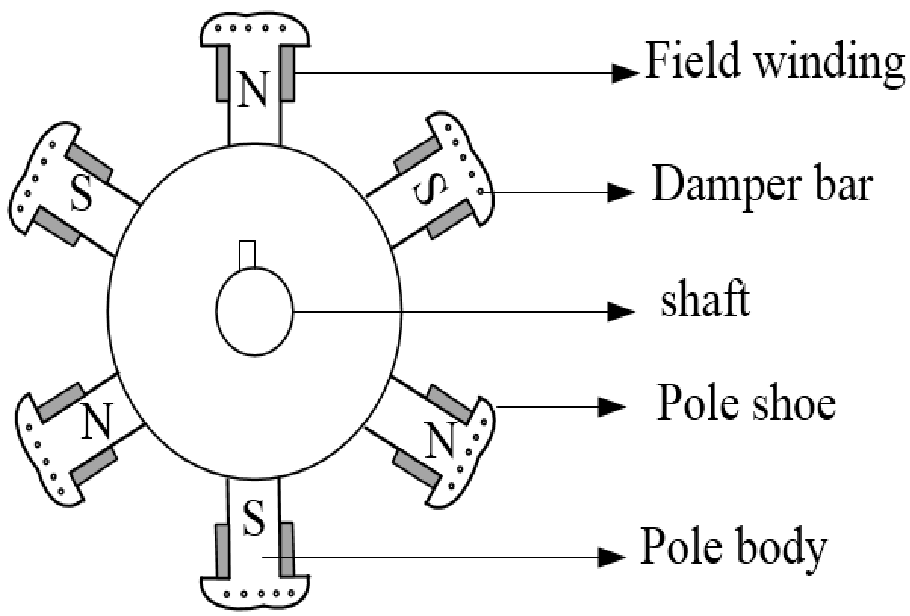

Figure 3.5: Salient pole rotor

c) Wound rotor:

The wound rotor will operate at the regular speed and has a very low starting current. The additional resistance combined with the rotor circuit will access the starting torque. The diagram of the wound rotor is given in Figure 3.6, the capability of the motor to work develops the additional resistance and it decreased when the motor speed increases. The wound rotor is a speed restraint and high torque.

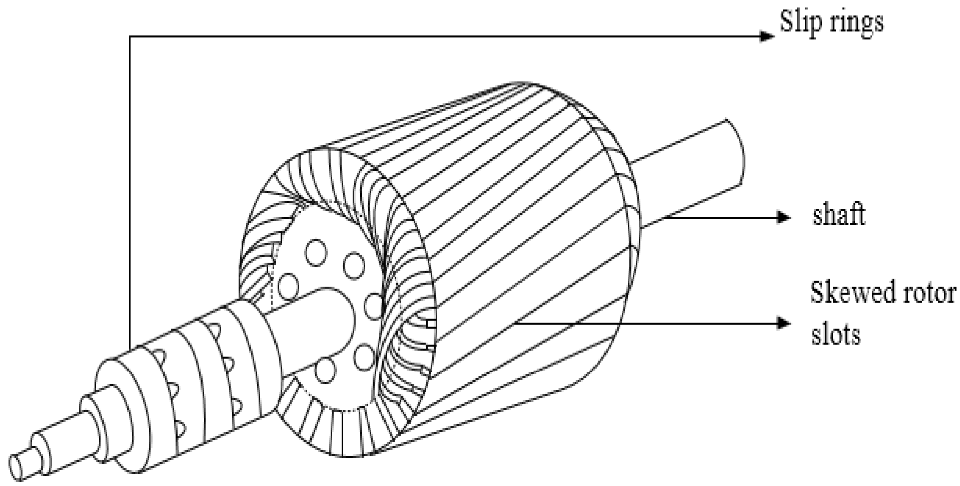

Figure 3.6: Wound rotor

d) Cylindrical rotor:

The speed between 1500-3000 rpm is the operating speed of the cylindrical rotor. In this type of rotor, the width is short and it has robust mechanical stability. Also, it has a broad axial length and needs a great torque when compared to the salient pole rotor.

An alternator rotor is developed by a coil of wire encircled over the iron core. To achieve the exact format, shapes, and size the magnetic equipment of the rotor is manufactured from steel laminations to care signature conducting slots. The magnetic field is conceived over the core when the current navigates through the wire coil, this current is invoked as field current. The ability of the field current restrains the power level of the magnetic field. While comes to the direction of flow of current the Direct Current flows the field current in a separate direction and is dispatched to the wire coil through a group of brushes and slip rings. The cylindrical rotor diagram is shown in Figure 3.7, as like other magnets, the magnetic field developed has a north pole and south pole. The ordinary clockwise direction of the motor that the rotor is emerging can be employed by adopting the magnets and magnetic fields embedded in the modeling of the rotor, granting the motor to operate in the backward or anti-clockwise direction.

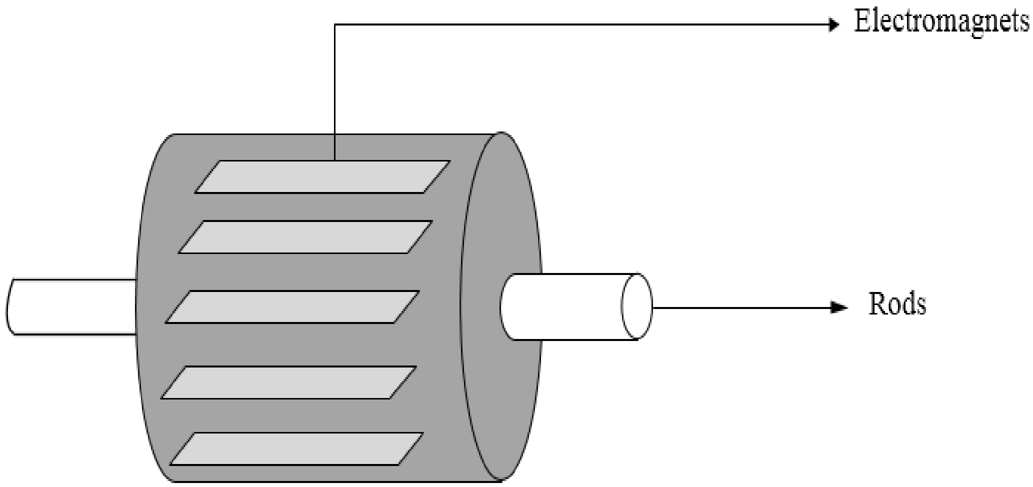

Figure 3.7: Cylindrical rotor

e) Torque in Rotor:

Torque is developed by the force generated through the co-operations of the magnetic field and current is expressed as,

$$F = CxE$$

$$T = HxV$$

F = Force

T = Torque

E = Rotor

Ferrite magnets are economical, anyhow they had low flux density for a disposed of volume. For advanced models unique earth alloy magnets are frequently used. Ferrite and boron (NdFeB), neodymium (Nd), and samarium cobalt (Smco) are some of the rare alloys. The rotor can be designed with disparate core configurations like the permanent magnet with a circular cone on the circumference, rectangular magnets with a circular cone, etc.

3.3.3 Hall sensor

The Hall Effect sensor is a transducer that differs gain voltage in feedback to a magnetic field. To locate, current discern appliance, speed identification, and concurrence switching Hall Effect sensors are drawn. A slim band of metal has a current enforced in the Hall Effect sensor. In the existence of a magnetic field, the electrons in the metal band are swerved against one corner, developing a voltage gradient beyond the small side of the band. The merits of Hall Effect sensor by inductive sensors in that, while inductive sensors behave to a dynamic magnetic field which activates the current in the wire containing the coil and generates the output as voltage.

Hall sensor affords the message to integrate stator armature excitation with rotor position. Since the compensation of the brushless DC motor is restrained electronically, to revolve the motor, the stator windings should be electrified in disposition. Hall Effect sensors can identify stable magnetic fields. Most efficiently, the sensor functions as an analog transducer, precisely revolving around a voltage. Its space from the Hall plate can be resolved by a familiar magnetic field. Before, energizing a singular stator winding confirmation of rotor position is important. Unusually the Hall Effect sensor is installed in the stator which senses the position of the rotor. The structure of the hall sensor is shown in Figure 3.8,

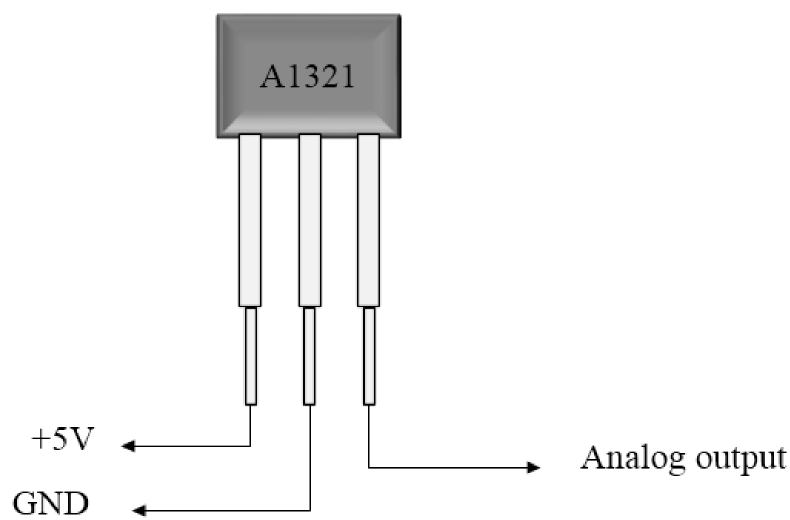

Figure 3.8: Structure of the Hall sensor

Most of the brushless DC motors organize three hall sensors that are installed into the stator. At any time, the rotor poles pass beside the individual sensor it develops low and high signals. The perfect commutation arrangement to the stator winding can be resolved which depends on the sequence feedback of these sensors.

3.4 Working of BLDC motor

The brushless DC motor will work on the principle that is related to a conventional DC motor. Especially the Lorentz force law states that whenever a current-carrying conductor is fixed in a magnetic field its exposures a force. The magnet will practice an equal and opposite force, as a payback of reaction force [41]. The current-carrying conductor is static in the condition when the permanent magnet shifts its position, in the process of brushless DC motor. When the stator coils are electrically switched by a supply source. The drive structure of the BLDC motor is shown in Figure 3.9, it turns into an electromagnet and starts generating the uniform field in the air gap. Though the origin of supply is DC, switching affords to develop an AC voltage waveform with a trapezoidal shape. By cause of the force of cooperation between permanent magnet rotor and electromagnet stator, the rotor sustains to rotate.

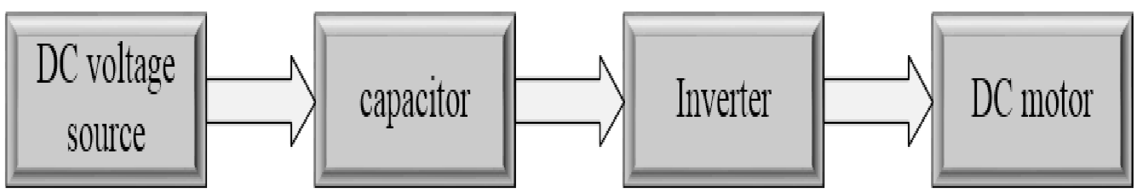

Figure 3.9: Drive structure of BLDC motor

The motor with the switching of windings as low and high signals, identically the winding is empowered as north and south poles. The permanent magnet rotors with north and south poles fix with the stator poles lead the motor to rotate. Examine that the motor generates torque because of the improvement of attraction force and repulsion force. By this approach, the motor rotates in a clockwise direction.

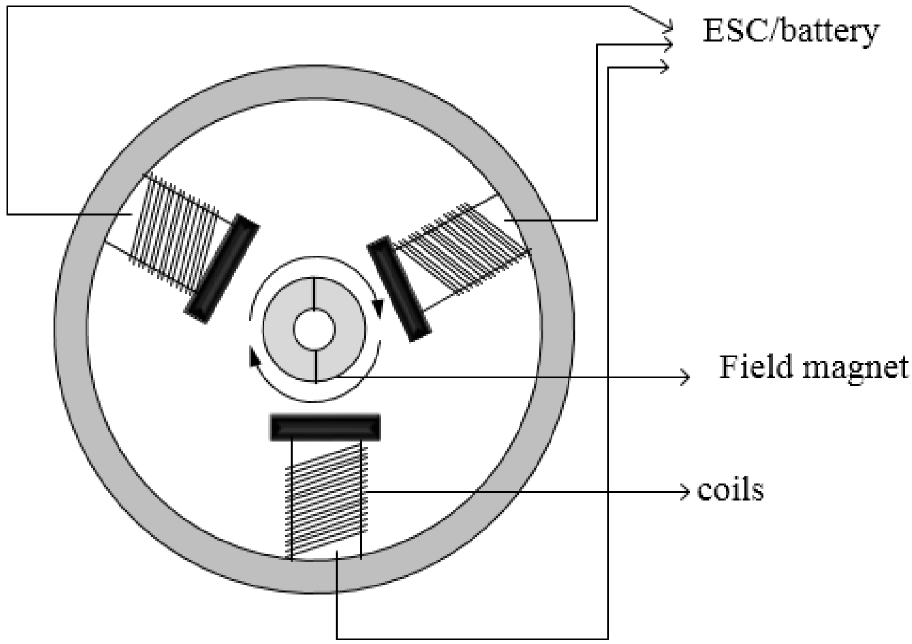

Figure 3.10: Inner surface of BLDC motor

Here, the doubt may arise on that how will we realize which stator coil is getting energized and when. Because of the repeated rotation of the motor based on the switching arrangements over the coils. As explained earlier that the shaft position response to the electronic control unit is given by the Hall sensors. Depend on the signal through the sensor, the controller concludes individual coils to strengthen. The internal structure of the BLDC motor is shown in Figure 3.10, When the rotor poles pass adjacent to it, Hall Effect sensors produce low- and high-level sensors. These signals regulate the location of the shaft.

3.5 Mathematical modeling of brushless DC motor

The brushless DC motor comprises three stator windings and also an unalterable magnet on the rotor and stator [42]. In the Brushless DC motor with trapezoidal back EMF, the number of phases empowered at a given contemporary of time is just only two phases. As like only two switches are operating at a given contemporary of time. A restraint approach with an individual switch PWM while preserving the alternate switch at ON condition for the total switching interruption is planned to operate the BLDC motor beyond the DC link capacitor. As one switch leftovers at ON condition, it affords a way for motor phase current to sustain during the restrained switch is at OFF condition.

$$r_{in}(t) = Ve_a(t) + B\frac{di_a(t)}{dt} + i(t) \tag{3.1}$$

$$Ve_a(t) + B\frac{di_a(t)}{dt} + i(t) = 0 \tag{3.2}$$

The motor that generates torque can be shown as,

$$T_i = \frac{1}{\omega(t)} i(t) e_a(t) \tag{3.3}$$

The derivation for the motion of the motor drive can be given as,

$$T_i - T_a = D\frac{d\omega(t)}{dt} + H\omega(t) \tag{3.4}$$

The joined inertia (Kgm2) of the rotor and load is D. Then the mechanical and electrical speed of the motor can be interrelated by,

$$Y\omega = \frac{d\theta_v}{dt} \tag{3.5}$$

The values stand for Y and θ_r can define the total amount of pole couples on the motor and the location of the rotor considerably, then consider an optimal full-wave rectifier, non-DC link capacitance and input voltage of buck converter $R_{in}(t)$ can be derived as,

$$R_{in}(t) = R_a\left|\sin(2\pi ft)\right| \tag{3.6}$$

Where R_a indicates the high value and f represents the frequency of main supply voltage.

The development of phase current governs by the curving inductance, winding resistance, and back EMF is feasible only at the time of one sector of the improved mains voltage, and the voltage beyond the inductance is announced as R_b is positive.

As noticeable from (3.1) and (3.2), phase current can be non-linear and regulated and then become non-regular. In the region of 2, it is undisciplined. Correspondingly, the torque will also be able to be unmanageable at the time of region 2. Consequently, it is necessary to examine the brunt on the generated torque because of unmanageable current at the time of region 2 in correlation to a typical drive. The amount $i(t)$ is stable at stable speed operation, and the detail to be disposed of by I. The duty cycle of the switch, which is determined as $J(t)$this is the time changing up by a half cycle $R_{in}(t)$. At the time of region 1, the voltage seconds produces over a single switching cycle beyond the inductance should be zero. Thus, from (3.1), (3.2), and (3.6),

$$\begin{aligned}&\left[R_a \left|\sin\left(2\pi ft\right)\right| - 2E_{ref}\left(t\right)V - I\right]J\left(t\right)/\ f_s \\ &\qquad = \left[2E_{ref}\left(t\right)V + I\right]\left[1 - J\left(t\right)\right]/\ f_s\end{aligned} \tag{3.7}$$

The switching frequency of U is f_s,

Evaluating (3.7)

$$J\left(t\right) = \frac{E_{ref}\,V + I}{R_a \left|\sin\left(2\pi ft\right)\right|} \tag{3.8}$$

The switch is performed by the controller at the ultimate feasible duty cycle of 100% at the time of region 2 as $e_m(t)$ is unmanageable. Therefore, $J(t)$ the switch can be derived as,

$$J\left(t\right) = \begin{cases} \dfrac{E_{ref}\,V + I}{R_a \left|\sin\left(2\pi ft\right)\right|} & in\ region\ 1 \\ & in\ region\ 2 \end{cases} \tag{3.9}$$

Alone the region 1prevail for conventional BLDC motor operates with a DC link capacitor and $J(t)$ is stable at a steady state for any inclined current quotation as $R_{in}(t)$ is a stable. It is considered that $R_{in}(t)$ is lined at the time of region 2 to determine the equations for $e_a(t)$. This guess cut down the complication of the equation $e_a(t)$ to a larger duration. T and T' are represented as time extant for $R_{in}(t)$ to achieve $E_{ref}\,V + I$ and I from 0 V, commonly. Hence, T and T' are expressed by,

$$T = \frac{1}{2\pi f} \sin^{-1}\left(\frac{E_{ref} V + I}{R_a}\right) \tag{3.10}$$

$$T' = \frac{1}{2\pi f} \sin^{-1}\left(\frac{I}{R_a}\right) \tag{3.11}$$

$e_a(t)$ is equated as a piecewise action of t in the course of region 2. $t1, t2\, and\, t3$ are detailed as pursue to explicit $e_a(t)$ as a piecewise behaviour and therefore to decrease the convolution in derivations.

$$t_1 = t - \left\{\frac{T_a}{4} + T\right\} \tag{3.12}$$

$$t_2 = t - \frac{T_a}{4} \tag{3.13}$$

$$t_3 = t - \left\{\frac{T_a}{4} + T'\right\} \tag{3.14}$$

T_a is the duration of the mains voltage. For example, $e_a(t1)$ performs the phase current in region 2 if $\{T_a / 4 - T\} \leq t \geq T_a / 4$.

Where $R_B(t_1)$ is equated as,

$$R_B(t_1) = \left(\frac{-e_a(t_1)V - I}{T}\right) t_1 \tag{3.15}$$

From (3.15) evaluating to $R_B(t_1)$ earns,

$$B\frac{de_a(t_1)}{dt_1} = \left(\frac{-e_a(t_1)V - I}{T}\right) t_1 \tag{3.16}$$

The familiar time concern solution for equation (3.16) can be represented as follows,

$$\ln\left[e_a(t_1)V + I\right] = \frac{-Vt_1^{\ 2}}{2BT} + K \tag{3.17}$$

Equating the steady-state basic condition, which is earned,

$$\ln(E_{ref} + I) = K \tag{3.18}$$

From (3.17) and (3.18)

$$e_a(t_1) = \frac{I}{V}\left(i^{\frac{-Vt_1^2}{2BT}} - 1\right) + E_{ref}\left(e^{\frac{-Vt_1^{\ 2}}{2BT}}\right) \tag{3.19}$$

From (3.19), it is feasible to check out that $e_a(t)$ is regular or irregular ahead $R_{in}(t)$ achieves 0, by the symbol of $e_a(t_1) at\, t_1 = T.$ If $e_a(t_1) > 0\ at\, t_1 = T.$ involves $e_a(t)$ is endless at zero crossings of $R_{in}(t)$. The range $e_a(t)$ of at zero crossings of $R_{in}(t)$, determine as E'_a will be equated by applying (3.19) by utilizing $t_1 = T.$

$$E'_a = \frac{I}{V}\left(i^{\frac{-VT}{2B}} - 1\right) + E_{ref}\, i^{\frac{-VT}{2B}} \tag{3.20}$$

Later the zero-crossing area $R_B(t_2)$ is given by,

$$R_B(t_2) = \left(\frac{I + e_a(t_2)V}{T'}\right)t - \left[I + e_a(t_2)V\right] \tag{3.21}$$

From (3.21) evaluating $R_B(t_2)$ earns,

$$B\frac{de_a(t_2)}{dt_2} = \left(\frac{I + e_a(t_2)V}{T}\right)t - \left[I + e_a(t_2)V\right] \tag{3.22}$$

The familiar time concern solution for (3.22) is written as,

$$\ln\left[I + e_a(t_2)V\right] = \frac{Vt_2^{\,2}}{2BT} - \frac{Vt_2}{B} + K \tag{3.23}$$

Substituting the basic condition in (3.20) to (3.23) earns,

$$K = \ln\left(I + E'_a V\right) \tag{3.24}$$

The entire time concern solution from (3.23), (3.24) for $e_a(t_2)$ at region 2 is given as,

$$e_a(t_2) = \frac{I}{V}\left(i^w - 1\right) + E'_a\, i^w \tag{3.25}$$

As previously mentioned, the derivations for phase current have drawn to resolve the stability $e_a(t)$ at the time of region 2. If $e_a(t)$ is irregular at region 2, it begins to develop after T'. To determine the developed current waveform $R_B(t_3)$ can be drawn.

$$R_B(t_3) = \left(\frac{e_a(t_3)V + I}{T'}\right)t_3 \tag{3.26}$$

From (3.26) executing to $R_B(t_3)$ earns,

$$B\frac{de_a(t_3)}{dt_3} = \left(\frac{e_a(t_3)V + I}{T'}\right)t_3 \tag{3.27}$$

The familiar time concern solution for (3.27) is written as,

$$\ln\left[e_a(t_3)V + I\right] = \frac{Vt_3}{2BT} + K \tag{3.28}$$

Then executing the steady-state basic position, $e_a = 0, at\, t = 0$

$$\ln(I) = K \tag{3.29}$$

From (3.28) and (3.29) the entire time concern solution for $e_a(t_3)$ is given as,

$$e_a(t_3) = \frac{I}{V}\left(i^{\frac{Vt_2^2}{2BT}} - 1 \right) \tag{3.30}$$

The equation (3.30) appears to react only when $e_a(t)$ interrupted at region 2.

The evaluated mathematical design $e_a(t)$ is drawn to attain the spontaneous and moderate ranges of torque of the motor at regular speed function. Furthermore, the design model shall be drawn to assess the devaluation of the torque because of the nonappearance DC link capacitor. Further, the design expedites a performance correlation between the prepared drive and the conventional BLDC motor drive by various performing positions for several motor parameters.

3.6 Advantages of BLDC motor

Some of the advantages of the brushless DC motor are given below,

- Long-life serves as a result of reduction of electrical and friction debt.
- Essentially less maintenance operation due to the absence of brushes and mechanical commutators.
- Decrease the EMI because of the rejection of ionizing nails from the brushes.
- More applicable for uncertain environmental surroundings (oil, muck, lubricant, and other foreign elements) because they are perfectly sealed.
- When the brush is not needed, the mechanical energy debt because of low erosion strengthens the capability.
- BLDC motors simply accelerate and decelerate freely because they obtain low rotor inertia.
- These motors can be cooled by conduction and no need for additional air flow for cooling the interior.
- Ionizing sparks will not come from the commutator and electromagnetic conflict is also get decrease.
- The performance of the motor is high and that establishes higher torque per cubic inch over a wide speed range.
- Some of the operational functions that consist,

- Bulky load
- High torque restraint
- Short duty cycle motion
- High speed
- Huge acceleration/deceleration efficiency

The benefits of that brushless DC motor over the conventional DC motor are more familiar [43]. Brushless DC motors generate their output torque as long as the cooperation between a magnetic field generated by the magnetic field and permanent magnet through a direct current in a stator design. This sequence, while correlated with conventional brush-type motors makes it simple to discard the heat obtained in the effective windings when generating a much thermally lasting device.

3.7 Disadvantages of BLDC motor

Some of the disadvantages of brushless DC motors are given below,

- These motors are a little expensive
- The electronic controller is needed to control this motor
- Moderate possibility of more electronic control solutions, normally for small brushless DC motors.
- Needs complicated drive circuits
- Sensors are additionally required
- Motor defect still happens in brushless motors and results in ability.

Mostly motor losses are frequently followed as in two processes [44]. Initially, torque-sensitive losses or load are normally restricted to winding losses, and the losses are in proportion to the square of the current passing along the resistance of windings times. Generally, windings consist of copper or aluminium conductors, in such kinds of metals the electrical resistance will rise with temperature. Hence, torque losses will enlarge during the motor heats high. The second types of loss include speed-sensitive losses which correspond to the speed of the motor. The superior losses have been assigned to the eddy current along with the hysteresis effect and short circuit currents for the brushless motors. The eddy currents are occurrences bring about by variation of magnetic flux or magnetic field between a medium that assists electric current flow. The housing portion of the motor comprises induced potential voltage for the brushless motors ad it also generates eddy current. The induced eddy currents have a prominent heating effect on the motor, and it is in proportion to the speed, specifically for small motors in which the current invention corresponds while operating at increased speeds.

3.8 Applications of BLDC motor

Brushless DC motors are mostly drawn for various kinds of application concerns like stable loads, unstable loads, and positioning utilization in the sectors of aeronautics, industrialized control, automotive, health care provisions, automation functions, etc. Also, some of the definite utilization of brushless DC motor are,

- Computer hardware and CD/DVD players
- Used in hybrid vehicles, electric vehicles, and electric bicycles
- Industrialized robots, CNC machine appliances, and an easy belt-driven scheme
- Compressors, washing machines, and dryers
- Blowers, fans, and pumps

3.9 H∞ controller process

The H∞ control arrives from the field of mathematics by which the optimization befalls. H∞ controller is a solid space of matrix assessed systems that are systematic, and encircled in the wide right half of the complicated plane which is determined by Re(s)>0; then the ultimate individual amount of the system along that space is the ∞norm. (It is explained as an ultimate gain and at any frequency for SISO schemes, and is energetically the ultimate magnitude of the frequency feedback.) To diminish the closed-loop clash perturbation [45] based on the issue conformation, the clash will either be deliberate in terms of equalization or enforcement H∞ techniques can be used.

Mixed weight H∞ controllers afford closed-loop feedback of the function confers to the model designation like model concern, disruption exhaustion at high frequencies, bandwidth requirements of the closed-loop scheme, etc. H-infinity controllers are the higher-order system that may tend to huge control effort demand. Furthermore, the design model can also base on the exact system and can desire its exact inquiry [10]. Further frequency-reliant weights are integrated with the function and are preferred to display individual capability. When H-infinity excellent control access is enforced to a scheme, and attainment conditions apply to the model objects.

Different methods have been applicable in composition for the structure of the H-infinity controller and the H-infinity loop frame is one of the generally approved frameworks among them as the achievement concern and that can be installed in the modeling step as achievement weights. The H∞ method in control theory structure shown in Figure 3.11, authorize in normal that weighing different loop signals in a path resolved by the design conditions, the scheme can develop probably to generate effective loop transfer function resolution. Here, a definite model is amplifying with convinced weight functions like awareness weight function, etc. unusually that aimed consummation of the closed-loop transfer function of the scheme has been ensured.

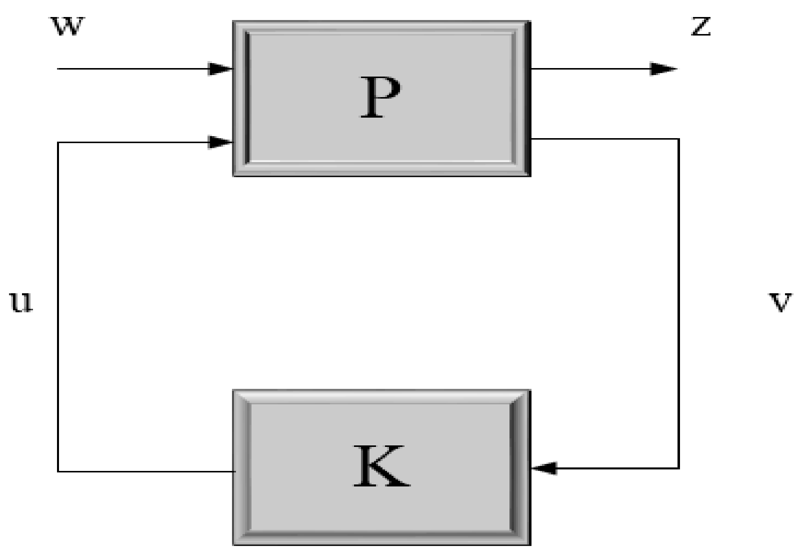

Figure 3.11: H∞ method in control theory

3.9.1 Design of H∞ controller

The design model of the H∞ controller is based on the mathematical field and also combined with the three major facts. The major facts are discussed below,

The controller K(s) will be imitated by the following three facts:

1) Stability criterion: This deals that the heritage of the characteristic equation 1+G(u) K(u)=0 should fall in the left part side of the s plane.

2) Enforcement criterion: This describes that the reactivity to be slight for every frequency where the disruption and set point variation is high.

3) Robustness criterion: It appeals for the cohesion and enforcement that to be preserved not only for the appearance but also for a group of nearby plant models that conclude from necessary habitation of designing faults [46].

The H-infinity controller design is in general based on minimization of the H-infinity norm of the selected closed-loop system described as

$$\left\| H_1(A,C) \right\|_\infty = \sup_\omega \bar{\sigma}\left(H_1(A,C)(d\omega)\right) \tag{3.31}$$

Where $\bar{\sigma}$ the peculiar is the value of the function $H_1(A,C)(d\omega)$ and C is the controller. The expression $H_1(A,C)$ is named as lower fractional transformation. It is denoted as $H_1(A,C)(d\omega)$ $= A_{11} + A_{12}\, C\left(E - A_{22}C\right)^{-1} A_{21}$. The attaining of the controller is later depending on the solution of Riccati equations. This is a little difficult thus few of the accessible powerful restraint design tools for the analytical solution are regularly drawn, e.g. MATLAB function.

$$\begin{bmatrix} \dot{X} \\ N_M \\ N_C \\ N_K \\ N_J \\ P \end{bmatrix} = \begin{bmatrix} \overline{M} & M_\Delta & C_\Delta & 0 & 0 & \overline{C} \\ E & 0 & 0 & 0 & 0 & 0 \\ 0 & 0 & 0 & 0 & 0 & E \\ E & 0 & 0 & 0 & 0 & 0 \\ 0 & 0 & 0 & 0 & 0 & E \\ \overline{K} & 0 & 0 & K_\Delta & J_\Delta & \overline{J} \end{bmatrix} \begin{bmatrix} X \\ j_M \\ j_C \\ j_K \\ j_J \\ s \end{bmatrix} \tag{3.32}$$

$$\begin{bmatrix} j_M \\ j_C \\ j_K \\ j_J \end{bmatrix} = \begin{bmatrix} \Delta_{\Delta M} & 0 & 0 & 0 \\ 0 & \Delta_{\Delta C} & 0 & 0 \\ 0 & 0 & \Delta_{\Delta K} & 0 \\ 0 & 0 & 0 & \Delta_{\Delta K} \end{bmatrix} \begin{bmatrix} N_M \\ N_C \\ N_K \\ N_J \end{bmatrix} \tag{3.33}$$

Where, $X = [x_1\, x_2]^T$, $\dot{X} = [\dot{x}_1\, \dot{x}_2]^T$, $N_M = N_K = X$, $N_C = N_J = S$, $P = \omega$, $S = \mu$, $j_M = \Delta_{\Delta M\ N_M}$, $j_C = \Delta_{\Delta C\ N_C}$, $j_K = \Delta_{\Delta K\ N_K}$, $j_J = \Delta_{\Delta J\ N_J}$ and certainly $-E \le \Delta_{\Delta M,C,K,J} \le E$.

$M_\Delta = M_{\max} - \overline{M}$ Where $M_{\max}$ is the state-space matrix of the example with the biggest concern in its criterion. $C_\Delta, K_\Delta, J_\Delta$ are attained correspondingly.

The converted matrix M then involves the details about the ambivalence. It was incorporated only $\Delta matrix$ previously in the transformation. The converted matrix M is the input criterion for the MATLAB functions (e.g. hinfsys) determining the Riccati equations to construct a powerful controller C .

The H∞ theory affords a directly integrate controller which perfectly entertains exceptional value loop shaping terms [47]. The classic setup of the restraint issue subsists of discovering a static or dynamic response controller to this extent the H∞ pattern of the closed-loop transfer function is lower than the enforced positive number under pressure that the closed-loop function is internally reliable.

Synchronously optimizing robust enforcement and robust equalization is troublesome. One technique that arrives near to attaining this is H∞ loop shaping, which permits the restraint designer to appeal academic loop shaping approach to the multivariable frequency feedback to earn excellent robust performance, and then the feedback is optimized close to the bandwidth of the system to obtain excellent robust stabilization.

3.9.2 H∞ control problem

We consider that $\sum$ to be a definite time constant scheme either in continuous or discontinuous time. Here need to figure out that $\sum$ is a function with dual different types of inputs and dual different types of outputs. The input Q is an extrinsic input defining the disruptions delegated to the system. The control problem of the H∞ controller is shown in below Figure 3.12,

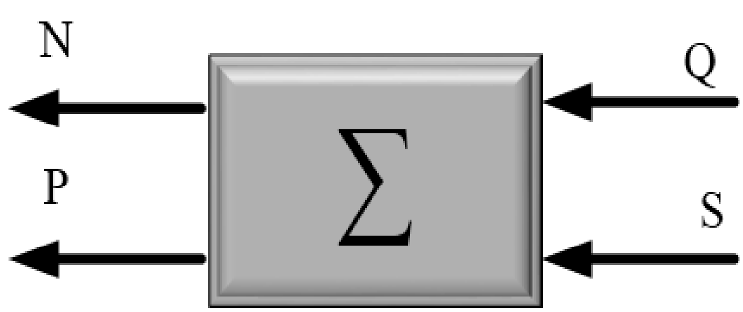

Figure 3.12: H∞ control problem

The gain N is an output of the scheme, whose dependency on the extracellular input Q is needed to be diminished. The output N is an assessment need to be done on the system, which will be drawn to select the needed input S , or in other words, this will act as a mechanism to reduce the effect W on N . A restraint to enforce is that this aligning from P to S should be alike that the closed-loop system is reliable at inside. This is normally instinctive since the states need not convert too enormous at the time of trying to govern the attainment. The issue of Q on N concluding the loop is deliberate in terms of power and very bad disruptions Q . Then the measurement, which will change out to equivalent to the closed-loop H∞ norm, is the absolute than all interruptions which are not equal to zero of the computation of energy to zero of the quotients of energy passing out of the system and the energy passing into the system.

3.10 Fixed order H∞ controller in BLDC motor

The fixed order H∞ controller for the BLDC motor is proposed for position analysis of the rotor. The de convolution filter in the H∞ controller involves a state input, a familiar input, and a disruption. The H∞ controller-based BLDC motor is shown in Figure 3.13; the function of the observer is to evaluate phase to phase trapezoidal behind electromotive force (BEMF) of the BLDC motor by employing certain line current and voltage for attaining the position and speed of the rotor [48].

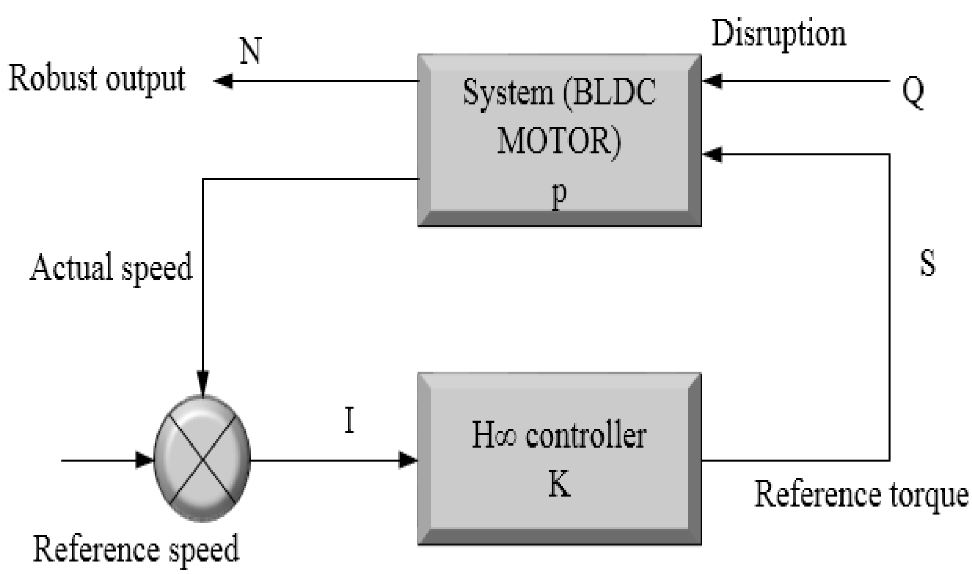

Figure 3.13: H∞ controller in BLDC motor

The progressive access to perfectly tune the BLDC motor, the acceleration controller like PID parameters by the genetic algorithm is the existing methods with H∞ controller by improved particle swarm optimization is the proposed process. The process deals with the execution of the H∞ controller with enhancing weights in a control criticism of the BLDC motor for developing durability and variation. For the optimization of electing position, an improved PSO method is installed.

3.11 Mathematical modelling of H∞ controller in BLDC motor

The fixed order H∞ controller is the feedback form of the BLDC motor and the normal configuration is given by (3.34).

$$\begin{bmatrix} e \\ c \end{bmatrix} = H_y \begin{bmatrix} \phi \\ u \end{bmatrix} \tag{3.34}$$

In the above derivation 'e' stands for the error speed and 'c' is the gain of the controller.

The weight function of the controller is given by,

$$H\infty = \min\ [weightning\ \ function] \leq 1$$

$$weightning\ function = \begin{bmatrix} w_u \\ w_{mu} \\ w_n \end{bmatrix} \tag{3.35}$$

$$W_u = \frac{U/R + F}{U + F\,m} \tag{3.36}$$

$$W_{mu} = Constant \tag{3.37}$$

$$W_n = \frac{U + F/R}{mU + F} \tag{3.38}$$

Where the values of 'F' and 'm' are 2 and 0.01 respectively and 'R' express the ultimate peak amplitude.

3.12 Advantages of H∞ controller

- H∞ controller methods have benefits over the classical restraint techniques.
- The H∞ control methods are eagerly relevant to issues concerning multi-variable functions [49].
- Also, the H∞ control techniques are feasible to modelling a strong state feedback
- The control law of the H∞ controller recognizes the parameter inferior Lyapunov function.

3.13 Disadvantages of H∞ controller

- The H∞ controller techniques combine a huge level of mathematical considerate.
- The mathematical formulations of H∞ controller required to apply them correctly
- The sensibly excellent model of the system needs to be restrained.
- The problem constitution is essential since any harmonized controller will be excellent in the developed sense.

3.14 Applications of H∞ controller

Some of the applications of H∞ controller are given below,

- Gas turbine restraint
- An aircraft gyro pilot modelling
- Used for peculiar systems
- H∞ control for distinct time systems
- Used in huge space network
- Reaction control of flexible field platform
- Vertical even agitation of an aircraft

3.15 Operation of improved particle swarm optimization algorithm

The communal behaviour of the birds gathering or fish schooling motivates the PSO. In these natural schemes, the combined behaviours of the humble characters are communicating with their atmosphere and everyone played a significant part. The PSO provokes the behaviours of biological swarms by arbitrarily seeking food in a region. One slice of food only searching in this area. The entire swarms cannot recognize the locality of food but they know how far away the food is available every test by noticing their strength. The query is that how the particle swarm will discover the food in an effective method [50]. The simple concept of resolving the swarm optimization issue is to monitor the emperor particle that is next to the food. From the time when the emperor particles characterize the ongoing optimum solutions, in PSO the particles in a population all the time shift via the difficult area by pursuing the present optimal particles.

The Particle Swarm Optimization is a community-centered stochastic optimization method. At first, this is begun with a set of arbitrary particles. Every particle is renewed by the succeeding two finest values are the personal best xp,i, and the global best xg in each repetition. The best solution of one particle xp,i have attained till now. The best value xg is attained till now by some particle in the community. The typical Particle Swarm Optimization algorithm has numerous disadvantages while dealing with certain problematic optimization complications. For example, an upgraded Particle Swarm Optimization algorithm was suggested by increasing an additional loop at the start of the algorithm to maintain the arbitrarily reinitializing impossible particles for confirming that they remain within the possible search space. The destructive Particle Swarm Optimization algorithm was generated by employing the self-arrangement process of the dissipative organization.

In this analysis, the important factor is to maintain effective stability between the investigation and the exploitation of particles in the swarm to develop the functioning of the benchmark PSO algorithm. The significant concept is common to maintain the diversity of both global and local optima to understand this idea in the usual method is to arbitrarily “perturb” these optima at present repetition. These perturbations are utilized for the disparity between the particle position and local best solution or between the particle current position and current global best solution in the benchmark particle swarm optimization algorithm. The advantage of this system is in limiting the investigation capacity of the particle swarm.

As the perturbations must be straight away utilized to the global best solution and local best solution to extending the investigation capability of the particle swarm [51]. The Metropolis algorithm is being applied to create this type of perturbations. Nevertheless, a probability density function (PDF) can highly boost the computational complication of the PSO algorithm. Hence, we use an easy method to create the arbitrary perturbations as in the benchmark Particle Swarm Optimization algorithm in this manuscript. The detailed flowchart of the IPSO algorithm is shown in Figure 3.14, the purpose of improving the enhanced PSO algorithm is to develop the union procedure of the particles in a swarm like this every particle has stopped from flying distant to the possible search space.

Step 1: Randomly boot the value of the position $P = P_e^1, P_e^2, ...P_e^z$ and the velocity can be declared by $V = V_e^1, V_2^2 ....V_e^z$.

Step 2: Assess the fitness operation of the particle. Every single particle has various values. The fitness operation is the phrase of the objective function.

Step 3: After that correlate both the fitness value local best and global best value. In which the global value is assumed as the perfect value. For a deprecation effort, the position earns a minor function value is noticed as carrying fitness, which is established as a local best. Then identifying the two perfect values the position and the velocity are restored.

Step 4: After that recent position and velocity by (3.39)

$$V_{new} = Q * v_e^z + k_e * rand(0) * \left(p_e^z - x_e^z\right) + k_d * rand(1) * \left(p_{gl} - x_e^z\right) \tag{3.39}$$

The inertia weight (Q) is drawn to restraint the velocity, and the attitudes develop into 0.7 then k_e and k_d are stable, p_{gl} performs as the global best value. the value of k_e and k_d inclines $0 \le k_e, k_d \le 2$. Then the situation can be restored by (3.40).

$$X_E^Z = x_e^z + v_e^z \tag{3.40}$$

The perfect position is the accession of instant position and the velocity of the particle.

Step 5: The developed crook value is the objective function. The election process is concluded under the perfect fitness value.

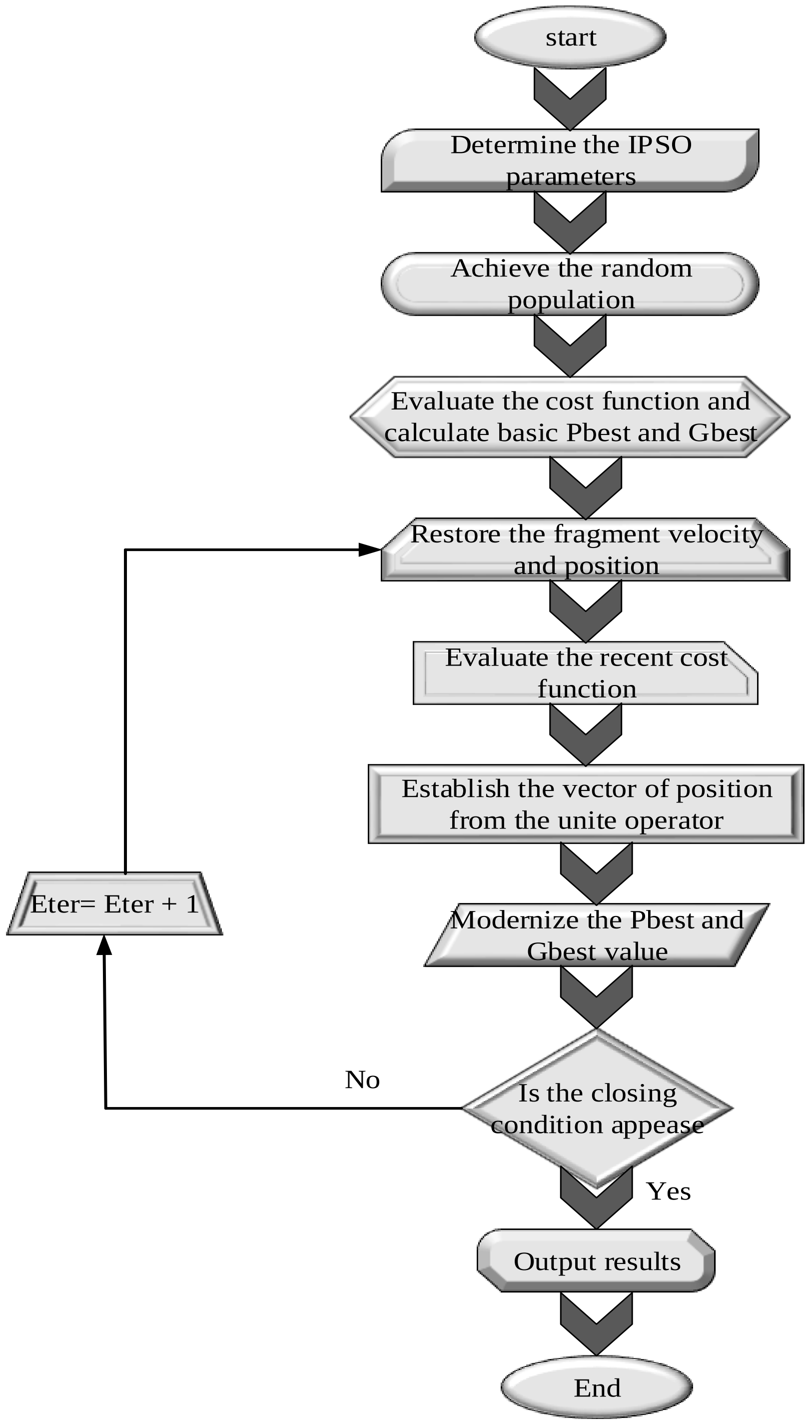

Figure 3.14: Flow chart of IPSO algorithm

3.15.1 Advantages of IPSO algorithm

One of the most energetic techniques for concluding irregular global optimization issues is the IPSO algorithm. Some of the advantages are given below;

- Like other examining optimization methods, the IPSO algorithm is also a subordinate-free approach. IPSO algorithm is easy in its approach and coding application correlated to other examining optimization methods.
- IPSO algorithm is low reactivity to the nature of the detached function correlated to the regular mathematical access and other examining techniques.
- IPSO algorithm has a constraint amount of criterion including only the inertia weight factor and two dispatch coefficients in contrast with another contest examining optimization techniques.
- The brunt of criterion to the clarifications is considered to be low sensitive when correlated with other examining algorithms.
- IPSO algorithm intimates to be considerably less reliant on a group of basic points compared with other developmental techniques, mentioning that convergence algorithm is tough.
- IPSO algorithm methods can develop high aspect solutions within a short estimation time and reliable convergence attribute than other imaging methods.

3.15.2 Applications of IPSO algorithm

One of the reasons that particle swarm optimization is glamorous is that there are very few constants to be regulated. One statement, with very small variations (or nothing perhaps) performs well in a wide array of applications [52]. Particle swarm optimization has been drawn for access that can be applied beyond a broad spectrum of applications, as well as for distinct utilization concentrate on an exact demand.

The basic application of Particle swarm optimization exhibits an approach or technique, which can be drawn for many utilization emerging unreal neural networks. Particle swarm optimization is being drawn to deriving not only the network density but even also the network formation. This technique is so easy and adequate that we have all about perfectly terminate employing classical neural network training criteria like rear generation. Rather, we emerge our network by particle swarm optimization. The access is efficient for several network architectures.

Particle swarm optimization is related to other progressive computation algorithms, which can be enforced to determine most optimization issues, and then the issues can be reformed to optimization defects. Though the application fields with the most probable system design, systematization, biological system designing, multi-objective optimization, pattern concession, signal processing, robotic application, organizing, games, decision making, simulation, and recognition. Then some of the examples embodied are fuzzy controller model, image analysis, speaker confirmation, heat diagnosing, time-frequency resolution, workshop organizing, EEG signal simulation, gesture concession, designing of escalation of antibiotic resistance, automatic target disclosure.

3.16 Existing method

In the proposed technology of position analysis of BLDC motor by using the fixed order H∞ controller involves some existing methods. The performance of the torque, speed and back EMF voltage all needs compare with the existing controllers such as fuzzy proportional derivative controller, fuzzy proportional integral derivative, and sensing algorithm.

3.17 Fuzzy PID controller

The PID controllers are suitably advanced and utilized for over half a century, and are highly applied for process control and industrial automation in recent times. Lately, encouraged by the advancement of digital processors and microelectronics, the conventional PID controllers have drained due to scientific advancements, from pneumatic.

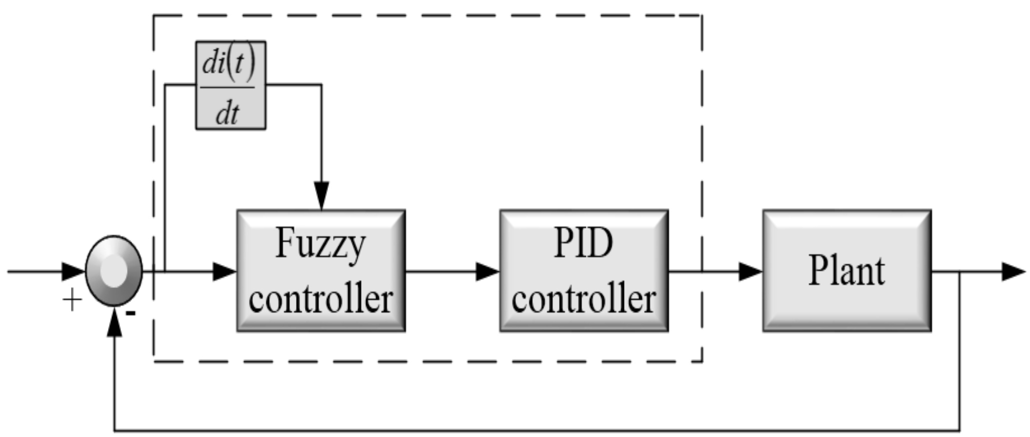

Figure 3.15: Block diagram of Fuzzy PID controller

Nevertheless, it comes to understand that the conventional PID controllers normally cannot perform better for nonlinear systems. Specific mathematical models are not applied for time-delayed and higher-order linear systems, and especially vague and complex systems [53]. The block diagram of the fuzzy PID controller is shown in Figure 3.15, Then, the special features of the fuzzy PID controller are given below.

1) The Fuzzy PID controller has a linear structure similar to that of the conventional PID controller, however, it has self-tuned control gains and constant-coefficient: the derivative, integral, and proportional gains are nonlinear functions of the input signals.

2) Depending on the classical discrete PID controller, the controller is modelled, using this the fuzzy control law has been acquired.

3) The membership functions are understandable simple triangular ones that comprise four fuzzy logic IF-THEN rules. The terminal fuzzy control law is formulated with fuzzification, control-rule execution, and defuzzification steps. The attained control law is a direct conventional formula, therefore the controller task is similar to the conventional PID controller, during the fuzzification–rules–defuzzification procedure cannot be required for the complete controlling process.

3.18 Design of fuzzy PID controller

The important work of a controller is to detect a proper set of commands that supports the system to attain an appropriate state with fewer deviations. The controlling equations have been coupled with nonlinear equations that are applied to several damping in different complicated systems. The framework of a typical fuzzy PID controller is depicted in Figure 3.16. In the general case, the equations of controlled systems are complex hence, the controller can have the capability to efficiently integrate nonlinear properties and unmodeled effects into its primary design.

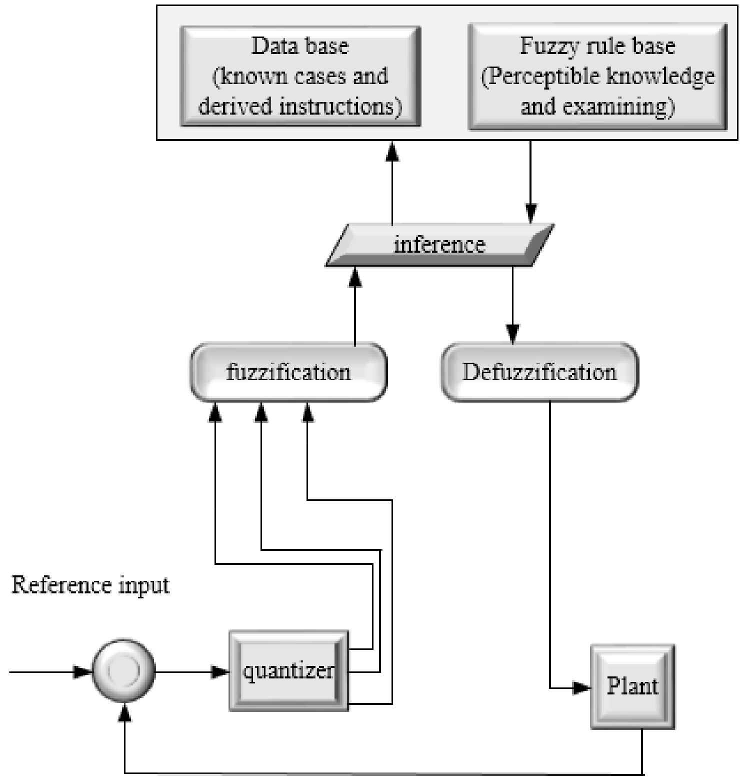

Figure 3.16: Structure of typical Fuzzy PID controller

Proportional-integral-derivative (PID) controllers are the most commonly used industrial controllers [54]. These controllers can easily know the mature design approaches and properties. The fundamentals for the designing method can be provided by the classical PID control law. As there is a need to transform the conventional PID control law into a digital version, due to the evolution of advanced control systems in computer processors for application.

The fuzzy logic controllers have been generally constructed with three primary components; A fuzzy rule base is built in the linguistic form ``if x is true then do y''. The rule base is constructed based on knowledge of the issue and normal observations and is normally straightforward for designing. Moreover, the next two distinct components are not similar. The numerical input signal is converted into some fuzzy values using a fuzzification unit, whereas during defuzzification the final fuzzy value from the controller is converted into an output signal.

The process of fuzzification and defuzzification needs membership functions and heuristic rules for encoding controller dynamics and response characteristics of the desired system. However, it is not clear how the fuzzy transformations can be, it is due to the fundamental conception of the physical system. It can be considered as an important problem for designing several fuzzy controllers, and for a reason, the fundamental justification is carried by utilizing a well-known PID controller as the elementary structure for the new design.

3.19 Mathematical modelling of fuzzy PID controller

The mathematical modelling of the fuzzy PID controller is detailed below and the result of the conventional analog PD controller on the frequency u-domain, is also be identified simply by,

$$u_{YJ} = \left(C_Y{}^K + uC_d{}^K\right)I(u) \tag{3.41}$$

Where $C_d{}^k$ *and* $C_y{}^k$ the typical derivative and proportional are gains commonly and $I(s)$ represent the tracing error signal [55]. This equation is remodelled into a distinct version by employing the bilinear conversion. $u=(2/T)[(n-1)/(n+1)]$, which T resembles the examining period which concludes in

$$u_{YJ} = \left(C_y{}^k + \frac{C_y{}^k T}{2}\,\frac{1-n^{-1}}{1+n^{-1}}\right)I(n) \tag{ 3.42}$$

Approving $C_y = C_y{}^k$ and $C_j = 2C_j{}^k/T$ after getting the inverse z transform the equation can be,

$$u_{YJ}(zT) + uYJ(zT-T) = C_y[i(zT)+i(zT-T)] + C_y[i(zT)-i(zT-T)] \tag{3.43}$$

Then dividing 3.43 by T and using z to mean zT from this instant we attain,

$$\Delta u_{YJ}(z) = C_y\, j(z) + C_j v(z) \tag{3.44}$$

Where,

$$\Delta u_{YJ}(z) = \frac{uYJ(z)+uYJ(z-1)}{T} \tag{3.45}$$

$$v(z) = \frac{i(z)-i(z-1)}{T} \tag{3.46}$$

$$j(z)=\frac{i(z)+i(z-1)}{T} \tag{3.47}$$

We can rewrite 3.45 as,

$$u_{YJ}(z)=-uYJ(z-1)+T\Delta uYJ(z) \tag{3.48}$$

Relocating the term $T\Delta uYJ(z)$ by a fuzzy control action gain. We conclusively reach at,

$$u_{YJ}(z)=-uYJ(z-1)+C_{uYJ}\,\Delta uYJ(z) \tag{3.49}$$

Where C_{uYJ} is a fuzzy control gain.

3.20 Advantages of fuzzy PID controller

- Normally, PID controllers are simple to implement
- Satisfied tuning rules are available
- Feasible PID tuning examining are easy to discern
- The process of operation is simple
- The design of the controller is the ease
- Cheap maintenance
- Minimum initial cost
- More effective for linear systems

3.21 Disadvantages of fuzzy PID controller

- PID controllers cannot treat large time delay processes effectively [56]
- PID controllers are not suitable for slow disturbance rejection or slow set point tracing
- The higher-order process is rare in PID
- In a system, the maximum overshoot is increased by this controller.
- Because of the existence of fuzzy PID controllers, there may be offset in the system

3.22 Applications of fuzzy PID controller

- Extremely used for industrial automation
- Human expertise can be accomplished with calm for PID gain scheduling

- PID controllers are most useful in power electronics utilizations like converters
- PID controllers will also use in the temperature control process
- To find MPPT, a PID controller is used and for that current and voltage setpoint is given to the controller.

3.23 Fuzzy PD controller

PD controllers are mostly used in industrial processes because of their effectiveness and simplicity. The suitably designed PD controller enhances damping and minimizes maximum overshoot, settling time, and rise time. Additionally, it enhances the stability of a feedback system. Recently, few attractive theoretical studies based on fuzzy logic controllers are expressed. And now, the most essential theoretical developments of fuzzy control, identified that Mizumoto, applying computer simulation, and then comparing every twelve different fuzzy reasoning approaches in the context of control in the view of first-order plant scheme along with a time delay.

Like that the detailed discussion about the static analysis of fuzzy controllers that involves various aspects of control protocol namely the connection between rules, completeness, robustness properties, and consistency [57]. Also need to verify that, the fuzzy PD controller exceeds its counterpart as the conventional linear PD controller.

To know the mentioned issues, need to understand detailed clarification of fuzzy PD controller, and its performance by comparing with a conventional PD controller. Therefore, the process needs to derive the analytical structure of the simple fuzzy PD controller by applying the output variable with three fuzzy sets and every input variable with two fuzzy sets during the fuzzification process, intersection T-norm, the center of the area (COA) defuzzification, rule base with four control rules, drastic product inference method, and Lukasiewicz OR T-conorm, method.

The stability of fuzzy control systems has been tested by categorizing them into frequency-domain and time-domain schemes. Besides, the conditions can be determined under the conventional linear PD controller, which is already in utilization for controlling the process, and it is restored by a nonlinear fuzzy PD controller for achieving better control performance without changing the stability of the system.

3.24 Design of fuzzy PD controller

The objective of the P-D controller is to maximize the system stability by enhancing control because the P-D controller can forecast the future error of the system feedback. The unexpected variations in the error signal value can occur, to solve this effect the derivatives are considered from the output system response variable than the error signal. Hence, to solve the unexpected changes caused in the output control from the error signal, D mode is applied as proportional to the variations in the output variable. Apart from this, D can directly expand the process noise hence D control has not been applied.

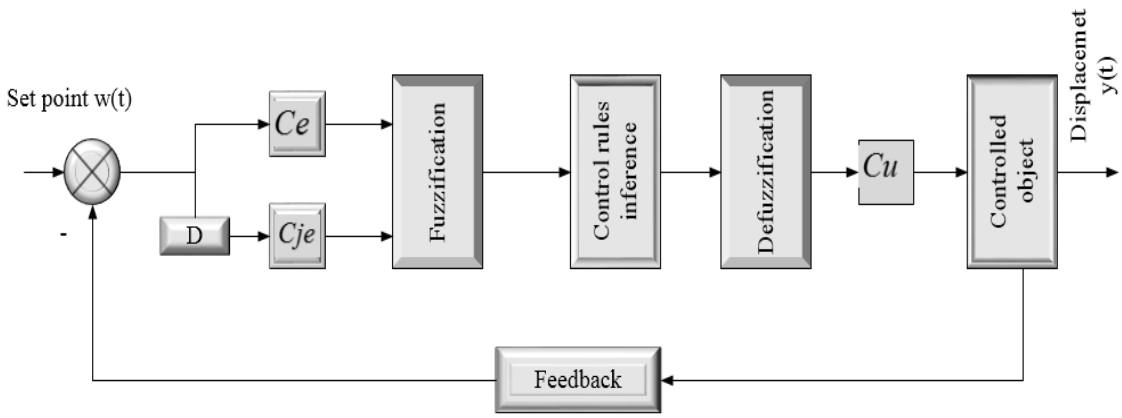

Figure 3.17: Typical structure of fuzzy PD controller

If the error prediction can control then D mode is utilized or if it is significant for system stabilization. By considering the frequency characteristic of the D element it is clear that the phase of the D element tends to 90°. Frequently the derivative from the system output variable than the error signal [58]. The typical structure of fuzzy PD controller is detailed in Figure 3.17, this process is performed to ignore the effects of unexpected change from the reference input that can make an immediate change in the error signal value.

The immediate change that occurred in the error signal tends to an unexpected change in the output control. To solve that it is necessary to model D mode to be proportional to the variation of the output variable. The PD controllers are frequently utilized for controlling moving objects including rockets, underwater vehicles, ships, flying vehicles, etc. The major reason is stabilizing effect of PD controller on unexpected variation in heading variable y(t). Usually, for determining the velocity a "rate gyro” is considered as the sensor of heading variations for moving objects.

3.25 Mathematical modelling of fuzzy PD controller

The mathematical modelling of the fuzzy PD controller is detailed below. Normally the design of the controller is generally based on the classical discrete PD controller [59], in which the derivative for fuzzy control law is evolved. Then, the conventional analog PD controller can be expressed as

$$u_{YJ}(t)=C_y{}^{k'}p(t)+C_j{}^{k}p(t) \tag{3.50}$$

The aforementioned equation in the form of frequency domain will be changed to,

$$u_{YJ}(S)=\left(C_y{}^{k'}+C_j{}^{k}s\right)p(s) \tag{3.51}$$

The above-mentioned equation is the continuous domain equation and it is transformed to discrete domain employing bilinear transformation,

$$s=\frac{2}{T}\frac{(n-1)}{(n+1)} \tag{3.52}$$

Where T>0 indicates the examining period. The succeeding term has a resulting equation,

$$u_{YJ}(n)=\left(C_y{}^{k'}+\frac{2}{T}\frac{(n-1)}{(n+1)}C_j{}^{k}\right)P(n) \tag{3.53}$$

The above equation 3.53 is simplified as,

$$u_{YJ}(n)+u_{YJ}(zT-T)=C'_y\left(p(zT)+p(zT-T)\right)+C_j\left(p(zT)-P(zT-T)\right) \tag{3.54}$$

Where,

$$\begin{gathered} C'_y=C_y{}^{k'} \\ and \\ C_j=\frac{2}{T}C_j{}^{k} \end{gathered} \tag{3.55}$$

While dividing the equation 3.54 by T we get,

$$\frac{u_{YJ}(zT)+u_{YJ}(zT-T)}{T}=\frac{C'_y\left(p(zT)+p(zT-T)\right)}{T}+\frac{C_j\left(p(zT)-p(zT-T)\right)}{T}$$

OR (3.56)

$$\Delta u_{YJ}(zT)=C'_y j(zT)+C_j\Delta p(zT)$$

Where,

$$\Delta u_{YJ}(zT)=\frac{u_{YJ}(zT)+u_{YJ}(zT-T)}{T}$$

$$j(zT)=\frac{p(zT)+p(zT-T)}{T}$$

$$\Delta p(zT)=\frac{p(zT)-p(zT-T)}{T}$$

Again, we have,

$$u_{YJ}(zT)=-u_{YJ}(zT-T)+T\Delta u_{YJ}(zT) \tag{3.57}$$

$\Delta u_{YJ}(zT)$ can be the fuzzy control action in the advanced design and the use of C_{uYJ} as a fuzzy control gain, later it can be decisive and expressed it as,

$$u_{YJ}(zT)=-u_{YJ}(zT-T)+C_{uYJ}\Delta u_{YJ}(zT) \tag{3.58}$$

3.26 Advantages of fuzzy PD controller

- Overall constancy of system will improve
- Has the capability to forecast the upcoming error
- Efficient in handling processes with the time lag
- Reduces settling time by developing damping and decreasing overshoot

3.27 Disadvantages of fuzzy PD controller

- Not suitable for fast responding systems which are commonly lightly damped or initially unstable.

- Amplifies noise at high frequencies which results in inaccurate handling of actuators [60].
- Does not eliminate steady-state error

3.28 Applications of fuzzy PD controller

- It can be widely used in most the industrial appliances
- Applied for the integrating process without the dead time
- The feedback of PD is utilized for varying the poles of the plant transfer function

3.29 Sensing algorithm

The radical new method for sampling the signals at a sub-Nyquist rate is known as compressive sensing. Compressive sensing is also described as compressed sensing. The analog signals are perfectly rebuilt from their samples using Nyquist/Shannon sampling theorem. When the signal is sampled at a rate of at least twice the maximum frequency, then the sampled rate of the signal is called as Shannon/Nyquist rate of the signal. Some signals like images or audio possess a high Nyquist rate.

Due to this reason, numerous samples can be acquired, and these samples are compressed in an attempt to transmit or store them, along with settling a high demand on the equipment required for sampling the signal. Since the compressive sensing method is established in recent times and that method will decrease the required number of measurements; somehow it is considered an automatic signal compressor [61]. When the original signal is sampled lower than the Nyquist rate, compressive sensing is a suitable method that supports fully rebuild the specific classes of signals.

The compressive sensing operates especially with sparse signals. The signal of interest is mainly zero for various applications as the signal consists of representation in several pre-determined bases over which many of the coefficients tend to 0. Typically, measurement approaches heavily over signal samples. Taking this into consideration, the samples are randomly drawn from the sparse signal, hence the sparsity fraction is equal to the probability of sampling at an “interesting” data point. The block diagram of compressive sensing is shown in Figure 3.18, Compressive sensing ignores the unrestricted oversampling by employing linear sampling operators which is the integration of compression and sampling.

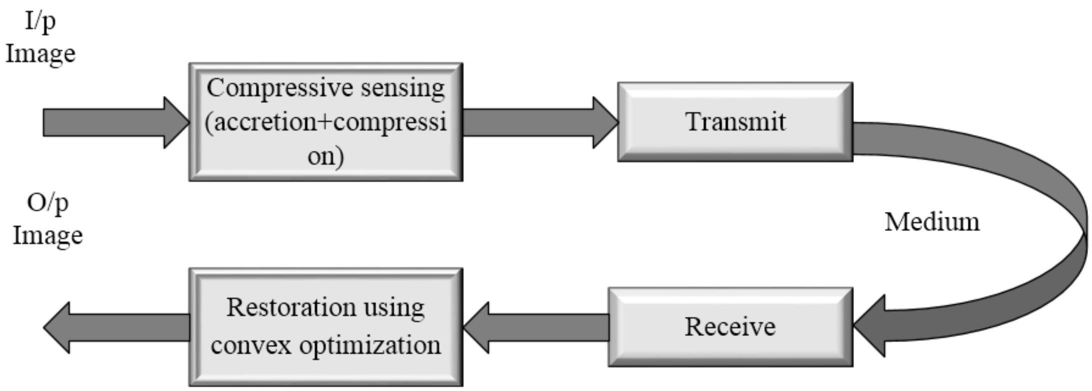

Figure 3.18: Block diagram of compressive Sensing

Nowadays, the standard method for signal acquisition is to evaluate the total copy of the signal and after measurement, it is processed and the crucial information is extracted. For instance, one normally determines an image considering the pixel basis and further executes JPEG compression for acquiring effective representation. Rather, the new method gathers the smaller number of deliberately selected (however non-adaptive) linear measurements that change the information contained in the signal. From the linear measurements, the signals are approximately rebuilt by employing sophisticated algorithms.

The conceptual work on compressive sensing is navigated by some exhilarating new advanced applications. The general linear estimation of the signal can be calculated by such advanced applications along with unit cost per measurement. Consequently, the cost of acquisition is proportional to the considered number of measuring signals. (This situation supports contrastingly with the digital computation of a dot product module by module.)

In conventional signal acquisition schemes, the measured signals contain an uncomplicated clarification. On the contrary, compressed Sensing makes use of measurements that resemble no actual intention. Normally, there has no easy map from signal domain to measurement data back. Finally, the time utilized to rebuild the signals from measurements can be concerned.

3.30 Major compliments in compressive Sensing

Besides, compressive sensing varies from classical sampling primarily by three significant considerations.

- Initially, sampling theory normally assumes continuous-time signals and infinite length. In comparison, compressive sensing is a mathematical theory concentrated on calculating the finite-dimensional vectors in Rn.
- Secondly, instead of sampling the signal at distinct points in time, the compressive sensing systems normally achieve measurements in the constitutions of inner products among many general test functions and the signal. Due to the essence of advanced sampling methods, the system normally achieves signals by many basic linear measurements [62].
- According to the two schemes, the third one varies as they handle the restoration of signal, which means the issue of restoring the original signal from the compressive measurements.

According to Nyquist–Shannon scheme, signal reconstruction is attained via sinc installation– a linear process that has uncomplicated clarification and needs small computation. The flowchart of the sensing algorithm is shown in Figure 3.19. In compressive sensing, anyway, the recovery of a signal is normally attained by employing highly nonlinear techniques.

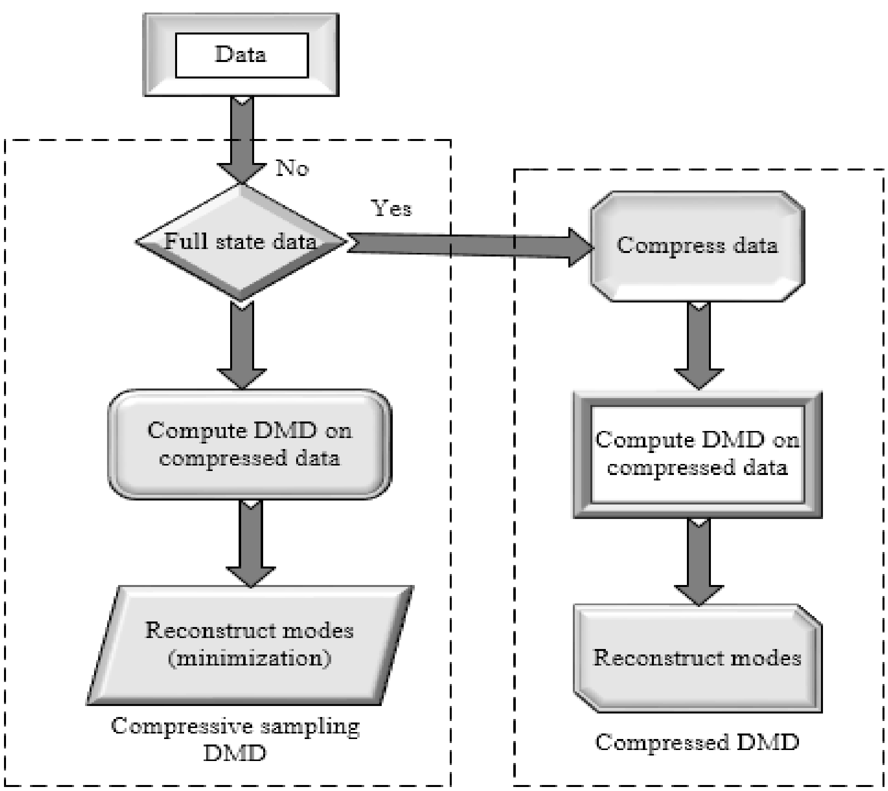

Figure 3.19: Flowchart of the sensing algorithm

3.31 Advantages of the sensing algorithm

- Reduction of the sampling rate of sparse signals
- Very few iterations can be used
- This helps in recovering images with sparse gradients
- It also effectively conceals and neglects any type of image noise and image artifacts such as streaking.

3.32 Disadvantages of the sensing algorithm

- Absence of tiny structure in reconstructed image or decadence of image resolution.
- It tends to have low relative error and higher interaction as compared to the TV method.
- It has low contrast regions.
- Tends to loss of low contrast information [63]

3.33 Applications of the sensing algorithm

- Performs in astronomy, biology, and communications
- Most probably used in image and video processing
- It can also be used for data collection in wireless sensor networks
- This can apply in detecting and estimating sparse physical signals

3.34 Summary

The position analysis of the Brushless DC motor is analyzed by using fixed order H∞ controller. The explanations of a Brushless DC motor and constructing parts like stator, rotor, and hall sensor are all detailed correctly. Then the H∞ control methods, H∞ control problems, and how the H∞ controller is used in Brushless DC motor are explained in detail. The existing methods like fuzzy PID controller, fuzzy PD control, and sensing algorithm are also mentioned in this chapter. The overall advantages, disadvantages, and applications of all the controllers are specified and the algorithm used here is IPSO, the principle of the IPSO algorithm and entire working process of the IPSO algorithm is detailed in step by step procedure.

CHAPTER 4

H-INFINITY CONTROLLER-BASED DISTURBANCE REJECTION IN CONTINUOUS STIRRED TANK REACTOR USING WATER WAVE OPTIMIZATION ALGORITHM

4.1 Introduction

This method is an H-infinity (H∞) controller-based disturbance rejection along with the appliance of a water wave optimization algorithm. H∞ controllers are used to synthesizing assured performance of certain applications as well as it affords maximum gain in any situation. It provide high disturbance rejection, guaranteeing high stability for any operating conditions. Continuous Stirred Tank Reactor (CSTR) is investigated for the application-oriented development as it includes complex reactions with high nonlinearity. The proposed work targets the contention of CSTR such as the difference in temperature and product concentration. The elimination of these issues is performed with the help of the proposed algorithm along with the controller operation. The planned work gives the enhanced performance employing disturbance rejection when compared with other existing controllers. Additionally, the proposed work improves the lifespan of the offered application through the destruction of disorders. The overall process is implemented in the MATLAB working platform and the results are compared with the preceding methods to show the expected performance.

4.2 Continuous stirred tank reactor

The Continuous stirred tank reactor (CSTR) is simply a structured, multipurpose, and inexpensive device that permits simple catalyst charging and substitute. Its combined nature allows the forthright regulation upon pH of the reaction and temperature and the supply or elimination of gases. The CSTRs are usually somewhat huge as the requirement to be effectively combined. Commonly, their volume of CSTRs is to be five to ten times the volume of the comprised powerless enzyme.

Nevertheless, it has the benefit that there is very slight resistance to the flow of the substrate stream that can comprise insoluble substrates or colloidal because the insoluble particles from the reactor are unable to swing the powerless enzyme. The backings are controlled by the mechanical nature of the stirring for the immobilized enzymes to materials that cannot simply collapse to provide 'fines' that can penetrate the creation stream [64]. But, fairly small particles (below around 10 mm diameter) can be utilized, while they are adequately dense to remain inside the reactor. Hence, it diminishes the issues because of the diffusional resistance.

The standard CSTR has entire combing resultant in a reduction of the substrate concentration and boosting of the product concentration and comparative to the last change, at each point inside the reactor the efficiency factor has been identified all over. So, the continuously stirred tank reactors are the chosen reactors and all the others are parallel for the methods including substrate inhibition or product activation. Moreover, it is helpful because the substrate stream comprises an enzyme inhibitor, although it is diluted inside the reactor.

Such result is very much visible while the inhibitor concentrations are higher than the inhibition continuous and [S]0/Km is maximum for uncompetitive inhibition or minimum for competitive inhibition while less outcome has attained by substrate dilution than the inhibitor dilution. The specifications of CSTR are shown in Table 4.1, The variations from the ideal CSTR behaviour appear while there is a fewer efficient combining regime and commonly, maybe win over by maximizing the stirrer speed and diminishing biocatalyst concentration or the solution viscidness or by efficient reactor baffling.

Table 4.1: Specifications of CSTR

Specification of the reactor	**Design dimensions**
Diameter of the reactor	1.683 m
Height of the reactor	1.346 m
Aspect ratio	0.8
Head depth	0.842 m

Shell thickness (vessel)	0.01115 m
Shell thickness (head)	0.411 m
Type of impeller	Four pitched blade turbine
Number of blades	4
Agitator diameter	0.561 m
Height of agitator from the tank bottom	0.561 m
Agitator blade width	0.1122 m
Input power	922.512 w
Agitator speed	14.703 m/s

The Continuous Stirred Tank Reactor (CSTR) to the adaptable regulator of the system in terms of polynomial synthesis along with the pole placement method. Frequently, the Computer simulation is utilized as its benefits over the experiment on an actual scheme that is every so often not possible and can be threatening, or time and money requires. The huge number of methods in the chemical industries are non-linear and the computer simulation will support to provide an understanding of the performance of the scheme. The arithmetical design is explained by differential equations, a set of nonlinear or linear equations. CSTR is broadly utilized for regulation since the cooling liquid or the input flow of the reactant may be simply restrained. According to the functional engineering attitude, CSTR concern with a set of nonlinear functions with bumped criteria. The analytical model of the reactors has been characterized by a group of nonlinear normal differential equations. Simulation results are then drawn for restraint, the initial process here is to identify convenient control schemes.

The polynomial access fulfilled the control needs together with furthermore needs, it can be drawn for a system with negative terms like non-minimum phase attitude and mechanism with time lags.

The accessing technique associated with pole placing satisfies the stability and non-associated tracing of the reference signal allowance of disruption. Two structures are applied for the control system among that the initial structure with one degree of freedom (1DOF), which governors on evaluation section, and next the second process with two degrees of freedom (2DOF) with evaluation and feed leading parts. The adaptation is assured by evaluating the parameters of the model with directional forgetting and recursive least-squares technique. An external linear constant time scheme is utilized as an input-output description for the regulated system because the model is nonlinear.

The need is the growth from the simulation of the behaviour to regulate a non-linear method signified by the continuous stirred tank reactor taken from. As is mentioned above, the structure is to explain the method from modelling and simulation to regulate a dynamic procedure. Four major steps are linked equally composed. The objectives of simulation analysis are required to describe containing a gathering of the entire obtainable information and the experimental experience with the researched kind of the plant. The main class of systems are non-linear or the variable quantity is more. This complication tends to be the starter of certain interpretations. The modelling is mainly the toughest stage.

The method is explained by its specific variables such as concentration, pressure, flow rate, temperature, etc., typically known as state variables and the arithmetical relations between variables later construct an arithmetical model. The arithmetical model arrived from the stability within the plant and it is indicated by a set of partial or ordinary differential equations, linear or nonlinear equations, etc. The simulation experiment outcomes are useful ways how to test the appropriateness of the acquired arithmetical model.

Normally, it contains two sections as static assessment and dynamic assessment. The outcomes of the static assessment are based on correct functioning points. Conversely, the dynamic assessment delivers frequency responses, step responses, etc. that show the system behaviour dynamically and they are the basis for selecting an external linear model. The contrast between simulated outputs and real system output and proves the sustainability of the arithmetical scheme. It is essential to rebound modelling and stop certain simplifications when the variation between the model and actual systems is unsuitable.

The objective is to discover the easiest model with an acceptable explanation of the actual procedure. After simulation, the issues are considered in the view of the control point i.e., to discover a controlling regulator for dynamic assessment in a suitable procedure. The acquired regulator should fulfil necessities including disturbance attenuation or asymptotic tracking of the reference, properness, and stability. To design such a type of controller various techniques are available. The regulating conditions are established by configuring two degrees-of-freedom (2DOF) and one degree-of-freedom (1DOF) along with groupings polynomial techniques.

These techniques can be utilized in a system with some negative control properties like transport delays, instability, or non-minimum phase on the systems. Then, the acquired regulators have been employed to simulate when the outcomes are satisfactory and are also utilized to regulate the dynamic issues [65]. The process which is explained in the earlier chapter has utilized on the actual nonlinear procedure signified by a Continuous Stirred Tank Reactor (CSTR). The next aim is the External Linear Model (ELM) and it can be acquired from the dynamic research. It is assumed that the cooling liquid and reactant are suitably mixed and, the heat capacities of reactant, volumes, cooling liquid, and densities are presumed to be stable.

4.3 Mathematical modelling of CSTR

Regrettably, in most cases, the formation of the attitude kinetics still extended to be unreliable. The existence of most of the unpredictability provides an unsuccessful control pattern that uses redundant instructions about the mechanism. Correspondingly to further research works in this field, some expectations have been developed in the endeavour to decrease the design complication. In peculiar, some of the considerations are following,

- There is an entire consistency of absorption and temperature inside the reactor and an entire consistency of temperature in the inner side of the jacket.
- The jacket and reactor quantity are stable.
- The reaction agitation is K^{-1} function.
- The thermal transfer between the jacket and the reactor is declared by a constant global heat transfer coefficient S and the magnitude of heat received in the activator walls can be examined inconsequential.

- The reaction enthalpies ΔF_{Ve} are self-reliant temperature is negative for exothermic reactions and positive for endothermic reactions.
- The heat quantities ky_1 *and* ky_2 of the mechanism fluids i.e. reactor contented and heat exchange medium is stable.

By the given above considerations, the energy and material harmonies enforced to jacket reactor gives the following mathematical model [66].

$$\begin{cases} \dot{x} &= Kv(x^v,T)+\dfrac{W}{R_1}\left(x^{in}-x\right) \\ \\ \dot{T} &= F_V{}^T V\left(x^v,T\right)+\dfrac{SM_t}{\rho_1 R_1 ky_1}\left(T_d-T\right)+\dfrac{W}{R_1}\left(T^{in}-T\right) \\ \\ \dot{T}_d &= -\dfrac{SM_t}{\rho_2 R_2 ky_2}\left(T_d-T\right)+\dfrac{J}{R_2}\left(T_d{}^{in}-T_d\right) \end{cases} \tag{4.1}$$

That can be recast as,

$$\begin{cases} \dot{x} &= Kv\left(x^v,T\right)+j\left(x^{in}-x\right) \\ \\ \dot{T} &= L\left(x^v,T\right)+w_1\left(T_d-T\right)+j\left(T^{in}-T\right) \\ \\ \dot{T}_d &= -w_2\left(T_d-T\right)+S \end{cases} \tag{4.2}$$

Where $x \in EV^z$ represents the vector of the z concentrations of products p and reactants r, $x \in EV^v$ indicates the vector of concentrations r of reactants, $k \in EV^{z\times a}$ resembles the characteristic matrix of the stoichiometric coefficients $v\left(x^v,T\right) \in EV^a$ is the vector of reaction kinetics, $F_v{}^T = \left[\dfrac{(-\Delta F_{V1})}{\rho_1 ky_1},\ldots.\dfrac{(-\Delta F_{Va})}{\rho_a ky_a}\right] = \left[L_1, L_2 \ldots L_a\right] \in EV^a$ is the vector of reaction enthalpies $T \in EV_+$ indicates the reactor temperature $j \in EV_+$ indicates the dilution rate, which is the ratio of the volume of the reactor and feeds stream flow rate $x^{in} \in V^z$ describes the vector of non-negative reactor feed concentrations, $L(x^v, T) = F_v^T v(x^v, T) \in EV$ specify the global reaction heat, $W_1 \in EV_+$ imply the heat transfer parameter of side reactor, $W_1 \in EV_+$ suggests heat transfer parameter of side jacket, $T_d \in EV_+$ highlights the jacket temperature $T^{in} \in EV_+$ represents the reactor feed temperature $T_d^{in} \in EV_+$ indicates the feed temperature of jacket stream and $S \in EV$ resembles the manipulated heat. The components l_e of the vector of reaction enthalpies, for endothermic reactions, F_v^T are positive and for exothermic reactions F_v^T are negative. Finally, the physical parameters of the model are listed in Table 4.2.

Let $x_{uu}, T_{uu}, T_d^{uu}, s_{uu}$ be steady-state values of input variables and state respectively and then the deviation variables can be given as,

$$
\begin{aligned}
\psi &= x - x_{uu} \in EV^z \\
\varsigma &= T - T_{uu} \in EV \\
\eta &= T_d - T_d^{uu} \in EV \\
\delta\mu &= S - S_{uu} \in EV
\end{aligned}
\tag{4.3}
$$

Table 4.2: Physical criterion for the CSTR model

PARAMETER	DESCRIPTION
M_t	Heat transfer field a^2
R_1	Reactor volume a^3
R_2	Jacket volume a^3
ky_1	Reactor fulfilled heat quantity $KJ / Kg\ ^\circ C$

ky_2	Heat exchange fluid heat quantity $KJ/Kg\ ^{\circ}C$
ρ_1	Reactor fulfilled density KJ/a^3
ρ_2	Heat exchange fluid density KJ/a^3
J	The volumetric flow rate of feed torrent $a^3/\min$
W	The volumetric flow rate of heat exchange fluid $a^3/\min$
S	Universal heat transfer coefficient $KJ/^{\circ}Ka^2 \min$
ΔF_{Vi}	The heat of the i^{th} reaction at temp $T, KJ/mol$

Where,

$$\psi = Y_e^{v} \psi_e \tag{4.4}$$

Here, Y_e^v is as in $x_e^{\ v} = Y_e^{\ v} x$ and $\left(\psi^v\right)^T = \left[\psi_1^{\ v} ....\psi_a^{\ v}\right] \in EV^a$ then the scheme (4.2) can be rewritten as,

$$\begin{cases} \dot{\psi} = K\tilde{v}\left(\psi^v, \varsigma\right) + j\left(\psi^{in} - \psi\right) \\ \dot{\varsigma} = -\left(w_1 + j\right)\varsigma + w_1\eta + \beta\left(T_{uu}, T_d^{\ uu}\right) + \tilde{C}\left(\psi^v, \varsigma\right) \\ \dot{\eta} = w_2\varsigma - w_2\eta - w_2\left(T_d^{\ uu} - T_{uu}\right) + S_{uu} + \int s \end{cases} \tag{4.5}$$

Where,

$\beta\left(T_{uu}, T_d^{\ uu}\right) = w_1\left(T_d^{\ uu} - T_{uu}\right) + d\left(T^{in} - T_{uu}\right), \tilde{v}\left(\psi^v, \varsigma\right) = v\left(\psi^v + x_{uu}^{\ v}, \varsigma + T_{uu}\right), \psi^{in} = x^{in} - x_{uu} \in EV^z$ and the reaction heat.

$$\tilde{L}\left(\psi^{v}, \varsigma\right)=L\left(\psi^{v}+x_{uu}{}^{v}, \varsigma+T_{uu}\right)$$

Can be declared as,

$$\tilde{L}\left(\psi^{v}, \varsigma\right)=L_{0}+L_{1}\psi^{v}+L_{2}\varsigma \tag{4.6}$$

In singular, if the agitation pursue the Arrhenius law, one has

$$L_{0}=L_{0}\left(x_{uu}{}^{v}, T_{uu}\right)=F_{v}{}^{T}\tilde{v}_{0}\left(x_{uu}{}^{v}, T_{uu}\right)=F_{v}{}^{T}\begin{bmatrix}\psi_{1}\left(x_{1uu}{}^{v}\right)c_{01e}-I_{1}/VT_{uu}\\ \psi_{2}\left(x_{2uu}{}^{v}\right)c_{02e}-I_{2}/VT_{uu}\\ \vdots\\ \vdots\\ \psi_{a}\left(x_{auu}{}^{v}\right)c_{0ae}-I_{a}/VT_{uu}\end{bmatrix}\in EV \tag{4.7}$$

$$L_{1}=L_{1}\left(x^{v}, T\right)=F_{v}{}^{T}\begin{bmatrix}L_{11} & 0 & \cdots & 0\\ 0 & L_{12} & \cdots & \vdots\\ \vdots & \vdots & \cdots & 0\\ 0 & 0 & \cdots & L_{1a}\end{bmatrix}\in\left(EV^{a}\right)^{*} \tag{4.8}$$

With

$$\begin{aligned}L_{11}&=L_{11}\left(x_{1}{}^{v}, T\right)=\left(\frac{\psi_{1}\left(x_{1}{}^{v}\right)-\psi_{1}\left(x_{1uu}{}^{v}\right)}{x_{1}{}^{v}-x_{1uu}{}^{v}}\right)L_{01e}-I_{1}/VT \quad \in EV\\ &\vdots\\ L_{1m}&=L_{1m}\left(x_{m}{}^{v}, T\right)=\left(\frac{\psi_{m}\left(x_{m}{}^{v}\right)-\psi_{m}\left(x_{muu}{}^{v}\right)}{x_{m}{}^{v}-x_{muu}{}^{v}}\right)L_{0me}-I_{m}/VT \quad \in EV\end{aligned} \tag{4.9}$$

And

$$L_{2}=L_{2}\left(x_{1uu}{}^{v}, T\right)=Fv^{T}\begin{bmatrix}\psi_{1}\left(x_{1uu}{}^{v}\right)c_{01}\left[\dfrac{e-I_{1}/VT-e-I_{1}/VT_{uu}}{T-T_{uu}}\right]\\ \psi_{2}\left(x_{2uu}{}^{v}\right)c_{02}\left[\dfrac{e-I_{2}/VT-e-I_{2}/VT_{uu}}{T-T_{uu}}\right]\\ \vdots\\ \psi_{m}\left(x_{muu}{}^{v}\right)c_{0m}\left[\dfrac{e-I_{m}/VT-e-I_{m}/VT_{uu}}{T-T_{uu}}\right]\end{bmatrix}\in EV \tag{4.10}$$

The functions $\psi_1\left(x_e^{\,v}\right)$ represent the diagonal matrix component at the reaction rate $v\left(x^v,T\right)=\psi\left(x^v\right)c\left(T\right)$. As the simplified form, deviation coordinates the system (4.5) is considered,

$$\begin{cases} \dot{\psi} = K\tilde{v}\left(\psi^{v},\varsigma\right)+ j\left(\psi^{in}-\psi\right) \\ \dot{\varsigma} = -\left(w_1 + j\right)\varsigma + w_1\eta + L_1\psi^{v} + L_2\varsigma \\ \dot{\eta} = w_2\varsigma - w_2\eta + \int s \end{cases} \tag{4.11}$$

4.4 Construction of CSTR

The traditional CSTR design is incapable of continuing the pH and the temperature in the suitable method. Established pH, digital pressure display, and the temperature sensor to acquire a nice regulator upon the system. The reactor is made up in the university workshop. In this exploration, the dimension of the CSTR reactor is considered and it is magnified by deciding the working volume (2.7 L) and reactor's total (4.5 L). The major digester is made of stainless steel and glass. And, it is firmly sealed using steel plate capping in combination with 6 nuts, and the plate is mounted by a stirrer motor. Some of the essential constructing parts of the CSTR are discussed below,

4.4.1. Wall jacket

The wall jacket present in the CSTR will conceive a double-wall, in which the water is dispersed for heating and cooling. By attaching the reactor to the outer surface recirculating water tub armed with a pump, then the temperature of the reactor can be restrained in the entire process. Every single CSTR can be heated separately or combined in series. Figure 4.1, shows the diagrammatic representation of a continuous stirred tank reactor. Even though several recirculating water bath pumps have the quantity to produce a great abundant flow rate (20-30/min).

4.4.2. Feeding port

Normally, the CSTR bioreactors comprise feeding ports in two various sizes. The biggest one conceives it simple for solid feedstock to achieve down beneath the surface of the reactor capacity.

Then in the smaller ones, the Liquids can be sustained, either self-regulating with the guidance of a syringe or instinctively by a pump.

4.4.3. Gas outlet

The gas outlet has been modelled to experience a precise with gas stiff tube-like Tygon® connected to it, for margin the gas into a pack or along with the disclosure unit.

4.4.4. Sampling port

On account of the global sampling port, it is desirable to haul samples for the offline evaluation of criteria including temperature and PH. The plastic adapter has been drawn to inject a PH sensor for online governing. However, the plastic adaptor will be equipped based on the demand.

4.4.5. Viewing port window

The stainless steel adaptation contains dual perceiving ports on their opposite sides, where scum arrangement has been identified at the time of the assimilation process. Then the important thing that needs to make clear is that the protective film is ejected. Glossal lamp through the back window, for the reason of getting an exact view inside the tank, while observing through the front window.

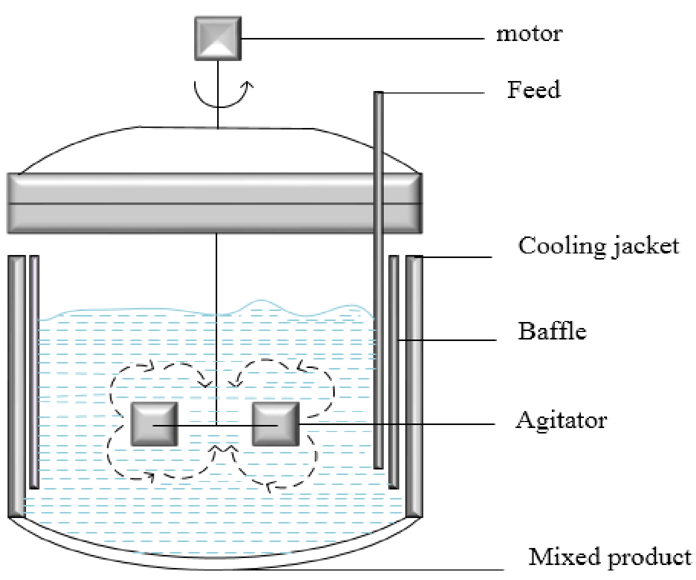

Figure 4.1: Diagram of CSTR

4.4.6. Ball valves for discharging and emptying

The ports for discharging and clearing the stainless-steel tanks have been closed and opened simply by the use of the ball valves. Here ON represents that the valve is open whereas OFF represents that the valve is closed.

4.4.7. Self-discharging port & auto slurry control

The stainless-steel composition attempts an automatic slurry level restraint. In the interior part of the reactor, the emptying tube achieves up between the surfaces of the tank to culvert any slurry that achieves over its rim.

4.4.8. Adjustable feet

When compared to other compositions the stainless-steel composition also had an adjustable foot, this makes the machine easy to authorize and able to change the level of the reactor.

Also, it would be with a speed regulating device and has a range of 100 to 260 rpm. A heater has also been mounted in the scheme to preserve the temperature. The feeding tank has been added for feeding purposes. The Biogas would be gathered via a biogas collection tank. In the digestor, a partial fraction is produced and it was encapsulated by a triangular-shaped biogas distributor with nearly 1 mm openings linked with a pump (230V, Deng Yuan).

In the digester, a digital gas flow meter had been mounted for monitoring the production of biogas. The CSTR would be verified for media degradation and blockage before initiating the recirculation of biogas. The CSTR was functioned at mesospheric state 28e37 C along with an electric heater. The efficiency of the CSTR had been assessed by deciding the biogas production, COD removal effectiveness mostly. Every value of the investigational parameters would be authenticated by triplicated investigational trials. Some of the raw materials drawn for the manufacturing process of the CSTR parts are given below,

Raw materials utilized for CSTR parts

a) Ng600wh is a plastic engraved from glass strengthened Nylon USP.

b) EPDM rubber is an ethylene propylene diene monomer rubber.

c) AISI316 is an acid criterion case stainless steel material with huge resistance to deterioration and heat.

d) Borosilicate glass is a form of glass, which has lesser nervous to thermal collapse.

e) FEP and PTFE are fluorinated and polytetrafluoroethylene, similarly a material called Teflon.

4.5 Working of CSTR

These days, reactors play a primary role in the numerous chemical industries. The Chemical reactions in a reactor are either exothermic or endothermic and need that the energy can either be eliminated or added to the reactor to retain the stable temperature. The exothermic reactions are highly nonlinear due to the potential safety issues and the likelihood of interesting behaviour like several stable conditions. The CSTR showing exothermic reaction is taken into consideration in the current work.

The permanent exothermic reaction comes in the CSTR procedure pattern. A coolant medium eliminates the heat of the reaction which runs via a 12 jacket around the reactor [67]. Through a pump, a fluid stream is fed to the reactor from the feed tank. The control of the CSTR is shown in Figure 4.2, for accelerating the reaction, a catalyst is positioned inside the reactor and as a result, it stays chemically unaffected during the reaction. By utilizing a conductivity meter, the concentration is quantified. By utilizing a thermocouple, the temperature of the fluid in the tank and the jacket are quantified.

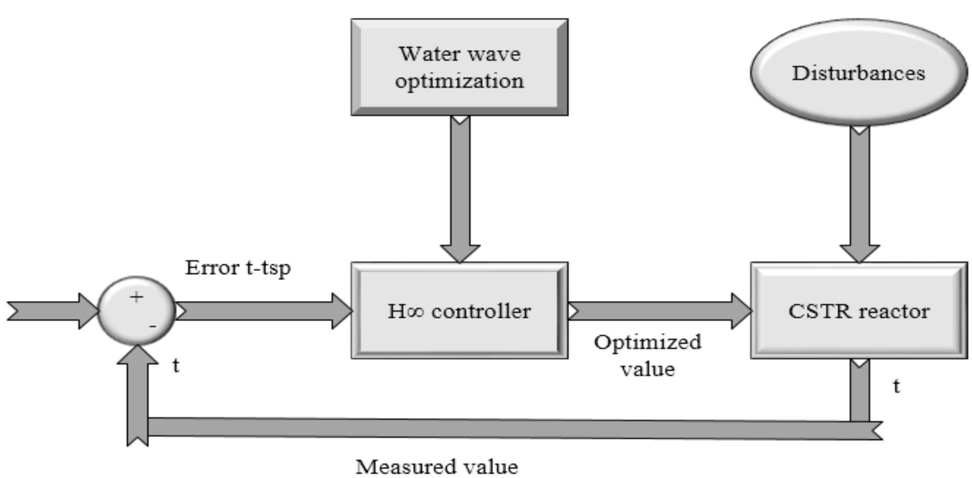

Figure 4.2: Control of the CSTR

Also, via a multi-input multi-output data attainment card, the sensor data are fed to the system. The liquid inside the reactor is rightly mixed and send out via the exit valve. The jacket has the coolant which is fed from the coolant feed tank via a pump. To make the cooling efficiency, the jacket is considered to be at a lower temperature than the reactor. The real feed flow rate of the coolant is decided and a changeable speed pump is actuated to regulate the operation changeably.

4.6 Mathematical modelling of H∞ controller in CSTR

The reaction succeeds inner the reactor is expressed in equation (4.12), and the heat condition of the system can restraint with the support of a scheduled feedback controller. It is evaluated on the exit portion of the reactor.

$$\begin{aligned} cyclopendtadiene + cyclopentenol &= cyclopen\tan ediol \;\; 2(cyclopendtadiene) \\ &= Dicyclopendtadiene \end{aligned} \tag{4.12}$$

The combination of the H∞ controller with CSTR will neglect the undesirable disruptions, which may distress the operating of the compensator. The function of the controller is to govern the gain variables like temperature or flow rate by correlating along with the setpoint is known as expected value. The variation among the consistent value and the desired value is known as fault signal and it is represented in equation (4.13).

$$fault\,signal = consistent\,value - set\,po\text{int} \tag{4.13}$$

The formula for manipulating the setpoint is inclined as follows,

$$\begin{aligned} t_{uy} &= \frac{I}{\ln\left(\gamma K_{out}\right) - \ln\left[\frac{W}{R}(K_{feed} - K_{out}) - \Delta\right]} \\ &where, \\ \Delta &= \frac{W}{R}\left(K_{feed} - K_{out}\right) - \gamma K_{out} \exp\left(-I\right) \end{aligned} \tag{4.14}$$

The temperature difference (Δt) can be computed with the support of equation (4.15).

$$\Delta t = \frac{W}{R}\left(t_{feed} - t\right) + \left(\frac{-f}{\sigma k}\right)\gamma\, k_{out} \exp\left(\frac{-I}{t}\right) t1 + \frac{W_k}{R}\left[1 - \exp\left(\frac{-\tau}{W_k \sigma_k} t_2\right)\right]\left(t_{feed} - t\right)$$

(4.15)

Where,

$$t1 = \exp\left(\frac{-0.0067I}{2t} T1\right) \;\&\; t2 = 1 - 0.01T2 \tag{4.16}$$

The time-changing approaches are determined as t1 and t2 in the previous equation (4.16). The consolidation of liquid inner the CSTR can be computed by employing the upcoming equation (4.17).

$$concentraction = \frac{0.0836}{1 + \left(6.37 \times 10^{-30}\right)\tau} \tag{4.17}$$

The formula given in equation (4.17), τ represents the time duration taken for the CSTR operation.

Tsp and t expressed as desired and systematic temperature. Reduction of external disruption is the major objective of the proposed technique. Then the transfer function of the scheme can be declared in equation (4.18).

$$Y = \begin{bmatrix} Y_{11} & Y_{12} \\ Y_{21} & Y_{22} \end{bmatrix} \tag{4.18}$$

From the above-mentioned equation, the measured and fault signals can be computed by applying the succeeding equations (4.19) and (4.20)

$$\eta = Y_{11}\delta + Y_{12}\gamma \tag{4.19}$$

$$t = Y_{21}\delta + Y_{22}\gamma \tag{4.20}$$

The actual and error signal can be expressed as t and η respectively. like that $\delta \,\&\, \gamma$ stands for exterior inputs (disruptions) and restraint signal (advanced value) respectively. By using the feedback law, the evaluation of the restraint signal is given in equation (4.21).

$$\gamma = ct \tag{4.21}$$

The concluding formula for the fault evaluation process is given in equation (4.22).

$$\eta = \left[Y_{11} + Y_{12} C\right]$$

(4.22)

The function $\Psi(Y,C)$ must be decreased to cancel the fault value. There are various conditions possible to attain the planned process. Some of them are given as follows,

- Excellent disruption evection at low-frequency regions can be set by creating the term $(1+YC)^{-1}$ as short as feasible $\delta = 0$.
- The decreasing of the closed-loop transfer function has been accomplished with the benefits of objective value $1-(1+YC)^{-1}$ $for\ f = \infty$.
- Preservation units for criterion deviations can be obtained by decreasing $C(1+YC)^{-1}$.

At last, the reduction function can be denoted by equation (4.23).

$$\Psi(Y,C) = \begin{bmatrix} Q_1 (1+YC)^{-1} \\ Q_3 1-(1+YC)^{-1} \end{bmatrix} \tag{4.23}$$

Where, $Q_1\ and\ Q_3$ are the frequency depending matrices.

4.7 Advantages of CSTR

Some of the advantages of the continuous stirred tank reactor are,

- It requires very low operating cost
- Simple to clean
- The design structure is simple
- Excellent control facility
- Great temperature control
- Regular continuous operation
- Back mixing of heat developed by exothermic reactions, which raises attitude rate and consequent reactor attainment.
- Neglecting of reactor circumstance for extreme exothermic reactions, accomplishing temperature easier to restraint.
- Promoting low-order reactions in the coordinate lateral reaction scheme.
- Operation is commercial when huge volumes need large contact time
- Improvement of heat transmission by mixing

4.8 Disadvantages of CSTR

Some of the disadvantages of CSTR are,

- CSTR has the least transformation per unit volume
- Have low disturbance when handling bypass and transmitting
- It can be observed that this kind of reactor occupy major benefits than its dupe
- Sometimes defects may occur on cable or further equipment. When this happens, the panel will not show the exact value and may disturb the entire mechanism of the operation.
- Time may be inadequate, this may cause the needed data not to attain.
- Usually, CSTR needs bigger reactor volumes, when related to other reactor systems.
- Stamina for agitation is needed in the tank.

4.9 Applications of CSTR

- Especially CSTR is favourable for reaction process that needs low concentrations like the distinction between various reactions or substrate obstacle in a chemostat.
- The reactor also had utilization for composite systems in this high mixing provides great association time among the phases.
- The type of liquid-liquid CSTR is drawn for the signification of fats and interruption and cosmetic polymerizations.
- The gas-liquid mixers are drawn for the decomposition of cyclohexane. Normally gas homogenous CSTR is intensely unique.

4.10 H∞ controller in CSTR

In the regulated system, the H-infinity controller design techniques are utilized to integrate the controllers for attaining steadiness with the promised execution. A control designer states the regulate issue like an arithmetical optimization issue to utilize the H-infinity technique and later, estimates the controller parameters. The block diagram of the H∞ controller in CSTR is depicted in Figure 4.3, the design-based methods to control the system models can be stated in the literature to assure the stability and the strong process of the system. An exciting contrast among the numerous methods is drawn in.

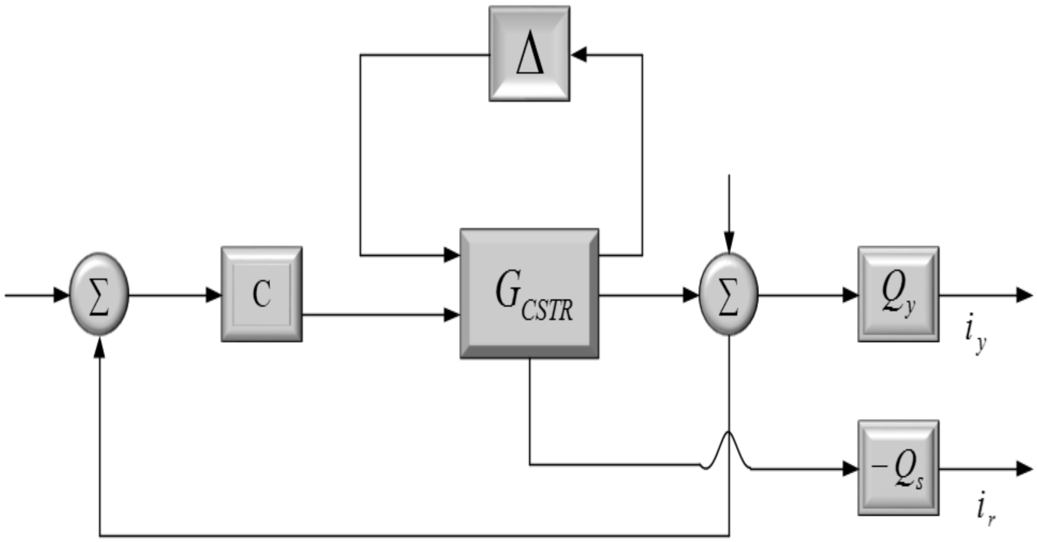

Figure 4.3: Block diagram of the H∞ controller in CSTR

The key to regulating the design issue in terms of the Riccati equation method usually generates a regulator which tolerates from the pole-zero cancellations between the regulator and plant [68]. Additionally, certain terms in the time domain like peak overshoot (closed-loop damping ratio), settling time do not obtain in a forthright way in the Riccati-based design. The Riccati-based model is deeply based on the suitable choice of weights for training the plant. In the design of the damping power system, there is no perfect process for the weight choice. The arithmetical method to solution via an LMI formulation contains different benefits however, the resulting regulator cannot undergo the issue of pole-zero cancellation.

4.11 Operation of water wave optimization

Water wave optimization (WWO) is a novel meta-heuristic that takes motivation from the shallow water wave patterns for universal optimization. An answer to the problem is similar to a wave in the wave water optimization and the stochastic search procedure of the algorithm is observed as a motion wave containing refraction, breaking, and propagation. The waves with high robustness most likely move to close places by propagation to strengthen the local strength when the waves with low strength tend to move to faraway places to make ease the global search.

Moreover, the finest wave breaks into a group of isolated waves to additional improve manipulation and the stable waves dropping their energy diverts to arbitrary locations to evade the search inactivity and rise the diversity of the population. In the WWO algorithm, the integration of the three processes offers a better balance between the investigation and exploitation [69]. The arithmetical investigates on the CEC 2014 standard suite display that the WWO algorithm surpasses an amount of the latest heuristics consisting of Bat Algorithm, Biogeography Based Optimization, Gravitational Search Algorithm, Invasive Weed Optimization, Hunting Search and novel Energy-Aware Bee Colony Approach[70]. The water wave optimization has been effectively applied to the actual world high-speed train arrangement issue in china.

The water wave optimization has an easy structure and it is simple to execute with a simple population size and contains only some regulated parameters. Additionally, the WWO algorithm is simplified by considering two alterations:

1) The refraction operator is letting out from the algorithm.

2) Considering the population size reduction policy, the convergence speed will be accelerated, at the same time (slightly) the weeding-out effect of the refraction operator is compensated.

The WWO algorithm is a novel nature motivated optimization technique in which the solution space of the issue is similar to the seabed region, and every solution is similar to the "wave" with a wavelength λ and height h, and then the fitness of every wave is quantified by the depth of seabed as the minimum distance to the still water level and higher fitness value. While preparing the population, every wave, t is set to a constant $t_{\max}$ and λ is set to 0.5. For every production, the WWO algorithm utilizes three kinds of processes, including refraction, breaking, and propagation to constantly develop the waves on the way to the global optimum.

4.11.1. Propagation:

For every wave Y , the propagation worker makes a new wave Y' by calculating a dissimilar displacement at every dimension j and included it with the original wave [71]:

$$Y'_j = Y_j + rand(-1,1).\lambda B_j \tag{4.24}$$

where B_j indicates the length in the j dimension of the search space and $rand$ represents the function that produces an arbitrary number same as that of distributing in the stated range.

Subsequently, the ability of $Y' : if\ f(Y)$ is estimated as higher than $f(Y), Y'$ utilizes the position of Y in the population, and $t_{\max}$ represents the reset height; Or else, Y can be remained and diminish its height by one, that imitates the energy excess because of bottom friction, vortex shedding, and inertial resistance. It is viewed as the waves placed in the deep water contain exceeding wavelengths with less height of the wave, and in shallow water, waves contain increased wave height and short wavelengths. While transferring a wave from deep water (low fitness location) to shallow water (high fitness location), then the wavelength gets diminution. After every generation, the WWO algorithm computes the wavelength of every wave Y as follows:

$$\lambda = \lambda.\alpha^{-\left(f(X) - f_{\min} + \in\right) / \left(f_{\max} - f_{\min} + \in\right)} \tag{4.25}$$

where $f_{\max}$ represents maximum fitness value, $f_{\min}$ indicates minimum fitness values amid the present population, $\in$ defines a small constant that evades division by zero and α resembles the parameter known as wavelength lessening coefficient,

4.11.2. Breaking:

Generally, the breaking operator splits a wave into a sequence of solitary waves while its wave celerity is surpassed by crest velocity. The WWO algorithm only executes splitting a wave Y to reaches a place more suitable than the present best solution Y_{best} [72]. Every isolated wave Y' Y is acquired by arbitrarily choosing C dimensions (C indicates a random number between a predefined number $c_{\max}$ and 1) and including a dissimilar offset to the initial location at every dimension j as:

$$Y'_j = Y_j + gaussian(0,1).\beta B_j \tag{4.26}$$

Where the braking coefficient is indicated by β , and Gaussian (0, 1) represents a function producing a Gaussian arbitrary number with standard deviation 1 and mean 0. While the fittest solitary wave Y' is more suitable than Y, Y' utilizes the position of Y in the population.

4.11.3. Refraction:

A wave Y is created by a refraction operator, with height diminutions from zero to learn Y_{best}, which imitates the difference of the wave while its beam is not vertical to the isobaths. By refraction, the new location Y' is computed for every dimension as an arbitrary number centered halfway between the initial position and $Y_{best,}\ j$:

$$Y'_j = gaussian\left(\frac{Y_{best,\,j} + Y_j}{2}, \frac{Y_{best,\,j} - Y_j}{2}\right) \tag{4.27}$$

Subsequently, the wave height X' is reset to $t_{\max}$, and updated wavelength is given as:

$$\lambda' = \lambda \frac{f(Y)}{f(Y')} \tag{4.28}$$

The detailed flow of the WWO algorithm is represented in Figure 4.4, In short, the propagation operator creates maximum strength waves utilize small region and minimum strength waves investigate huge regions, local search is increased by the breaking operator among the best wave to develop the solution precision,

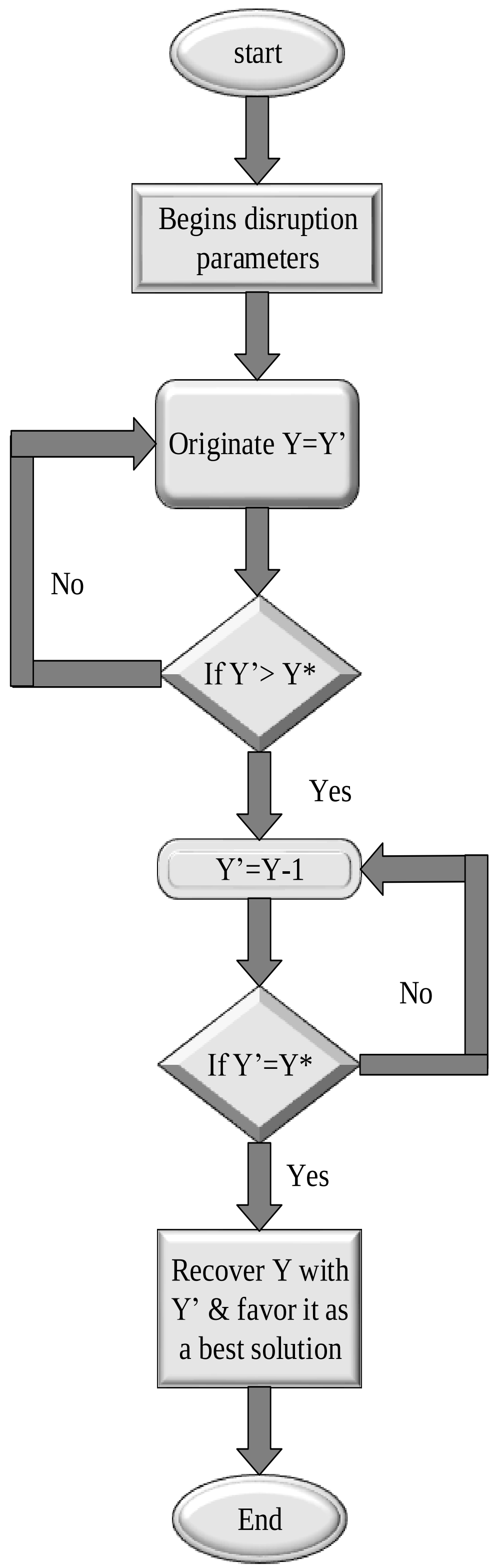

Figure 4.4: Flow chart of WWO algorithm

4.12 Advantages of WWO algorithm

- It is a simple scheme.
- Requires only a few control parameters [73].
- It is easy to recognize.
- Does not require bulk calculation as it dominance a mini population.
- Make an energetic search in a large dimensional solution area.
- Large span positions can be conquered

4.13 Disadvantages of WWO algorithm

- Inability to comply with the different heights and frequency of waves.
- Restrain optimization through flexibility [74]
- The broad waves will decrease the efficiency of the equipment's
- When the waves are too strong it may cause damage

4.14 Applications of WWO algorithm

- Used in real-world engineering development issues.
- The design is sustaining constant developments, on account of velocity, certainty & abstraction.
- To clear the high-speed train organizing issues
- It explains the effectiveness and workability of metaheuristics in the real-world appliance.

4.15 Existing methods

In the proposed technology of H∞ controller-based disturbance rejection in CSTR involves some existing methods. The performance of the temperature, time and concentration are all needed compare with the existing controllers such as the Proportional Integral Derivative controller, Artificial Neural Network, and Active Disturbance Rejection Controller.

4.16 Artificial neural network

ANN is a new effective computing and information-processing method explored by biological neuron processing. ANN models are broadly employed in different fields of science and technology including process control, pattern recognition, time series forecasting, etc. ANNs are being applied successfully for designing diverse functions since the 1980s. An automatic training process is utilized to understand these functions effectively to the network. Moreover, various problems considering the network architecture are not known properly. The classification of the ANN algorithm is detailed in fig 4.5. Various researchers have considered ANNs as a black-box model that is not able to establish useful and crucial understandings of the basic nature of the physical processes.

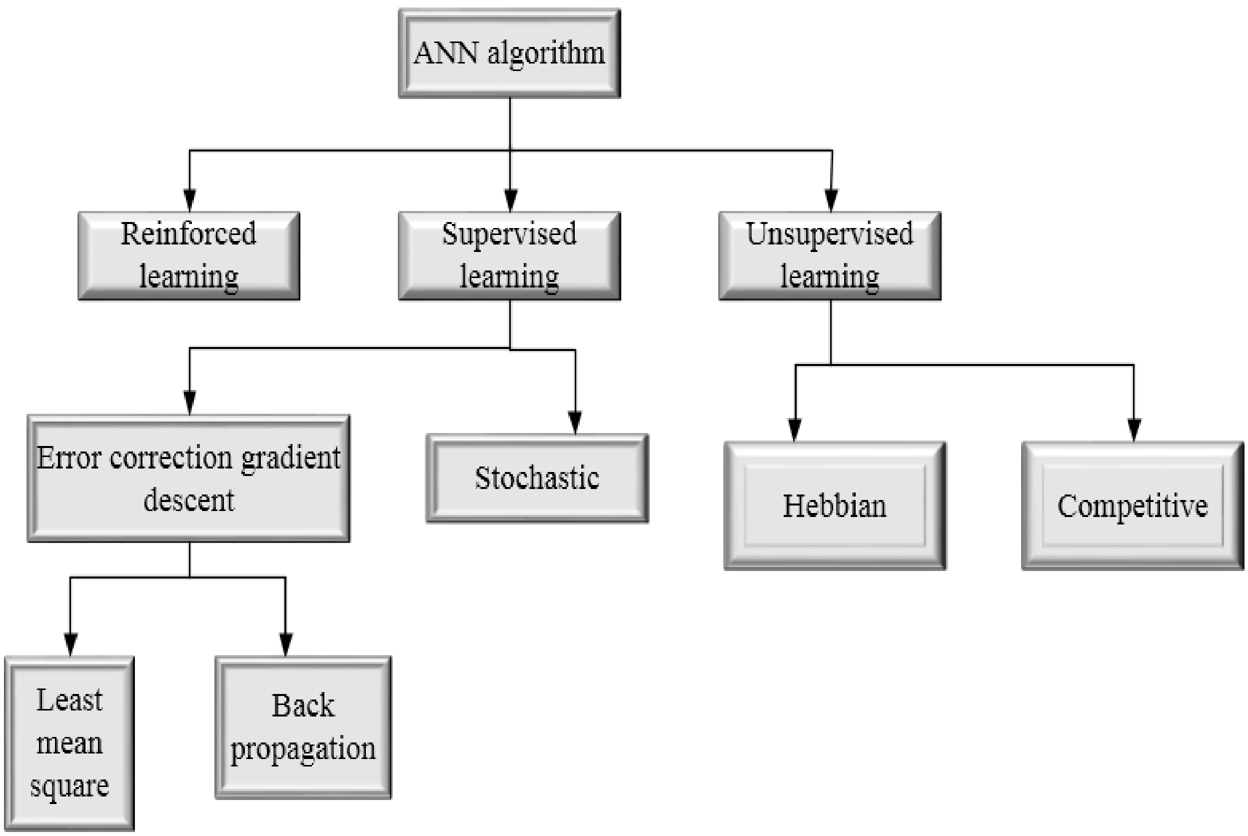

Figure 4.5: Classification of ANN algorithm

An ANN tries to imitate, in a simplified manner, the neural functions and structure and human mental. It comprises numerous simple neurons which are parallelly interconnected so that it performs as a collective system [75]. In network topology, ANN usually contains several layers and set of neurons (nodes) that are interconnected by links. The block of the ANN algorithm is given in Figure 4.6. The weighted input from a previous layer is received and processed in every node present in the layer and forwards its output to the nodes present in the next layer via links. The weight is assigned for every link, and the weight represents the numerical evaluation of the interconnection capability. Typically, based on the transfer function the weighted sum of inputs to a node is transferred to an output (generally a sigmoid function).

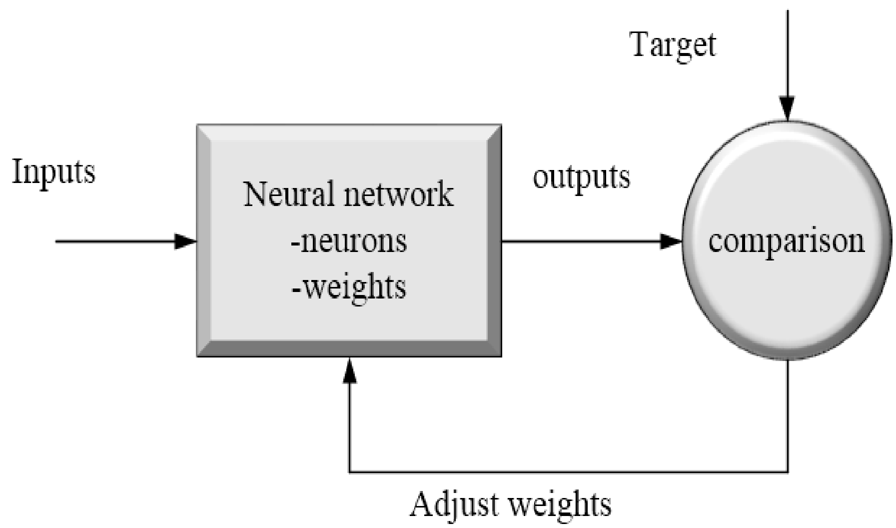

Figure 4.6: Block of ANN training

The layers of artificial neural networks are as follows,

- The input layer is drawn to current information in the network.
- The output layer is considered to obtain a suitable response for the corresponding input.
- Then one or more intermediate layers are considered to play as a group of feature detectors.

One of the most significant tasks is establishing a proper network architecture, and the complex task is a model-building process. The function process of the ANN algorithm is shown in Figure 4.7. It is expected to model ANN carefully otherwise, it tends to over parameterization, which causes large redundant network.

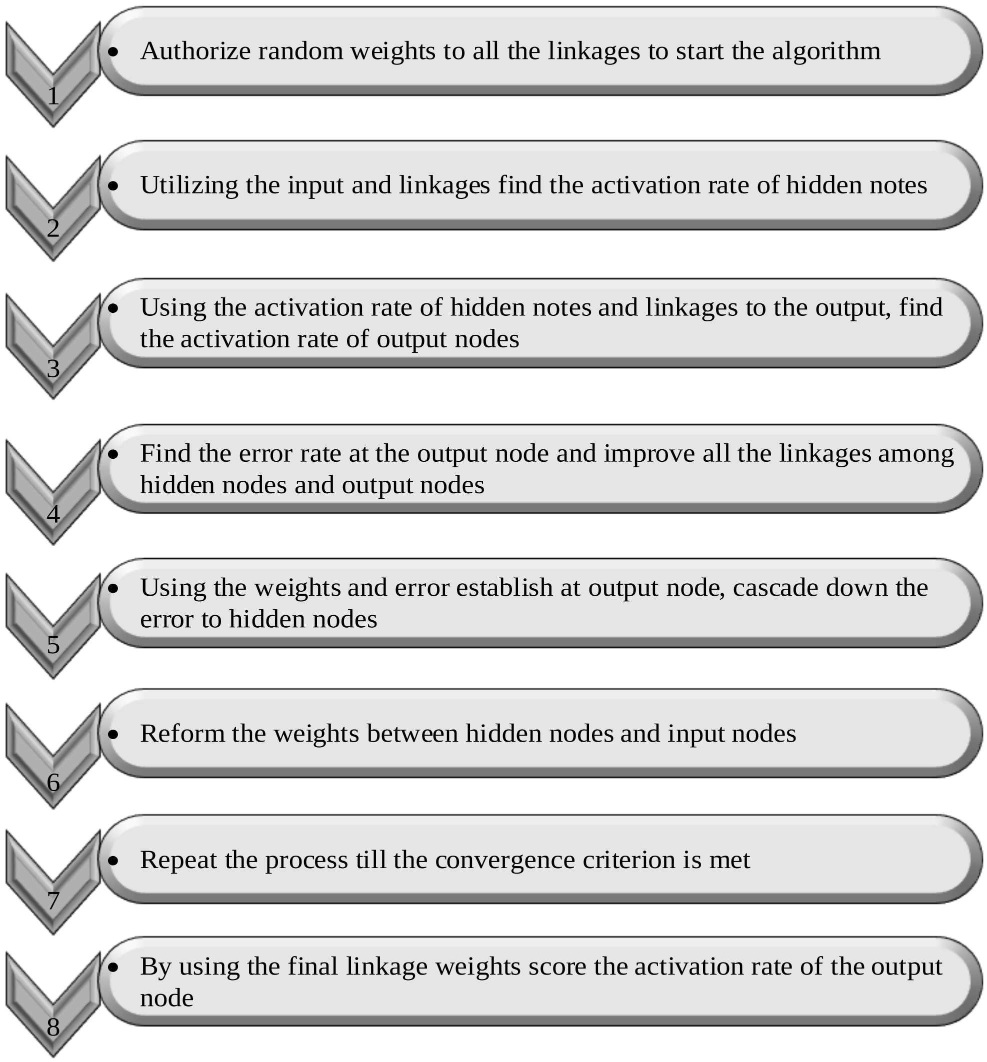

Figure 4.7: Function of ANN algorithm

The learning process attains the capability of a neural network for processing the knowledge, and this process is the adjustment of link weights therefore the network will generate a proper output. Normally, the learning scheme of an ANN can benefit an exact response to an input of the system by developing the current matrix strength of nodal weights. Hence, the similarity of generating a similar output if the same inputs break out in the future can maximize. The nodal weights are adjusted so that the inappropriate response from the systems are dejected. Therefore, the system can make responses contrastingly if it experiences similar inputs lately.

The learning process can be unsupervised or supervised depending on the convenience of the target output. In supervised learning, inputs are processed by the network and obtain an output [76]. The error has resembled in the variation between the target output and the output then, the error is propagated back by the network for training it. The network can automatically determine the significant features and categorizes the input data into various classes by considering these features.

In the learning process, numerous information about neural networks is determined. While learning, the error function is reduced by applying iterative methods, and if the error function value attains a predefined objective the iteration will end, hence the learning process ends. Moreover, learning will be terminated after achieving the satisfactory error value is small.

4.17 Types of ANN algorithm

Mainly the ANN algorithm consists of three major types they are listed below,

- Single-layer feed-forward network
- Multilayer feed-forward network
- Recurrent network

4.17.1 Single layer feed-forward network

In a neural network, the input layer of origin nodes is subjected into an output layer of the nodes and not inversely is known as an acyclic network or single feed-forward. For a single-layer network, 'single layer' represents the computation nodes of the output layer as shown in Figure 4.8.

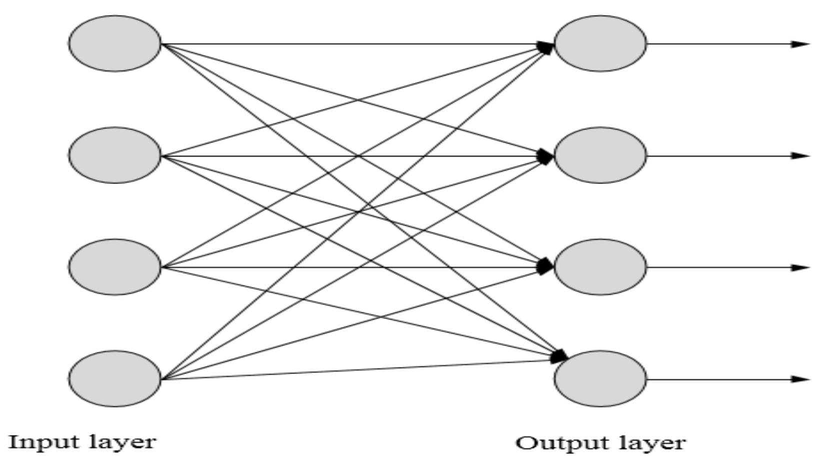

Figure 4.8: Single layer feed-forward network

4.17.2 Multilayer feed-forward network

The multilayer feed-forward network (Figure 4.9) comprises more than one hidden layer of which the estimation nodes are named as hidden units or hidden neurons. The objective of hidden units is to make collaboration between the network output and external input in an effective way and for extracting higher-order statistics. In a network, the input signal is contributed to the nodes in the next layer (1st hidden layer) by the source nodes in the input layer. Similarly, the output signals from the second layer are drawn as inputs to the succeeding layer and so on. In the output layer of the network, the group of output signals provides the overall response to the activation pattern provoked by source nodes in the first input layer.

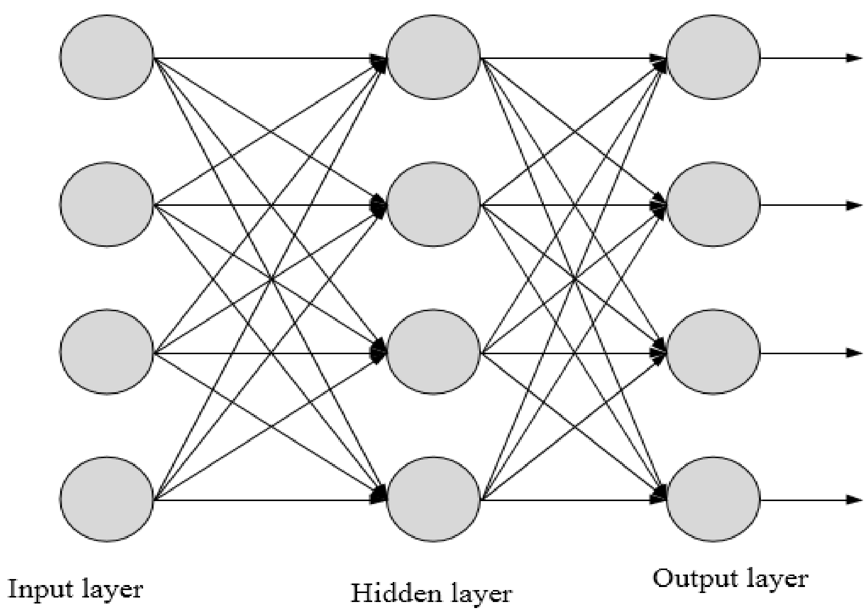

Figure 4.9: Multilayer feed-forward network

Some of the attributes of feed-forward networks:

- Normally, fed forward is an activation function from the input to output via ‘hidden layers’, by various existing architectures [77].
- These networks mathematically accomplish static input-output mappings.

- The back propagation algorithm is the most prominent supervised training algorithm.
- It is helpful for several realistic applications as the approximations of pattern classifications and nonlinear functions.

4.17.3 Recurrent network

A feed-forward neural network that contains more than one hidden layer with slightly one response loop is called a recurrent network as is depicted in Figure 4.10. The feedback can be a self-feedback which means the output of a neuron is delivered back to its input. Frequently, feedback loops concern the need for unit delay components, which tend to nonlinear dynamic characteristics, considering that neural network yielding nonlinear units.

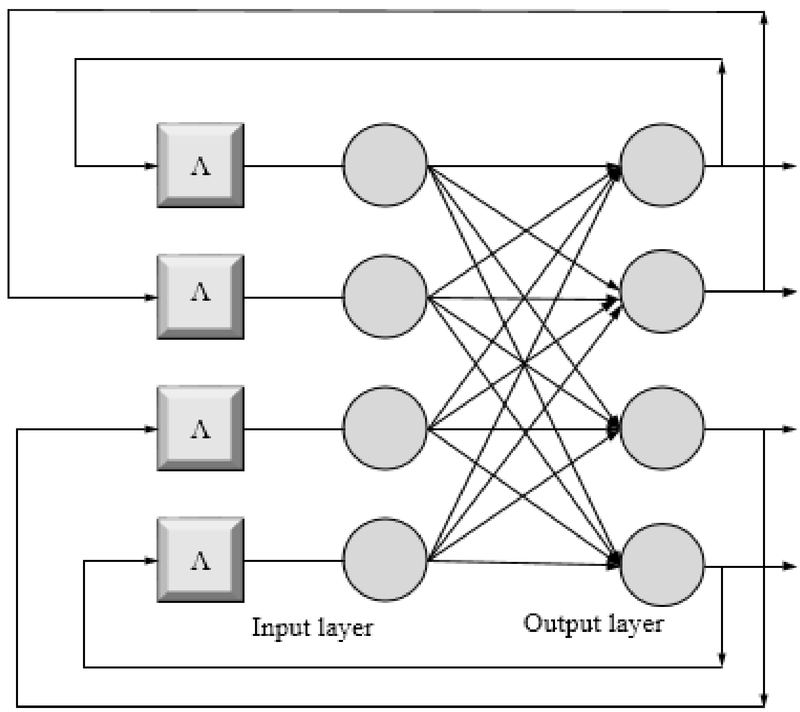

Figure 4.10: Recurrent network

Indeed, Vector quantization, spatial-temporal pattern, counter propagation, probabilistic, Hamming, adaptive resonance, Boltzmann, bidirectional associative memory, self-organizing map, recirculation, Hopfield, delta bar delta, etc., are some of the types of networks.

There is at least one cyclic path of synaptic connections are considered in a recurrent neural network. However, the fundamental characteristics are:

- Every biological neural network is recurrent.
- They are mathematically employed in dynamic systems.
- Different kinds of training algorithms have been coming to known, but no perfect winner.
- Analytical and practical problems are reduced in experimental applications till now.

4.18 Advantages of ANN algorithm

- Within a reasonable amount of time, one can attain a highly accurate mathematical model of the system
- Unlike many other forecasting techniques, ANN does not enforce any restraint on the input variables
- ANN can learn and model nonlinear relationships, which is essential many relationships among input and output are nonlinear as well as complex
- Information stored can be replaceable means new data can be added by deleting an old one.
- Response time is in nanoseconds

4.19 Disadvantages of ANN algorithm

- It is incapability for extrapolations [78].
- ANN needs processors with parallel processing power following their structure.
- When ANN produces a probing solution, it does not give a clue as to why and how. This reduces trust in the network.
- There is no specific rule for determining the structure of artificial neural networks.
- The network is reduced to a certain value of the error on the sample means that the training has been completed. This value does not give us optimum results.

4.20 Applications of ANN algorithm

- It can be used in many chemical engineering appliances
- It can be applied for image processing and character recognition
- Also used in many fields like medicine, security, banking/finance, as well as agriculture and defense

- ANN can be utilized in recognition areas like speech recognition, character recognition, and face recognition.

4.21 Active disturbance rejection controller (ADRC)

The primary key point of ADRC is compiled in detail and it depends on the information of the controlled process. Every external and internal disturbance indicating the contingency of the process has been referred to as the total disturbance. After all, the total disturbance has been observed, determined, and terminated on time.

ADRC was initially proposed by J. Han and it is an independent framework. On the other way, ADRC attains control access without an exact mathematical model. Additionally, its strength to solve every disturbance is assessed to manage the distributed parameter systems. The basic block diagram of ADRC is given in Figure 4.11. In the distributed parameter systems, the independent model could not be utilized to overcome the controlling issues. Besides, for some industrial processes, the independent model has been broadly used for the existing goals.

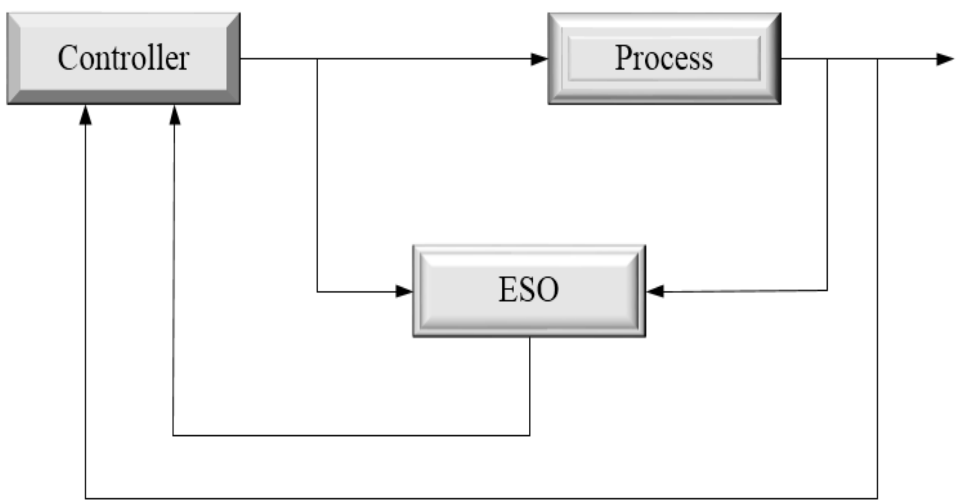

Figure 4.11: Block diagram of ADRC

The second ADRC controller was being modelled for the main engine in the ship due to overcoming the complex wave disturbances. Also, the attitude tracking had explained for modelling spacecraft with inertia uncertainty [79]. In dynamics, the design was nonlinear. The issues with the nonlinear dynamic design were solved by designing ESO. However, ADRC cannot rely on the exact mathematical model, but it is better to solve various disturbances namely indelible noises and changing parameters. In the complete working region, to a particular extent, the ADRC ignores the disturbances. Finally, the above mentioned two applications determine that the ADRC control algorithm has better disturbance rejecting strength to solve the uncertain disturbances. Hence, ADRC is employed for control issues.

4.22 Design structure of ADRC

The basic pattern of ADRC is comprised of extended state observer, nonlinear state error feedback control law, and tracking differentiator. In comparison with existing model-based designs, the ADRC technique needs some data about the plant. The ADRC describes the discrepancy between the model and plant, and generalized disturbance as an external disturbance that is determined effectively by ESO and then, remunerates with control law.

The investigation of the capability and tracking behaviour of a separate class in linear ESO and the correlated response for the control system, linear ADRC for nonlinear time-varying systems that are greatly unrevealed [80]. Comparable inquiry of rejecting disturbance concern for Markovian jump systems or Markovian jump nonlinear systems with several lossy measurements and disturbance. Admitting that the ADRC technique is mostly drawn and joined with different control schemes, SMC and ADRC compound control is approximately uncommon.

The correlation between SMC and ADRC technique in tracing performance, disruption resistance, and durability attach SMC and ADRC technique to restraint the level of the water steam generator (SG) whereas SMC displaces the nonlinear state response restraint fault rate of the ADRC. The design structure of ARDC is shown in Figure 4.12. While analysing various authors, the issues of combining the LCAMC technique with the ADRC technique cannot be determined.

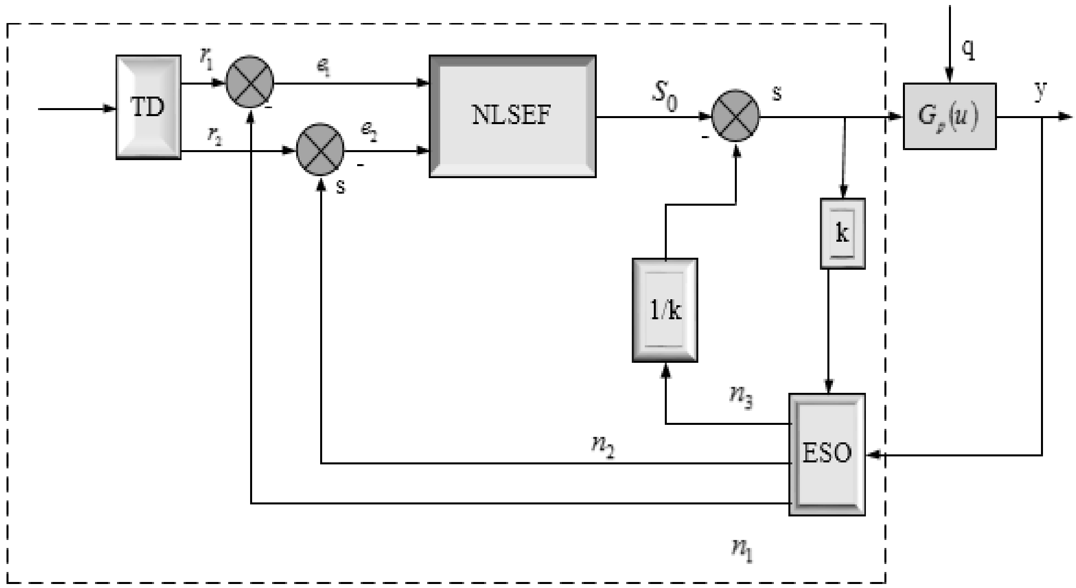

Figure 4.12: Design structure of ADRC

4.23 Working principle of ADRC

Generally, the classical PID controller is popularly utilized in the industry due to its effective and simple action, however, it has some inherent restrictions and these restrictions are given below.

- ❖ The controlled plant is typically a dynamic system, and so the outputs cannot move immediately but, a fixed value is provided with the command signal [81]. Hence, the initial error between the command and actual output is high, and it cannot be practicable for computing directly.
- ❖ The differential signal (velocity) is commonly determined in many motion control cases by the backward variation of the position signal. Further, the position signal is noisy and it may restrict the overall performance.
- ❖ The control law is generally in the form of a linear weighted sum, which is not in optimal form and is oversimplified.
- ❖ ADRC technology is introduced to solve the limitations of PID.

4.24 Mathematical analysis of ADRC

The active disturbance rejection concept is utilized to solve various issues namely single-input single-output (SISO) and multi-input multi-output (MIMO), plants that are, time-varying, uncertain and nonlinear. The second-order motion system is commonly applied for illustration can be given below,

For second-order nonlinear system model, the approximation for a dynamic system can be structured as:

$$\ddot{Y} = h(t, y, \dot{y}, q) + ls \tag{4.29}$$

Where Y defines the determined output to be controlled, s indicates the input, l resembles the parameter that is represented as: $l \approx l_0$. h indicates the combinational effect of the external disturbances q and internal dynamics. Generally, a clear mathematic description h is frequently unreachable. To solve this issue, ADRC establishes as a highly suited method. The common idea is: in some way, it h is obtained in real-time, it is eliminated by applying the control signal, and that lowers (4.29) to a double integral plant. The nonlinear time-varying unknown plant of (4.29) is considerably minimized to a linear time-invariant cascade integral plant. Then, the linear time-invariant cascade integral plant will be simply controlled [82].

Further, this inspired objective that transforms the control issues into a measurable ones. The process is resembled below as follows,

4.24.1. Extended state observer

The system (4.29) is revised in state-space form can be expressed as:

$$\begin{cases} \dot{x}_1 = x_2 \\ x_2 = x_3 + l_0 s \\ x_3 = \dot{h} = f \\ y = x_1 \end{cases} \tag{4.30}$$

With $x_3 = h$, the state is extended and it can be expressed in matrix form:

$$\begin{cases} \dot{x} = Mx + Ls + IF \\ y = Kx \end{cases} \tag{4.31}$$

Where,

$$M = \begin{bmatrix} 0 & 1 & 0 \\ 0 & 0 & 1 \\ 0 & 0 & 0 \end{bmatrix}, L = \begin{bmatrix} 0 \\ l_0 \\ 0 \end{bmatrix}, I = \begin{bmatrix} 0 \\ 0 \\ 1 \end{bmatrix}, k = \begin{bmatrix} 1 & 0 & 0 \end{bmatrix} \tag{4.32}$$

With f unknown the state observer of (4.31) is,

$$\begin{cases} \dot{n} = Mn + Ls + B(y - \hat{y}) \\ y = Kn \end{cases} \tag{4.33}$$

Where n_1, n_2, n_3 are the determinates of $y, \dot{y}$, and h approximately. This is considered as the ESO however, the state vector in (4.30) exceeds to add f and this observer is modeled to promote an estimation. It is modeled and implemented properly and the observers' state (4.32) can trace that the plant (4.31). Then, the parameter vector B is determined; for instance, the pole-placement approach. Consider,

$$\lambda(u) = |uE - (M - BK)| = (u + \omega_0)^3$$

We can obtain,

$$B = \left[3\omega_0, 3\omega_0^{\ 2}, \omega_0^{\ 3}\right]^T$$

The ESO contains two parameters l_0 *and* ω_0. The precedent is normally familiar to designers and also it is estimated from the open-loop response. The tuning parameter is lately mentioned and it tends to the observer’s bandwidth. The trade-off between noise sensitivity and performance can be smoothly attained by adapting ω_0 .

4.24.2. Controller design

As $n_3 = h$ evaluated by the ESO, then the control law can be given as,

$$s = (s_0 - h)/l_0 \tag{4.34}$$

Reduces (4.29) to an estimated double integral plant:

$$\ddot{y} \approx s_0 \tag{4.35}$$

It can simply control by employing a PD controller, which is expressed below as:

$$s_0 = c_p(r - n_1) - c_j n_2 \tag{4.36}$$

Certainly, the basic quality in ADRC is to determine f in real-time nullify it in the controller law.

4.24.3. First-order systems

In a first-order nonlinear system, the design of the controller can be entirely the same. Consider,

$$\dot{y} = h + l_0 s \tag{4.37}$$

The second-order ESO is represented as,

$$\dot{n} = \begin{bmatrix} -2\omega_0 & 1 \\ -\omega^2{}_0 & 0 \end{bmatrix} n + \begin{bmatrix} l_0 & 2\omega_0 \\ 0 & \omega_0{}^2 \end{bmatrix} \begin{bmatrix} s \\ y \end{bmatrix} \tag{4.38}$$

Where n_1 tracks y and n_2 tracks f. The controller is,

$$s = (s_0 - h)/l_0 \tag{4.39}$$

Then, an integral form of the lower plant is derived in (4.40),

$$\dot{y} = s_0 = c_p(r - n_1) \tag{4.40}$$

4.25 Advantages of ADRC

- The ADRC can estimate both the modelling discrepancies and the external disturbances in a unified matter.

- In the circumstance, due to rising in practicality and performance establishing solutions for pressing engineering issues.
- ADRC is known for its ability to contain both external disturbances and internal concerns.
- In system variables, after setting up for the fault in a prearranged variation range, no tuning is required to start up or allowance for variations in the disturbance and dynamics of the system [83].

4.26 Disadvantages of ADRC

- High dimension of the resulting controller.
- The main defect is that they require information about higher-order derivatives of the plant output signals.
- When compared to other controllers time consumption is slightly high.

4.27 Applications of ADRC

- Mostly used in industrial control problems.
- It can applicable in DC-DC power converters, motion control, velocity regulation, and web tension.
- In an electromagnetic linear actuator, ADRC technology is applied for trajectory tracking control.
- ADRC can also be used for time-delay systems
- To manage extreme nonlinear dynamics of the disturbances and converter, a digital signal processor-based ADRC has been introduced.

4.28 Summary

The $H\infty$ controller-based disturbance rejection in CSTR is the objective function of this method. The explanations of CSTR and constructing parts of CSTR like wall jacket, gas outlet, viewing port window, adjustable feet, etc are all detailed correctly. Then the $H\infty$ control methods, $H\infty$ control problems, and how the $H\infty$ controller is used in CSTR are explained in detail. The existing methods like PID controller, ANN algorithm, and ADRC controller are also mentioned in this chapter. The overall advantages, disadvantages, and applications of all the controllers are specified and the algorithm used here is the WWO algorithm, the principle of the WWO algorithm, and the entire working process of the WWO algorithm is a detailed step by step procedure.

CHAPTER 5

RESULT AND DISCUSSION

5.1 Introduction

The BLDC motor is designed and constructed by the robust fixed order H-infinity controller. The operation of the BLDC motor and the performance aspects of the BLDC motor like speed, torque, and back EMF are evaluated and correlated with the existing method controllers, namely fuzzy PD controllers and fuzzy PID controllers. The use of the controllers in the BLDC motor is to achieve the set speed and to reject the torque ripples from the motor. Then the process of the IPSO algorithm is to examine the position of the rotor. The simulation results are carried out under the platform of MATLAB R 2016a.

5.2 Weight function of the H-infinity controller

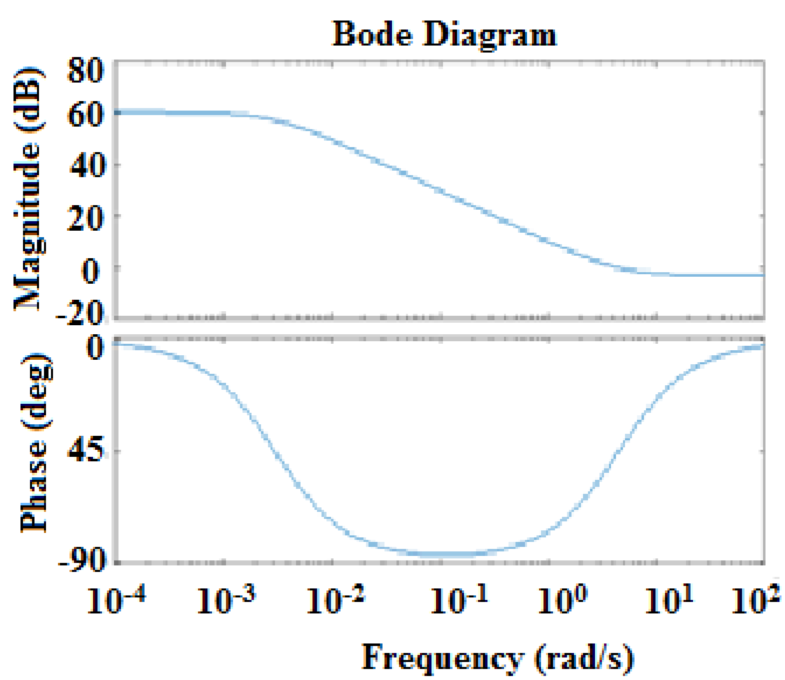

(a) Weight function (W_u)

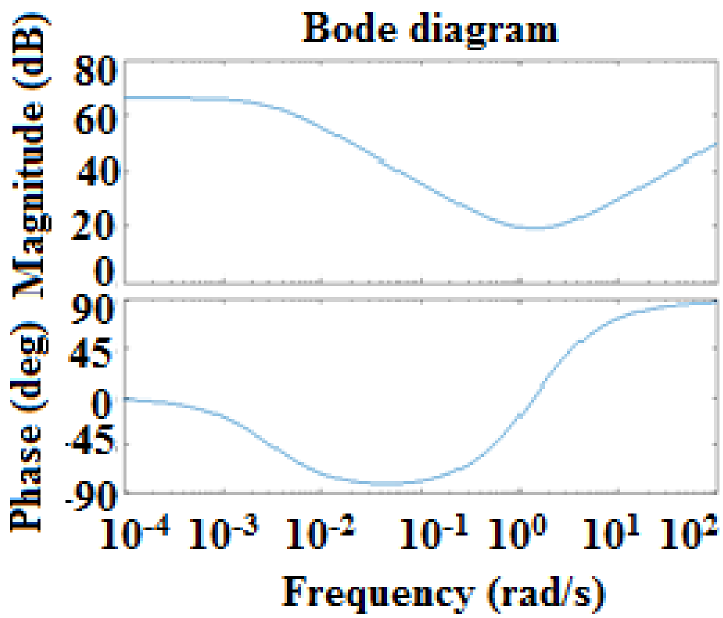

(b) Weight function (W_{cu})

5.3 Transfer function of the H-infinity controller

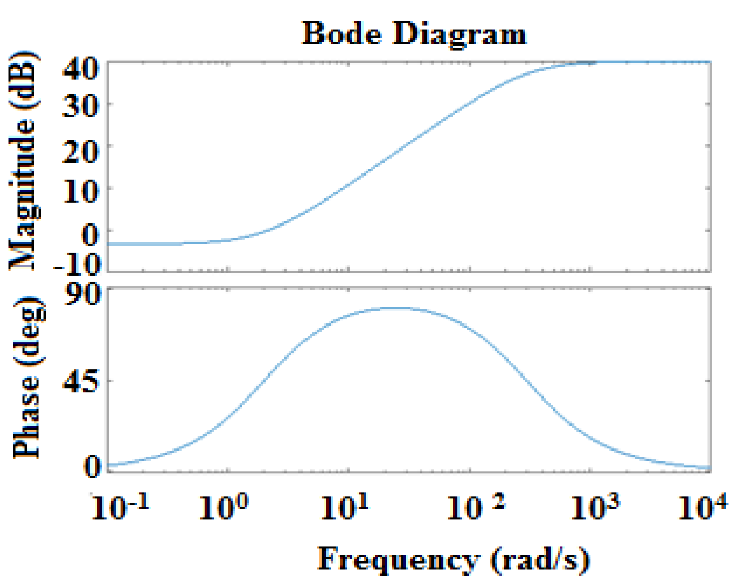

(c) Transfer function of the H-infinity controller

Figure 5.1: Output of the H-infinity controller

The bode plots of the H-infinity controller are depicted in Figure 5.1. In the H-infinity controller, the weight function can be evaluated. Figure 5.1(c) shows the transfer function of the controller. Like that the phase and the magnitude are given in the weighting function. For both the process, the phase value is denoted as 60 dB and 65 dB among that the phase value is 0 and 90^0. The angle value will get increases in the transfer function correspondingly to the frequency and the magnitude is given as 40 dB. To minimize the error function the controller can be drawn.

5.4 Speed of the rotor

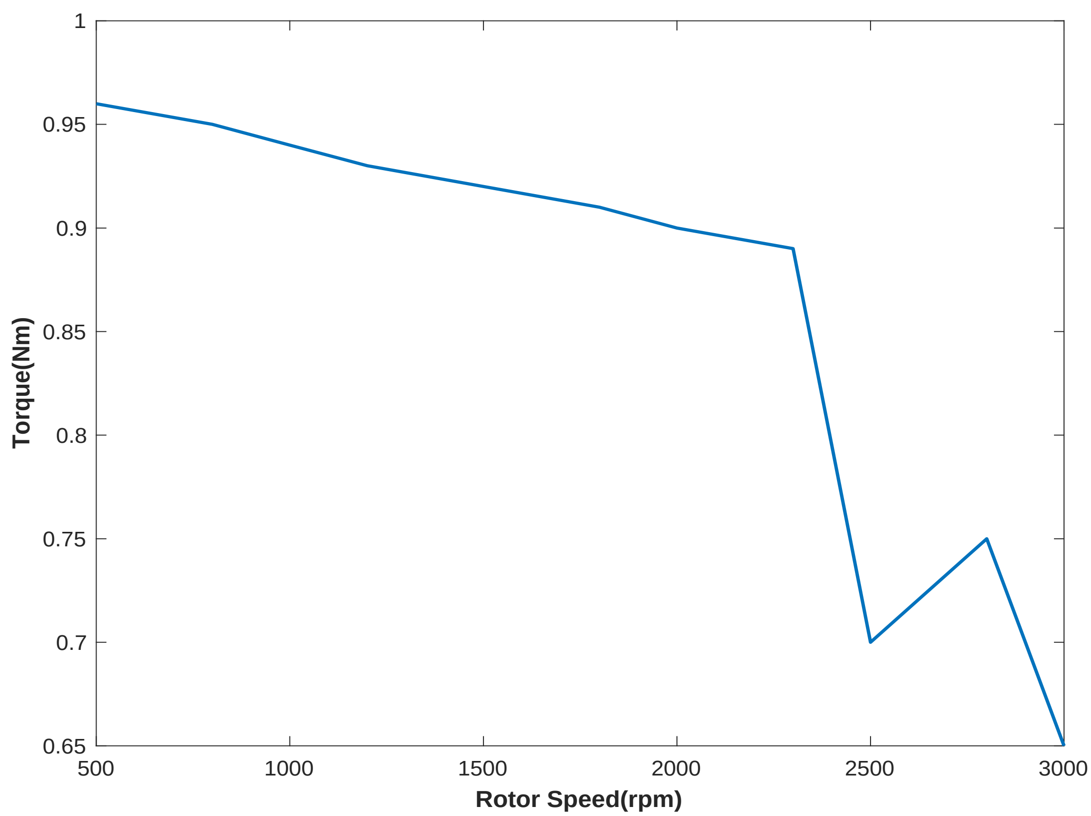

Figure 5.2: Speed vs Torque

The relation of the speed and torque are inversely proportional which is shown in Figure 5.2.When the torque gets decreases, the speed will get increases. Simultaneously the speed gets decreases and the torque will get increased. When the speed of the rotor is at 500 rpm then the torque is huge at the rate of about 0.96. Due to the vibrational effect of the rotor, the rotor speed increased with an increase in torque, which is common in every motor. But the proposed model provides very low transient than the other method. After a short period of time this effect got mitigated and reached the speed of about 3000 rpm, where the torque value is diminished at the range of about 0.65.

5.5 Position of the rotor

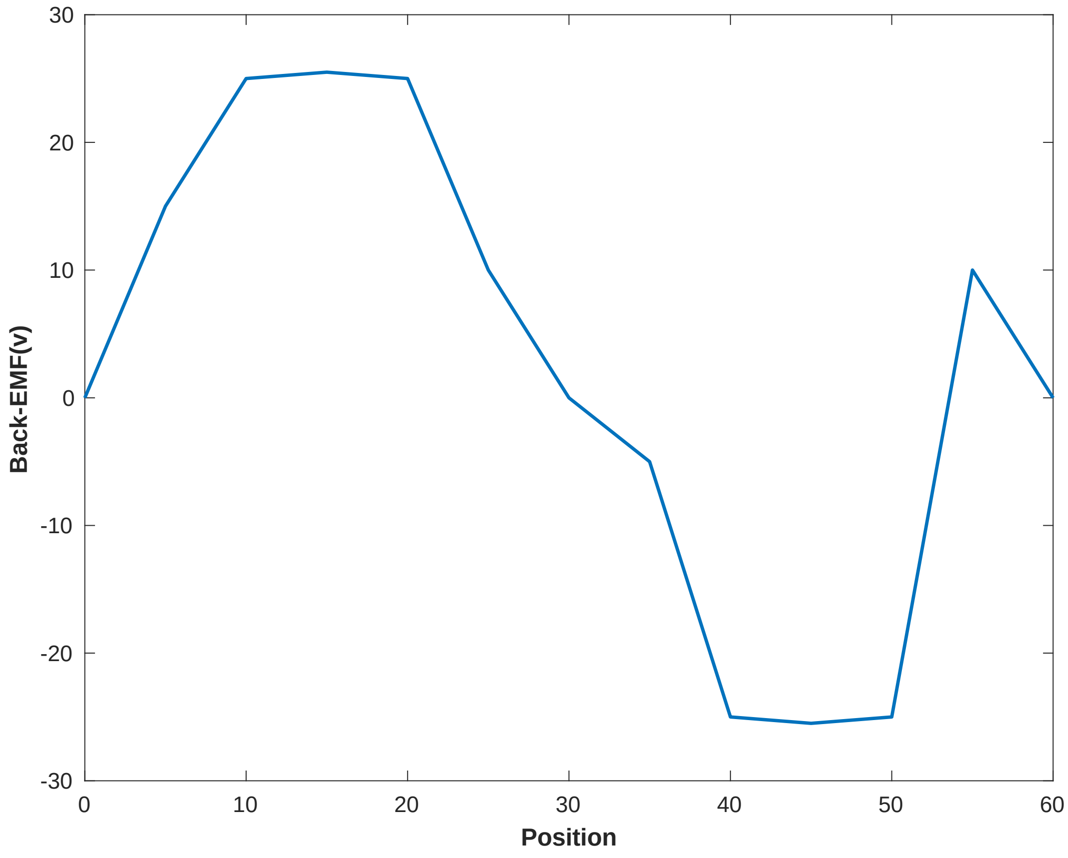

Figure 5.3 : Position vs Back EMF

The rotor position and the voltage of the motor is shown in Figure 5.3. By using the IPSO algorithm the position of the rotor can be attained and the angle value is about 10° to 20°. At that time the voltage level will be high and abruptly decreased. The developed position produces a good voltage in the motor at 25 V.

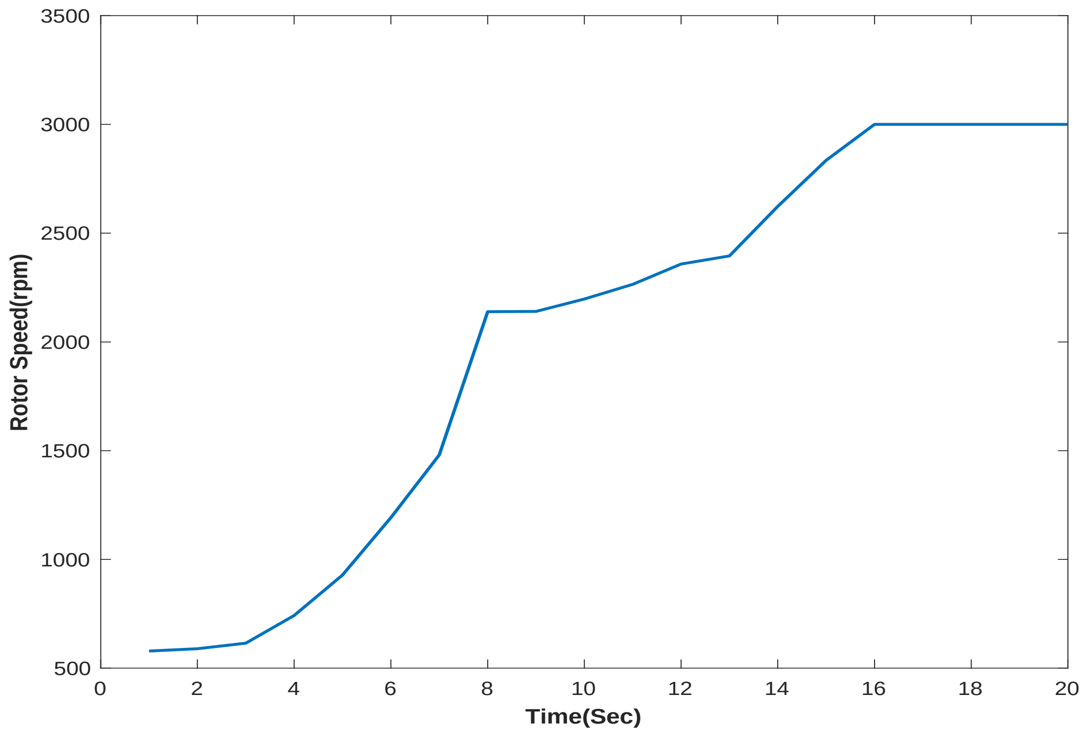

Figure 5.4: Time vs Rotor speed

Figure 5.4, displays the speed value concerning time. The speed of the motor is greatly improved at every single interval of time. The speed level is constant in 16 to 20 seconds interval time. Like that speed of the rotor is slightly vary concerning time.

Table 5.1 Parameters of IPSO algorithm

Size of swarm	64
Maximum iteration	50
Inertia weight	1
Lower bound	0
Upper bound	180

The parameter details of the IPSO algorithm is detailed in Table 5.1, in which the swarm size is assumed as 64, inertia weight is 1, maximum iteration level is about 50, then the upper bound and lower bound is about 180 and 0. In every single iteration, it will differ concerning time.

5.6 Comparison of the existing and proposed method

Table 5.2 Comparison of the proposed method with the existing method

TYPE OF CONTROLLERS	PARAMETERS		
	Torque (N-M)	**Speed (rpm)**	**EMF (v)**
Fuzzy PD controller [84]	1.2	2000	40
Fuzzy PID controller [85]	1.6	1500	30
Sensing algorithm [86]	1.8	2500	35
Proposed controller	0.65	3000	25

The comparison results of the existing controllers like fuzzy PD controller, fuzzy PID controller, and sensing algorithm are detailed in Table 5.2. The EMF of the existing controllers is 40, 30, 35 respectively and in our proposed controller EMF is 25. The speed is 2000 rpm, 1500 rpm, and 2500 rpm respectively, but in the proposed controller the maximum speed is 3000 rpm. The torque is reduced in the Fuzzy PD controller, Fuzzy PID controller, Sensing algorithm, and proposed H-infinity controller is about 1.2, 1.6, 1.8, and 0.65 respectively.

5.7 Summary

The designing of the BLDC motor is concluded with the guidance of the robust fixed order H-infinity controller. The position of the rotor is identified with the help of the IPSO algorithm and the developed angle to produce the current, voltage, and torque at an optimized angle to generate the current, voltage, and torque at a decreased level. The achievement of speed, torque, and EMF is examined, along with the weighting parameters and transfer function are computed under the MATLAB environment. At last, the correlation results are carried out over the existing controllers like fuzzy PD controller and fuzzy PID controller admits the proposed adaptive controller of H-infinity. Thus the speed of the motor is enlarged at the rate of 3000 rpm and at the same, time the torque is diminished at the level of 0.65. The performance of the controller is reinforced with the help of the proposed optimization algorithm. When compared the proposed method with the existing method, it clearly explains that the proposed technique is superior to the existing methods.

CHAPTER 6

RESULT AND DISCUSSION

6.1 Introduction

The H-infinity (H∞) controller-based disturbance rejection in the CSTR along with the utilization of the water wave optimization algorithm has been evaluated. The proposed work targets the conflicts of CSTR, such as variation in temperature and product concentration. The temperature and concentration of CSTR with disturbance need to evaluate and then reduction of error is made by the WWO algorithm. After that, the temperature and concentration of CSTR without disturbance are needed to evaluate. Then compare the results with existing methods like PID controller, ANN algorithm, and ADRC. The simulation results are carried out under the platform of MATLAB R 2016a.

6.2 Temperature and concentration of CSTR with disturbance

The criterion such as temperature and product concentration is taken as the disruptions from the CSTR. The setpoint for the planned system is evaluated by using the applicable equa244 ^{0} C and 0.0836 mol/liter are the measured values for temperature and product concentration respectively.

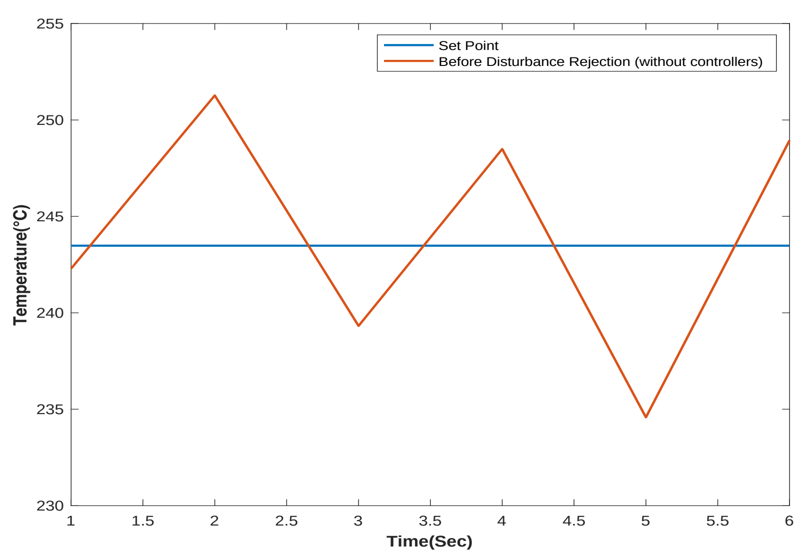

(a) Temperature

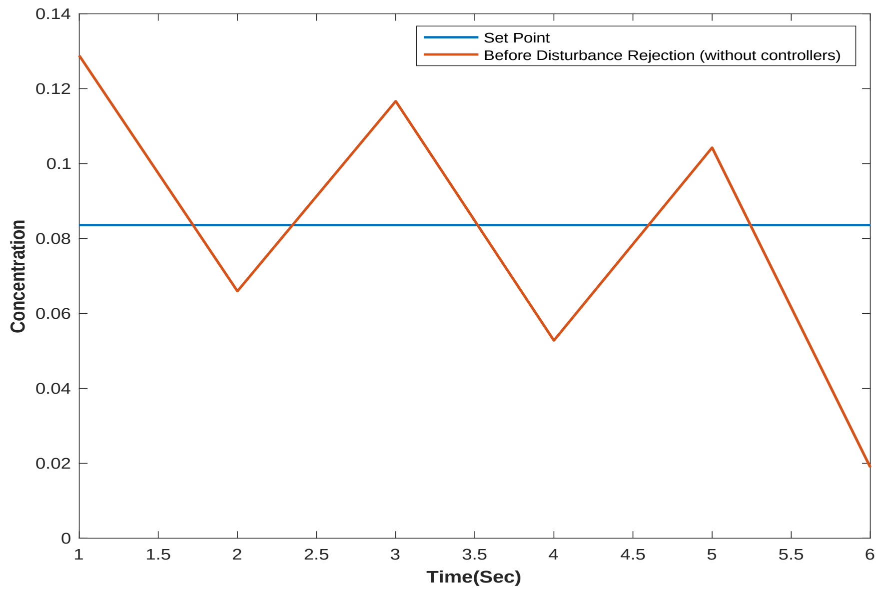

(b) Concentration

Figure 6.1: CSTR with disturbance (a) Temperature (b) Concentration

Due to the brisk change of temperature and concentration the disturbance may occur. Both the conditions are shown in Figure 6.1. They may corrupt the lifetime of the system so that, the proposed method concentrate on the elimination of such concern with the help of the H∞ controller.

6.3 Reduction of error by WWO algorithm

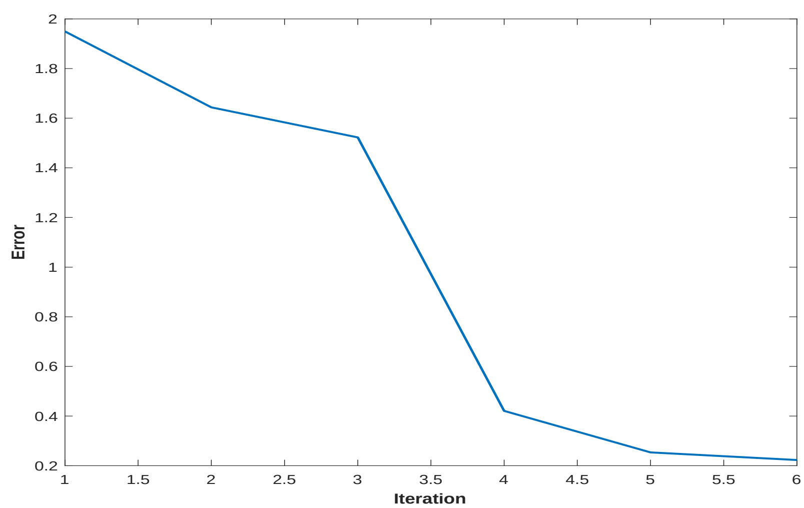

(a) Temperature

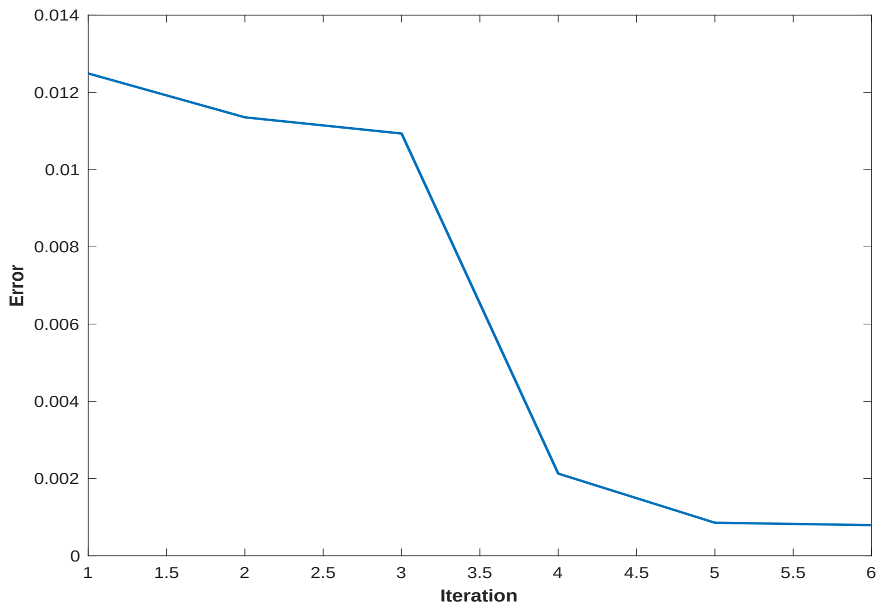

(b) Concentration

Figure 6.2: Error reduction using WWO algorithm (a) Temperature (b) Concentration

The reduction of error by employing the proposed controller is shown in Figure 6.2. For the reason of error reduction, the water wave optimization approach is drawn. When the number of iterations get increased, the error for both the parameters will get decreased constantly. Adjacent to the fourth iteration more amount of faults are disqualified to the desired value. After the clearance of fault, the CSTR will produce the output which is shown in Figure 6.3.

6.4 Temperature and concentration of CSTR after disturbance rejection

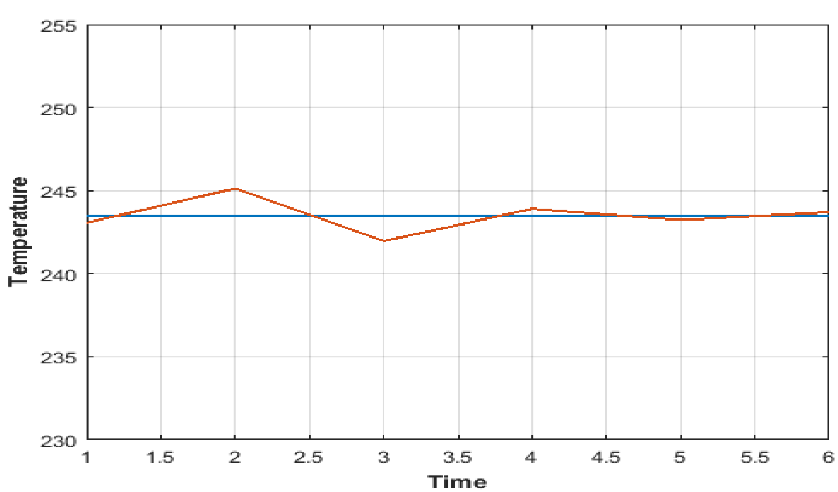

(a) Temperature(°C)

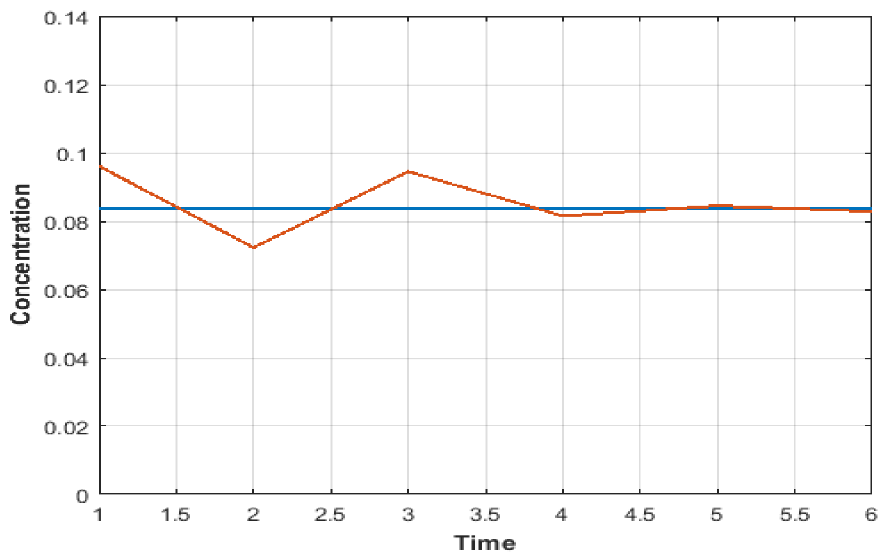

(b) Concentration

Figure 6.3: CSTR after disturbance rejection (a) Temperature (b) Concentration

The CSTR output after the disturbance rejection is shown in Figure 6.3. The relation of the Temperature(°C) and time(sec) after disturbance rejection. This output represents the graph with less amount of error. For both criteria, the red colour line (disturbed value) varies nearer to the setpoint value.

6.5 Comparison with the existing and proposed method

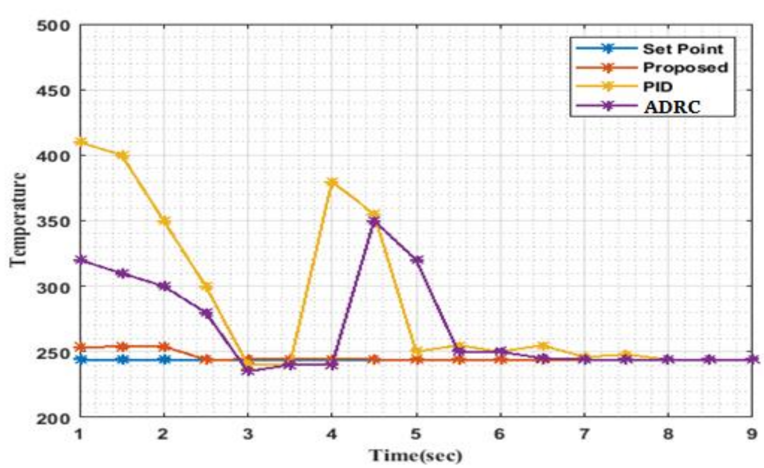

Figure 6.4: Temperature comparison with existing methods

The comparison of temperature (°C)with the existing methods is shown in Figure 6.4. This explains that the excellent performance of the proposed controller is more or less appropriate to the setpoint value. Generally, there is a vast deviation from the needed value in the case of existing methods. Among the existing techniques, when compared to other controllers, PID controller shows the bad performance when related to Active Disturbance Rejection Controller.

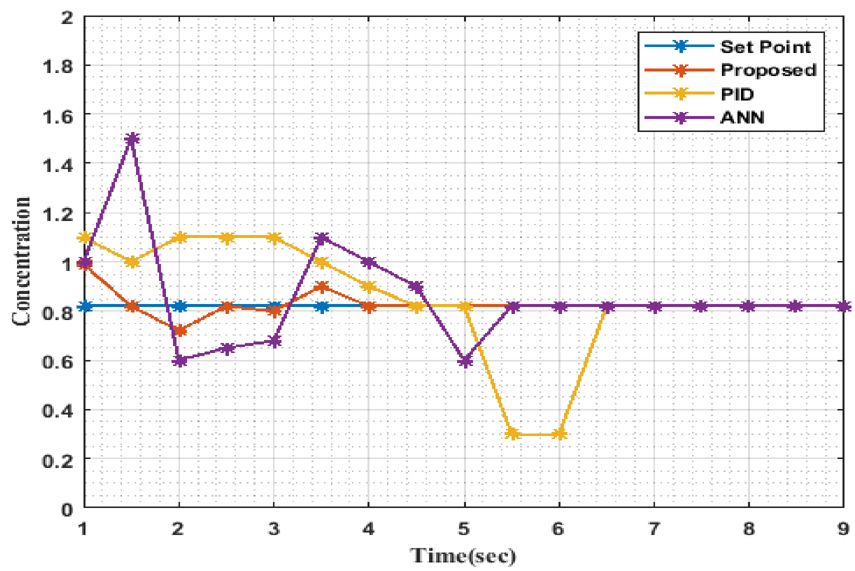

Figure 6.5: Concentration comparison with existing methods

The comparison of concentration with the existing systems is shown in Figure 6.5. Here, the ADRC, PID controller, and artificial neural network-based controllers are taken as the existing methods for performance evaluation. As well as, the time at which setpoint attainment for the existing methods is longer than the planned work.

Table 6.1: Comparison of a time requirement

Parameter	Time required to reach set point
PID Controller	7.5 Sec
ADRC Controller	7 Sec
ANN Controller	5.5 Sec

Proposed Controller	2.5 Sec

The proposed method reaches the desired value within 2.5 sec after the rejection of instabilities due to the usage of the H∞ controller. It is represented in Table 6.1along with the comparison of previous practices. Among the prevailing systems, PID, ARDC & ANN controllers take 7.5 Sec, 7 Sec, and 5.5 Sec to reach the preferred value, respectively. Furthermore, the H∞ controller performs the disturbance rejection through the utilization of the water wave optimization algorithm. Hence it provides better performance than other methods.

6.6 Summary

An H∞ controller was offered for effective disturbance rejection through the utilization of a water wave optimization algorithm. H∞ controllers are widely used to provide high gain in any kind of complex situation. The application taken for the development of the proposed work is a continuous stirred tank reactor in which non-linear complex reactions are very common. Variation in temperature and product concentration has been taken as the disturbances in continuous stirred tank reactor. So, an algorithm was proposed along with the controller action for eliminating these issues. The implementation results were compared, with the existing controllers and performance enhancement has also been shown in the result analysis.

CHAPTER 7

CONCLUSION AND FUTURE SCOPE

7.1 Conclusion

The motor consists of two types which are the brushless direct current (BLDC) motor and conventional direct current (DC) motor. In the conventional DC motor, the current produces the flux in the coil. But in the case of brushless DC motor, the permanent magnet is provided rather than wire wound field poles. These have the merits like free maintenance, simple structure, and better reliability. The brushless direct current motor needs the electronic speed controllers to run the motor, which is superior to the brushed direct current motor because of its efficiency and better-operating speed. In the past, the PI controllers were used due to their simple structure. But it has load disturbance, control complexity, and some parametric variations. The above facts can be avoided by the proposed controller. The $H\infty$ controllers are used to synthesize the guaranteed performance of certain applications as well as provides a maximum gain in any situation. The brushless direct current motor is designed with the novelty of fixed order H-infinity controller. The appropriate weight functions and transfer functions have been used to design the controller. The controller is applied to the brushless direct current motor to obtain the position. Thus, the improved particle swarm optimization algorithm to obtain the optimal position of the rotor. The IPSO algorithm is used for the examination of position and the optimized angle to generate the current, voltage and torque at reduced level. The new controller can reduce the torque as much as possible so that the speed is high. The performance of the BLDC motor enhance with the help of suggested optimization algorithm and the comparison result clearly show that the proposed method show better results than the existing methods. The disturbance in the controller can be avoided through the water wave optimization algorithm. Continuous stirred tank reactor (CSTR) is considered for application-oriented development as it includes complex reactions with high nonlinearity. The proposed work focuses on the conflicts of CSTR, such as variation in temperature and product concentration. $H\infty$ controller was offered for effective disturbance rejection through the utilization of the water wave optimization algorithm. $H\infty$ controllers are widely used to provide high gain at any kind of complex situations. The elimination of these issues is performed with the help of the proposed algorithm along with the controller operation. The planned work gives the enhanced performance utilizing disturbance rejection when compared with other existing controllers. Additionally, the proposed work improves the lifespan of the offered application through the elimination of disorders. The overall process is implemented in the MATLAB working platform and the results are compared with the preceding methods to show the expected performance. The performance of the torque, speed, and back EMF voltage is analyzed and compared with the existing controllers such as fuzzy proportional integral derivative, sensing algorithm, and fuzzy proportional derivative controller.

7.2 Future scope

The new controller, which is more effective than the $H\infty$ controller with advanced technology and the real-time process, is developed for future work to enhance the torque and speed and choose the better algorithm to avoid the error presented in the system. The new proposed controller improves the performance of new generations of high-speed underwater vehicles.

REFERENCES

[1] R.H. Daugherty and C.H. Wennerstrom, "Need for industry standards for AC induction motors intended for use with adjustable-frequency controllers", **IEEE Transactions on Industry Applications**, Vol. 27, No. 6, pp: 1175-85, 1991, doi: 10.1109/28.108471

[2] P.C. Sen, "Electric motor drives and control-past, present, and future", **IEEE Transactions on Industrial Electronics**", Vol. 37, No.6, pp:562-75,1990, doi: 10.1109/41.103462

[3] M. Yildirim, M. Polat and H. Kürüm, (2014) "A survey on comparison of electric motor types and drives used for electric vehicles", **In Power Electronics and Motion Control Conference and Exposition (PEMC), 21-24 Sept. 2014, Antalya, Turkey**, pp:218-223, doi: 10.1109/EPEPEMC.2014.6980715

[4] S. Ogasawara and H. Akagi, "An approach to position sensorless drive for brushless DC motors", **IEEE Transactions on Industry Applications**, Vol. 27, No. 5,pp: 928-33,1991 Sep;27(5):928-33, doi: 10.1109/28.90349.

[5] T. Sekiya, H. Uchida, H. Yamauchi and K. Umeda, inventors; Sony Corp, assignee. "Brush-less DC motor". **United States patent US** 4,167,692. 1979 Sep 11.

[6] N. Hemati, "Strange attractors in brushless DC motors", **IEEE Transactions on Circuits and Systems I: Fundamental Theory and Applications.**, Vol. 41, No. 1, pp: 40-45,1994, doi: 10.1109/81.260218

[7] J.C. Gamazo-Real, E. Vázquez-Sánchez and J. Gómez-Gil, "Position and speed control of brushless DC motors using sensorless techniques and application trends", **Sensors**, Vol. 10, No. 7, pp: 6901-47,2010, doi:10.3390/s100706901.

[8] H. Melkote and F. Khorrami, "Nonlinear adaptive control of direct-drive brushless DC motors and applications to robotic manipulators", **IEEE/ASME Transactions on Mechatronics**, Vol. 4, No. 1, pp: 71-81,1999, doi: 10.1109/3516.752086.

[9] E.M. Elhaji and C.J. Hatziadoniu, “Interarea oscillation damping using H-infinity control for the permanent magnet wind generator”, **Electric Power Systems Research**, Vol. 151,pp:319-28,2017, doi.org/10.1016/j.epsr.2017.05.037.

[10] A. Bansal and V. Sharma, “Design and analysis of robust H-infinity controller”, **Control Theory and Informatics**, Vol. 3,No.2,pp:7-14,2013.

[11] P.P. Khargonekar, I.R. Petersen and K. Zhou, "Robust stabilization of uncertain linear systems: quadratic stabilizability and H/sup infinity/control theory", **IEEE Transactions on Automatic Control**, Vol. 35, No. 3, pp. 356-361, 1990.

[12] D. Simon, “Optimal state estimation: Kalman, H infinity, and nonlinear approaches”, **John Wiley & Sons,** 2006.

[13] J.A. Laghari, H. Mokhlis, A.H. Bakar and H. Mohammad, “A comprehensive overview of new designs in the hydraulic, electrical equipment’s and controllers of mini hydro power plants making it cost effective technology”, **Renewable and Sustainable Energy Reviews**, Vol. 20, pp:279-93,2013, doi.org/10.1016/j.rser.2012.12.002

[14] N. Aziz, M.A. Hussain and I.M. Mujtaba, “Performance of different types of controllers in tracking optimal temperature profiles in batch reactors”, **Computers & Chemical Engineering**, Vol. 24, No. (2-7), pp:1069-75,2000, doi.org/10.1016/S0098-1354(00)00526-3

[15] P. Roy and B.K. Roy, “Sliding mode control versus fractional-order sliding mode control: Applied to a magnetic levitation system”, **Journal of Control, Automation and Electrical Systems**, Vol. 31, No. 3, pp.597-606, 2020.

[16] Q. Li, D.W. Gao, H. Zhang, Z. Wu and F.Y. Wang, “Consensus-based distributed economic dispatch control method in power systems”, **IEEE Transactions on Smart Grid**, Vol. 10, No. 1, pp.941-954, 2017.

[17] Z.Y. Zhao, M. Tomizuka and S. Isaka, “Fuzzy gain scheduling of PID controllers”, **IEEE Transactions on Systems, Man, and Cybernetics** , Vol. 3,No. 5,pp: 1392-98,1993, doi: 10.1109/21.260670

[18] W.K. Ho, C.C. Hang and L.S. Cao, (1992) “Tuning of PI controllers based on gain and phase margin specifications”, **Proceedings of the IEEE International Symposium on Industrial Electronics, 25-29 may 1992, Xian, China,** doi: 10.1109/ISIE.1992.279722

[19] G. Herbst, “A simulative study on active disturbance rejection control (ADRC) as a control tool for practitioners”, **Electronics**, Vol. 2, No.3, pp: 246-79, doi.org/10.3390/electronics2030246

[20] Z.G. Li, C.Y. Wen and Y.C. Soh, “Switched controllers and their applications in bilinear systems”, **Automatica**, Vol. 37, No. 3,pp: 477-81,2001, doi.org/10.1016/S0005-1098(00)00172-2

[21] M. Sznaier and A. Sideris, “Feedback control of quantized constrained systems with applications to neuromorphic controllers design”, **IEEE Transactions on Automatic Control**, Vol. 39, No. 7, pp:1497-502,1994, doi: 10.1109/9.299643

[22] M. Athans, “The role and use of the stochastic linear-quadratic-Gaussian problem in control system design”, **IEEE Transactions on Automatic Control**, Vol. 16, No. 6, pp. 529-552, 1971.

[23] S.Y. Jung, Y.J. Kim, J. Jae and J. Kim, “Commutation control for the low-commutation torque ripple in the position sensorless drive of the low-voltage brushless DC motor”, **IEEE Transactions on Power Electronics**, Vol. 29, No.11,pp:5983-94, 2014, doi:10.1109/TPEL.2014.2298113

[24] M. Baszynski and S. Pirog, “A novel speed measurement method for a high-speed BLDC motor based on the signals from the rotor position sensor”, **IEEE Transactions on Industrial Informatics,** Vol. 10, No. 1,pp:84-91,2014, doi: 10.1109/TII.2013.2243740

[25] R. Shanmugasundram, K.M. Zakariah and N. Yadaiah, “Implementation and performance analysis of digital controllers for brushless DC motor drives”, **IEEE/ASME Transactions on Mechatronics,** Vol. 19, No. 1,pp: 213-24,2014, doi: 10.1109/TMECH.2012.2226469

[26] J.M. Patel, H.V. Hirvaniya and M. Rathod, “Simulation and Analysis of Brushless DC Motor Based on Sinusoidal PWM Control”, **International Journal of Innovative Research in Electrical, Electronics, Instrumentation and Control Engineering**, Vol. 2, No. 3,pp:1236-38,2014.

[27] K. Vinida and M. Chacko, (2016) “A novel strategy using H infinity theory with optimum weight selection for the robust control of sensorless brushless DC motor”, **In Sensorless Control for Electrical Drives (SLED), 5-6 june 2016, Nadi, Fiji**, doi: 10.1109/SLED.2016.7518799

[28] H. Dong, Z. Wang, S.X. Ding and H. Gao, “On H-infinity estimation of randomly occurring faults for a class of nonlinear time-varying systems with fading channels”, **IEEE Transactions on Automatic Control,** Vol. 61, No.2, pp:479-84, 2005 doi: 10.1109/TAC.2015.2437526

[29] Z. Liu, C. Gao and Y. Kao, “Robust H-infinity control for a class of neutral-type systems via sliding mode observer” **Applied Mathematics and Computation**, Vol. 271,pp:669-81,2015, doi.org/10.1016/j.amc.2015.09.007

[30] S.P. Ribas, L.A. Maccari, H. Pinheiro and V.F. Montagner, “Design and implementation of a discrete-time H-infinity controller for uninterruptible power supply systems” **IET Power Electronics**, Vol. 7, No. 9, pp: 2233-41,2014, doi: 10.1049/iet-pel.2013.0794

[31] D. Zhao, Q. Zhu and J. Dubbeldam, “Terminal sliding mode control for continuous stirred tank reactor”, **Chemical Engineering Research and Design**, Vol. 94, pp: 266-74,2015, doi.org/10.1016/j.cherd.2014.08.005

[32] F.J. Hurtado, A.S. Kaiser and B. Zamora, “Fluid dynamic analysis of a continuous stirred tank reactor for technical optimization of wastewater digestion”, **Water Research**, Vol.71, pp:282-93,2015, doi.org/10.1016/j.watres.2014.11.053.

[33] A. Uppal, W.H. Ray and A.B. Poore, “On the dynamic behavior of continuous stirred tank reactors”, **Chemical Engineering Science**, Vol. 29,No. 4,pp:967-85,1974, doi.org/10.1016/0009-2509(74)80089-8

[34] U.V. Ratnakumari and M.B. Triven, (2016) “Implementation of adaptive model predictive controller and model predictive control for temperature regulation and concentration tracking of CSTR”, **International conference on Communication and Electronics Systems (ICCES), 21-22 Oct. 2016, Coimbatore, India**, pp: 1-6, doi: 10.1109/CESYS.2016.7889843

[35] T.M. Silva Filho, B.A. Pimentel, R.M. Souza and A.L. Oliveira, “Hybrid methods for fuzzy clustering based on fuzzy c-means and improved particle swarm optimization”, **Expert Systems with Applications,** Vol.42, No. (17-18), pp:6315-28,2015, doi.org/10.1016/j.eswa.2015.04.032

[36] D. Saha, A. Datta, B.K.S. Roy and P. Das, “A comparative study on the computation of directional overcurrent relay coordination in power systems using PSO and TLBO based optimization”, **Engineering Computations (Emerald),** Vol. 33, no. 2, 2016. DOI 10.1108/EC-06-2015-0152.

[37] K.S. Sandhu and A. Mahesh 2016. A new approach of sizing battery energy storage system for smoothing the power fluctuations of a PV/wind hybrid system. **International Journal of Energy Research**, Vol. 40, No. 9, pp.1221-1234,2016.

[38] X. Chu, J. McAllister and R. Woods, (2011) “A Low Complexity Real-time MIMO-Preprocessing for Fixed Complexity Sphere Decoder”, **Paper presented at SDR'11 Technical Conference and Product Exposition, Washington D.C., United States**, pp-601-604, 2011.

[39] X. Wu, Y. Zhou and Y. Lu, “Elite opposition-based water wave optimization algorithm for global optimization”, **Mathematical Problems in Engineering**,2017, doi.org/10.1155/2017/3498363

[40] P. Yedamale, “Brushless DC (BLDC) motor fundamentals”, **Microchip Technology Inc**., Vol. 20, No. 1 pp:3-15,2003

[41] V. Bist and B. Singh, “An adjustable-speed PFC bridgeless buck–boost converter-fed BLDC motor drive”, **IEEE Transactions on Industrial Electronics**, Vol. 61, No.6, pp:2665-77,2014, doi: 10.1109/TIE.2013.2274424.

[42] H.S. Ransara and U.K. Madawala, (2013) “Modelling and analysis of a lowcost Brushless DC motor drive”, **IEEE International Conference on Industrial Technology, 25-28 Feb. 2013, Cape Town, South Africa**, pp. 356-61, doi: 10.1109/ICIT.2013.6505698

[43] R.L. Mulgrave, inventor; Cleveland Machine Controls Inc, assignee. Brushless DC motor. **United States patent US** 5,710,474. 1998 Jan 20.

[44] B.K. Lee, T.H. Kim and M. Ehsani, “On the feasibility of four-switch three-phase BLDC motor drives for low cost commercial applications: topology and control”, **IEEE Transactions on Power Electronics**, Vol. 18, No. 1, pp: 164-72,2003, doi: 10.1109/TPEL.2002.80712

[45] P. Gahinet and P. Apkarian, “A linear matrix inequality approach to H∞ control”, **International Journal of Robust and Nonlinear Control**, Vol. 4, No. 4, pp:421-48,1994, doi.org/10.1002/rnc.4590040403

[46] L. Březina and T. Březina, “H-infinity controller design for a DC motor model with uncertain parameters”, **Engineering Mechanics**, Vol. 18, No. (5-6), pp:271-79,2011.

[47] I. Tolaimate and N. Elalami, “Robust Control Problem as H2 and H∞ control problem applied to the robust controller design of Active Queue Management routers for Internet Protocol”, **International Journal of Systems Applications, Engineering & Development**, Vol. 5, No.6, pp: 683-91,2011.

[48] K. Vinida and M. Chacko, (2016) “An optimized H infinity strategy for robust control of sensorless BLDC propulsion motor in submarines for improved maneuverability”, **IEEE International Conference on Power Electronics, Drives and Energy Systems (PEDES), 14-17 Dec. 2016, Trivandrum, India**, pp: 1-6, doi: 10.1109/PEDES.2016.7914280

[49] X.C. Méndez Cubillos and L.C. de Souza, “Using of H-infinity control method in attitude control system of rigid-flexible satellite”, **Mathematical Problems in Engineering**,2009, doi.org/10.1155/2009/173145

[50] B. Jiao, Z. Lian and X. Gu, “A dynamic inertia weight particle swarm optimization algorithm”, **Chaos, Solitons & Fractals**, Vol. 37, No.3, pp: 698-705,2008, doi.org/10.1016/j.chaos.2006.09.063

[51] Q. Bai, “Analysis of particle swarm optimization algorithm”, **Computer and Information Science**, Vol.3, No.1, pp:180-84,2010, DOI: 10.5539/cis. v3n1p180

[52] M.R. Faieghi and S.M. Azimi, (2010) “Design an optimized PID controller for brushless DC motor by using PSO and based on NARMAX identified model with ANFIS” **12th International Conference on Computer Modelling and Simulation, 24-26 March 2010, Cambridge, UK**, pp: 16-21, doi: 10.1109/UKSIM.2010.12

[53] K.S. Tang, K.F. Man, G. Chen and S. Kwong, “An optimal fuzzy PID controller”, **IEEE Transactions on Industrial Electronics**, Vol. 48, No.4, pp:757-65,2001, doi: 10.1109/41.937407

[54] J. Carvajal, G. Chen and H. Ogmen, “Fuzzy PID controller: Design, performance evaluation, and stability analysis”, **Information Sciences**, Vol.123, No. (3-4), pp:249-70,2000, doi.org/10.1016/S0020-0255(99)00127-9

[55] H.A. Malki, D. Misir, D. Feigenspan and G. Chen, “Fuzzy PID control of a flexible-joint robot arm with uncertainties from time-varying loads”, **IEEE Transactions on Control Systems Technology,** Vol. 5, No.3, pp:371-78,1997, doi: 10.1109/87.572133

[56] M. Petrov, I. Ganchev and A. Taneva, (2002) “Fuzzy PID control of nonlinear plants”, **First International IEEE symposium intelligent systems, 10-12 Sept. 2002, Varna, Bulgaria, Bulgaria**, pp: 30-35, doi: 10.1109/IS.2002.1044224,

[57] B.M. Mohan and A.V. Patel, “Analytical structures and analysis of the simplest fuzzy PD controllers”, **IEEE Transactions on Systems, Man, and Cybernetics, Part B (Cybernetics),** Vol. 32, no.2, pp: 239-48,2002, doi: 10.1109/3477.990881

[58] J. Sun, G. Chen, K.T. Ko, S. Chan and M. Zukerman, (2003) “PD-controller: A new active queue management scheme”, **GLOBECOM '03. IEEE Global Telecommunications Conference (IEEE Cat. No.03CH37489), 1-5 Dec. 2003, San Francisco, CA, USA,** Vol. 6, pp. 3103-3107, doi: 10.1109/GLOCOM.2003.1258806

[59] M.P. Majhi and C. Mahanta, (2004) “Fuzzy proportional integral-proportional derivative (PI-PD) controller”, **Proceedings of the 2004 American Control Conference, 30 June-2 July 2004, Boston, MA, USA,**Vol. 5, pp: 4028-4033,doi: 10.23919/ACC.2004.1383938

[60] J.H. Kim, J.H. Park, S.W. Lee and E.K. Chong, “Fuzzy precompensation of PD controllers for systems with dead zones”, **Journal of Intelligent & Fuzzy Systems**, Vol. 1, No. 2, pp:125-33,1993, doi: 10.3233/IFS-1993-1203

[61] G. Pope, “Compressive sensing a summary of reconstruction algorithms”, **(Master's thesis, ETH, Swiss Federal Institute of Technology Zurich, Department of Computer Science),**2009.

[62] D.L. Donoho, “Compressed sensing”, **IEEE Transactions on Information Theory,** Vol. 52, No.4, pp: 1289-306, 2006, doi: 10.1109/TIT.2006.871582

[63] M.F. Duarte and Y.C. Eldar, “Structured compressed sensing: From theory to applications”, **IEEE Transactions on Signal Processing**, Vol. 59, No.9, pp: 4053-85,2011, doi: 10.1109/TSP.2011.2161982

[64] N.I. Siddique, M.S. Munaim and Z.A. Wahid, “Role of biogas recirculation in enhancing petrochemical wastewater treatment efficiency of continuous stirred tank reactor”, **Journal of Cleaner Production,** Vol. 91, pp: 229-34, 2015, doi.org/10.1016/j.jclepro.2014.12.036

[65] A.K. Mishra, V. Singh and A. Rani, “H-Infinity Controller Design for a Continuous Stirred Tank Reactor”, **International Journal of Electronic and Electrical Engineering**, Vol. 7, No. 8, pp: 767-72,2014.

[66] R. Antonelli and A. Astolfi, “Continuous stirred tank reactors: easy to stabilise?” **Automatica,** Vol.39, No.10, pp:1817-27,2003, doi.org/10.1016/S0005-1098(03)00177-8

[67] B. Chaudhuri, B.C. Pal, A.C. Zolotas, I.M. Jaimoukha and T.C. Green, “Mixed-sensitivity approach to H/sub/spl infin//control of power system oscillations employing multiple FACTS devices”, **IEEE Transactions on Power Systems**, Vol. 18. No.3, pp: 1149-56,2003, doi: 10.1109/TPWRS.2003.811311

[68] Y.J Zheng, “Water wave optimization: a new nature-inspired metaheuristic”, **Computers & Operations Research,** Vol. 55, pp: 1-11,2015, doi.org/10.1016/j.cor.2014.10.008

[69] Y.J. Zheng and B. Zhang, (2015) “A simplified water wave optimization algorithm”, **IEEE Congress on Evolutionary Computation (CEC), 25-28 May 2015, Sendai, Japan**, pp:807-813. doi: 10.1109/CEC.2015.7256974

[70] Zaheeruddin, D.K. Lobiyal and A. Pathak, “Energy-aware bee colony approach to extend lifespan of wireless sensor network”, **Australian Journal of Multi-Disciplinary Engineering (Taylor & Francis),** Vol. 13, no. 1, pp. 29-46, 2017 (DOI: 10.1080/14488388.2017.1358896

[71] A.F. Falcão, J.C. Henriques, L.M. Gato and R.P. Gomes, “Air turbine choice and optimization for floating oscillating-water-column wave energy converter”, **Ocean Engineering**, Vol. 75, pp: 148-56,2014, doi.org/10.1016/j.oceaneng.2013.10.019

[72] W. Xu, Z. Ye and Y. Hou, (2017) “A fast image match method based on water wave optimization and gray relational analysis”, **9th IEEE International Conference on Intelligent Data Acquisition and Advanced Computing Systems: Technology and Applications (IDAACS), 21-23 Sept. 2017, Bucharest, Romania**,Vol. 2, pp: 771-776,doi:10.1109/IDAACS.2017.8095193

[73] H.L. Tolman, V.M. Krasnopolsky and D.V. Chalikov, “Neural network approximations for nonlinear interactions in wind wave spectra: direct mapping for wind seas in deep water”, **Ocean Modelling,** Vol. 8, No.3, pp:253-78,2005, doi.org/10.1016/j.ocemod.2003.12.008

[74] Y.J. Zheng, “Water wave optimization: a new nature-inspired metaheuristic”, **Computers & Operations Research**. Vol. 55, pp 1-11, 2015. doi.org/10.1016/j.cor.2014.10.008

[75] K.P. Sudheer, A.K. Gosain, D. Mohana Rangan and S.M. Saheb, “Modelling evaporation using an artificial neural network algorithm”, **Hydrological Processes**, Vol. 16, No.16, pp:3189-202 ,2002, doi.org/10.1002/hyp.1096

[76] D.C. Park, M.A. El-Sharkawi, R.J. Marks, L.E. Atlas and M.J. Damborg, “Electric load forecasting using an artificial neural network”, **IEEE Transactions on Power Systems**, Vol. 6, No.2, pp:442-49,1991, doi: 10.1109/59.76685

[77] K.L. Hsu, H.V. Gupta and S. Sorooshian, “Artificial neural network modeling of the rainfall-runoff process”, **Water Resources Research,** Vol. 31, No.10, pp:2517-30, 1995, doi.org/10.1029/95WR01955

[78] E. Arce-Medina and J.I. Paz-Paredes, “Artificial neural network modeling techniques applied to the hydrodesulfurization process”, **Mathematical and Computer Modelling**, Vol. 49, No. (1-2), pp:207-14, 2009, doi.org/10.1016/j.mcm.2008.05.010

[79] J. Xiao, D. Li and J. Zhou, (2015) “Active disturbance rejection controller design for distributed parameter systems”, **Chinese Automation Congress (CAC), 27-29 Nov. 2015, Wuhan, China,** pp: 202-207, doi: 10.1109/CAC.2015.7382496.

[80] Y.J. Wu, Y.Y. Hua and X.D. Liu, “Design method of active disturbance rejection variable structure control system”, **Mathematical Problems in Engineering**,2015, doi.org/10.1155/2015/195720

[81] X.X. Shi and S.Q. Chang, “Application study of active disturbance rejection control technology”, **Advanced Materials Research,** Vol. 383, pp: 701-706, 2012, doi.org/10.4028

[82] Z. Chen, Q. Zheng and Z. Gao, (2007) “Active disturbance rejection control of chemical processes” **IEEE International Conference on Control Applications, 1-3 Oct. 2007, Singapore, Singapore,**pp: 855-861, doi: 10.1109/CCA.2007.4389340

[83] Y. Xia, B. Liu and M. Fu, “Active disturbance rejection control for power plant with a single loop”, **Asian Journal of Control**, Vol. 14, No.1, pp:239-50,2012, doi.org/10.1002/asjc.240

[84] K. Premkumar and B.V. Manikandan, “Bat algorithm optimized fuzzy PD based speed controller for brushless direct current motor”, **Engineering Science and Technology, an International Journal,** Vol. 19, No.2, pp:818-40,2016, doi.org/10.1016/j.jestch.2015.11.004

[85] K. Premkumar and B.V. Manikandan, “Fuzzy PID supervised online ANFIS based speed controller for brushless DC motor”, **Neurocomputing**, Vol. 157, pp: 76-90, 2015, doi.org/10.1016/j.neucom.2015.01.032

[86] W. Li, J. Fang, H. Li and J. Tang, “Position sensor less control without phase shifter for high-speed BLDC motors with low inductance and nonideal back EMF”, **IEEE Transactions on Power Electronics**, Vol. 31, No. 2, pp: 1354-66, 2016, doi: 10.1109/TPEL.2015.2413593

LIST OF PUBLICATION

- **Sikander Hans and Smarajit Ghosh** “Position Analysis of Brushless Direct Current Motor Using Robust Fixed Order H-infinity Controller”, Assembly Automation, Emerald insight, Vol. 40, no. 2, pp. 211-218. https://doi.org/10.1108/AA-05-2019-0084 **(Published) (Impact Factor- 1.256)**

- **Sikander Hans and Smarajit Ghosh** “H-infinity Controller based Disturbance Rejection in Continuous Stirred Tank Reactor”, Intelligent Automation & Soft Computing, Tech Science Press, Vol. 31, No. 1, 2021. DOI:10.32604/iasc.2022.019525 **(Published) (Impact Factor- 1.647)**

BIOGRAPHY

SIKANDER HANS was born in Hisar, Haryana, India on 6^{th} August,1984. He did his B-Tech (Electronics and Instrumentation Control) from Y.M.C.A College Faridabad, Haryana, India in 2007 and M.E (Electronics Instrumentation and Control) from Thapar University Patiala, Punjab, India in 2011.He got admitted in PhD as a regular research scholar in the Department of Electrical and Instrumentation Engineering of Thapar Institute of Engineering and Technology(Deemed to be University), Patiala, Punjab, India. Under the supervision of Prof. Dr. Smarajit Ghosh. His areas of interest are H-infinity control, Controller Design, Artificial Intelligence, Optimization using Nature Inspired Algorithms (PSO, WWO, ESO), etc. He has above 6 year of academic and research experience.

Contact email: shans_phd16@thapar.edu

Contact email: sikihans995@gmail.com

SMARAJIT GHOSH: Born in Ghatal, West Bengal, India on 16 August,1967. He did his B.Sc. (Physics Hons). B. Tech. (Electrical Engineering), M. Tech. (Electrical Machines and Power Systems) from Calcutta University in 1991, 1994 and 1996 respectively. Finally, he did his Ph.D. from Indian Institute of Technology, Kharagpur, India in 2000. His research areas include load flow study, network reconfigurations, optimum capacitor allocation, application of soft computing in Electrical Power Distribution systems, data-security. He has already served REC (Durgapur), BITS Pilani and Sikkim Manipal University, as a lecturer, an Assistant Professor and a Professor respectively. He has authored a number of books published by Prentice Hall of India Private Limited and Pearson Education as a single author.

Smarajit Ghosh is presently serving as a Professor at Thapar Institute of Engineering and Technology (Deemed to be University), Patiala in Department of Electrical and Instrumentation Engineering from 01-08-2007.

Contact email: smarajitg@hotmail.com

Contact email: sghosh@thapar.edu